Computationally Efficient Spatial and Cooperative Diversity Techniques for Wireless Communication Networks

Vom Fachbereich Elektrotechnik und Informationstechnik
der Technischen Universität Darmstadt
zur Erlangung des akademischen Grades eines
Doktor-Ingenieurs (Dr.-Ing.)
genehmigte Dissertation

von

Samer Alabed, M.Sc.

Geboren am 18 Aug. 1981 in Amman, Jordanien.

Referent:	Prof. Dr.-Ing. Marius Pesavento
Korreferent:	Prof. Dr. Ing. Babak Khalaj
Tag der Einreichung:	3 Feb., 2012
Tag der mündlichen Prüfung:	8 Mai, 2012

D17

Darmstadt 2012

Zusammenfassung

Mehrantennensysteme wurden in den vergangenen Jahren intensiv erforscht. Die Verwendung mehrerer Antennen erlaubt es, drahtlose Kommunikationssysteme robuster zu machen, die Übertragungsrate zu erhöhen und Störungen z.B. durch Mehrwegeausbreitung und Interferenzen zu überwinden. Mehrantennensysteme erlauben es, diese Verbesserungen zu erreichen, ohne zusätzliche Frequenzbandbreite oder Übertragungsleistung zu benötigen. Allerdings könenn Mehrantennensysteme z.B. aus Platz- oder Kostengründen nicht in allen Anwendungen eingesetzt werden. Als Alternative zu Mehrantennensystemen wurden kooperative Systeme vorgeschlagen. Diese erlauben es, ähnliche Gewinne wie Mehrantennensysteme zu erreichen.

In dieser Arbeit werden Signalverarbeitungsverfahren für Mehrantennensysteme und kooperative Systeme entwickelt. Ziel dabei ist es, einen möglichst guten Kompromiss zwischen Rechenkomplexität, Bitfehlerrate und Datenübertragungsrate zu erreichen.

Wir betrachten zunächst die Raumzeitcodierung für Mehrantennensysteme. Wir entwickeln einen Decoder für quasiorthogonale Codes mit niedriger Rechenkomplexität. Sowohl die kohärente als auch die inkohärente Implementierungen dieses Decoders werden untersucht. Der vorgeschlagene Decoder erreicht in etwa die gleiche Performance wie der optimale Maximum Likelihood Decoder bei einer deutlich geringeren Rechenkomplexität.

Verschiedene kooperative Strategien wurden für drahtlose Zwei-Wege Relay-Netze vorgeschlagen basierend auf Amplify-and-Forward und Decode-and-Forward Protokollen. Die gleichzeitige Zwei-Wege Decode-and-Forward Strategie ermöglicht es, höhere Datenübertragungsraten zu erreichen als anderen Decode-

and-Forward Strategien. Allerdings erfordert die gleichzeitige Zwei-Wege Decode-and-Forward Strategie eine hohe Rechenkomplexität für die Decodierung und eine direkte Verbindung zwischen den Nutzern wird nicht unterstützt.

In dieser Arbeit schlagen wir neue kooperative kohärente und inkohärente gleichzeitige Decode-and-Forward Strategien vor, die einen höheren Codierungsgewinn bieten und eine wesentlich geringere Rechenkomplexität für die Decodierung benötigen als existierende Verfahren. Außerdem ermöglicht es die vorgeschlagene Technik, eine direkte Verbindung zwischen den Teilnehmern zu nutzen.

Zusätzlich entwickeln wir ein nichtkohärentes Amplify-and-Forward Codierungsverfahren für Zwei-Wege Relay-Netze. Dieses Verfahren erreicht einen signifikant höheren Kodierungsgewinn als herkömmliche Verfahren. Zudem ist es energieeffizienter als existierende Verfahren und es ermöglicht, eine direkte Verbindung zwischen den Teilnehmern zu nutzen.

Weiterhin stellen wir ein inkohärentes verteiltes Beamformingverfahren vor. Da die Schätzung des Kanalzustands einen erheblichen Aufwand erfordert und in vielen Anwendungen nicht realisierbar ist, verwenden wir ein differentielles Verfahren, das die Kenntnis des Kanalzustands nicht benötigt. Der vorgeschlagene Beamformer erreicht eine hohe Performance und optimale Latenzzeit bei einer geringen Decodierungskomplexität.

Abstract

Several techniques are recently proposed to improve the robustness of wireless communication systems, increase the throughput, and overcome channel impairments such as multi-user interference and multi-path fading. Among them, using multiple-antennas is one of the most remarkable techniques as it allows to improve the error performance and the data rate without an increase in the frequency bandwidth or transmitted power. However, multiple-antenna techniques are not applicable in all ad-hoc networks due to hardware constraints. As an alternative, cooperative diversity techniques have been proposed to achieve gains similar to that of multiple-antenna techniques.

In this thesis, we develop computationally efficient multiple-antenna and cooperative diversity techniques for wireless communication networks which offer an improved tradeoff between computational complexity, error performance, and data rate. We first consider space-time block coding for conventional multiple-antenna systems. We propose a low complexity decoder for quasi-orthogonal space-time block codes. Both the coherent and non-coherent implementations of this decoder are developed. The proposed decoder can provide a substantially improved tradeoff between the complexity and performance as compared to state-of-the-art decoding techniques. The proposed decoder enjoys a nearly linear decoding complexity and it approximately achieves the optimal performance of the maximum-likelihood decoder.

Recently, cooperative diversity strategies for two-way wireless relay networks have been proposed using the amplify-and-forward and the decode-and-forward protocols. Although the simultaneous bidirectional decode-and-forward transmis-

sion has been shown to outperform other decode-and-forward strategies, it has mainly two disadvantages: high relay decoding complexity and the impossibility to use the direct link between the communicating terminals. In this thesis, we propose novel coherent and non-coherent simultaneous bidirectional decode-and-forward distributed space-time coding strategies that provide a higher coding gain and enjoy a substantially lower relay decoding complexity than the state-of-the-art strategies at the same symbol rate. In the proposed strategies, the communicating terminals can benefit from the direct link which is not exploited by other existing simultaneous bidirectional transmission strategies.

Various differential distributed space-time coding strategies for two-way relay networks using the amplify-and-forward protocol which do not require channel state information either at the relays or at the terminals have been proposed. The simultaneous two-way differential distributed space-time coding strategy using the amplify-and-forward protocol has been shown to outperform the conventional differential four-phase strategy in the low to medium signal-to-noise ratio region. However, there are mainly three disadvantages associated with it: i) the relay power wasted for transmitting redundant information at either side, ii) The direct link between the communicating terminals can not be used and iii) the considerable bias at high signal-to-noise ratio. In this work, amplify-and-forward differential distributed space-time coding strategies for two-way wireless relay networks are developed, that provide a higher coding gain than the state-of-the art strategies. In the proposed strategies, the relays do not waste power to transmit redundant information at either side and the communicating terminals can fully use the direct link between them.

Although differential distributed space-time coding strategies do not require channel state information at the relays, they are associated with a low error performance, a high latency, and decoding complexity. Another strategy used in relay networks relies on coherent processing of the relay signals using distributed beamforming techniques.This strategy enjoys a good error performance and low decoding complexity while offering an optimal decoding delay. However, a common requirement in distributed beamforming is the availability of perfect

channel state information at all nodes. To avoid this requirement, we introduce a distributed differential beamforming strategy that combines the differential diversity and the distributed beamforming strategy while retaining the benefits of both approaches. The proposed strategy does not require channel state information at any node and enjoys a good error performance, optimal delay, and low decoding complexity.

Dedication

(And ye have no good thing but is from Allah)
To Prof. Dr. Alex B. Gershman
To Prof. Dr. Eng. Marius Pesavento
To my family members
To my faculties
To my colleagues
To the people I care about
To those who I love
To those who appreciate the glory of the creation
To those who convert the beauty into reality

Samer Jamil Alabed

Acknowledgment

First and foremost, I would like to express my deepest gratitude to my supervisors, *Prof. Dr. Eng. Marius Pesavento* and *Prof. Dr. Alex Gershman*, for all support and guidance they have offered me during my PhD study. I am very grateful for the knowledge they have shared with me throughout the development of my thesis and academic papers. Many thanks also to my co-supervisor, Prof. Dr. Eng. Babak Khalaj, for his time and interest in my work. I would like to gratefully thank and acknowledge my colleague, *Dr. Eng. Javier Paredes*, for all interesting discussions and helpful comments and suggestions.

Special thanks to all the past and actual members of the Communication Systems Group (Marlis Gorecki, Dana Ciochina, Ahmed Abdelkader, Michael Ruebsamen, Mohammed El-Korso, Nima Sarmadi, Nils Bornhorst, Xin Wen, Adrian Schad, Yang Yang, Young Cheng , Imran Wajid, Liang Li, Ka Law, Pouyan Parvazi, and Terasan Niyomsataya) and to anyone who contributed in one way or another in the successful completion of this work.

I would like to thank the *German Academic Exchange Service(DAAD)* for the prestigious scholarship that I received during my PhD study. Finally, I am grateful to my parents for their support and encouragment.

Samer Jamil Alabed

Contents

List of Figures

List of Tables

Chapter 1

Introduction

Multiple-antenna and cooperative diversity techniques have been an active area of research in wireless communications due to their ability to significantly increase the error performance and the data rate. In this chapter, we first present an overview to multiple-antenna and cooperative diversity techniques. Afterwards, a review of preliminary works and motivation for this work are covered. Finally, we outline the contributions of this thesis.

1.1 Overview

Over the last decade, new wireless communication networks have been developed in order to enable communication to be carried out anywhere and anytime. Therefore, the demands for high data rate and guaranteed quality of service (QoS) in wireless communication systems have increased substantially. However, the capacity in single-antenna wireless communication systems is limited mainly due to multi-user interference and multi-path fading. The physical limitations of the wireless medium and limitations due to hardware cost conflict with the achievable data rate and QoS demands.

Several techniques have been proposed for wireless communication systems to improve the data rate and overcome various channel impairments occurring

in practical situations. Theoretically, transmitter power control is one of the techniques to reduce the effect of signal fading in the wireless communication channel where in conventional single-antenna wireless communication systems, the bit error rate (BER) decreases linearly with the increase of the signal-to-noise ratio (SNR). Practically, in order to overcome a certain level of signal attenuation at the receiver due to multi-path fading and path loss, the concept of transmit power control is to increase the transmitted power which, in most cases, is not practical due to the cost and size of the amplifiers and radiation power limitations enforced by regulations. In addition to that, the transmitter, in some cases, does not have any knowledge of channel state.

Other communication techniques that improve spectral efficiency and reduce the effects of multi-path fading and interference have been proposed. One of these successful communication techniques is the use of diversity which improves the overall error performance and the achievable data rate by transmitting more than one independently attenuated replica of the information signal. Diversity techniques can be mainly categorized into time, frequency, and spatial diversity [3, 19–21]:

- Frequency diversity: Redundant information is transmitted simultaneously on different frequency blocks. This improves transmission performance at the cost of additional frequency bandwidth.
- Time diversity: Redundant information is transmitted in different transmission time intervals. This reduces the symbol rate.
- Spatial diversity (antenna diversity): Redundant information is transmitted and received using multiple antennas. This improves the overall system performance in terms of BER and capacity with no penalty in the bandwidth efficiency or transmitted power at the expense of additional hardware costs [1, 2].

Spatial diversity techniques have been introduced as an efficient solution for future wireless communication systems and received considerable attention in

the scientific community. These techniques can be merged with other diversity techniques such as time and frequency diversity. In order to exploit the spatial diversity provided by multiple-antenna transceivers, various multiple-antenna techniques have been proposed [3–7]. Among them, the *space-time coding* (STC) is one of the most successful techniques.

STC techniques improve the diversity gain over the fading channels without requiring multiple receive antennas and channel state information (CSI) at the transmitter [8–13]. The gain is obtained by exploiting the independent signal pathes between the communicating terminals and transmitting multiple redundant copies of a data stream. In this step some of the copies may arrive at the receiver in a better state than others. The data stream is transmitted using multiple antennas over multiple consecutive time slots. Using this technique, the achievable data rate and BER performance are improved by many orders of magnitude.

In recent years, many interesting STC techniques for transmit diversity have been proposed such as: *space-time trellis codes* (STTCs) [9] which enjoy high coding gain. However, their decoding complexity for a fixed number of transmit antennas increases exponentially with the transmission rate. As a solution to the large decoding complexity of STTCs, Alamouti proposed a remarkable space and time diversity technique using two transmit antennas [12]. Later, Tarokh generalized Alamouti code and presented *space-time block codes* (STBCs) to an arbitrary number of transmit antennas [10, 11].

If the use of multiple antenna devices is impractical, multiple single antenna devices can cooperative to provide similar diversity gains. Cooperation among different relays in wireless communication systems has been recently envisioned as an alternative approach to achieve transmit diversity in the face of these limitations [14, 15]. This new form of transmit diversity has been proposed under the name of user cooperation, cooperative diversity, or cooperative communication.

Similar to multiple-antenna techniques, cooperation between, e.g., pairs of wireless communication relays increases the achievable data rates and decreases multi-path effect by allowing two single-antenna terminals to transmit and re-

ceive their information signals using multiple single-antenna relay nodes [14, 15]. Cooperation can be used in several types of wireless communication networks such as sensor networks, cellular networks, and ad hoc networks. Recently, different cooperative transmission protocols have been proposed [14–16]. They can be classified into the two main categories: the amplify-and-forward [17] and the decode-and-forward protocols [16, 17].

In [18], an efficient cooperative strategy called *distributed space-time block coding* that combines both STC and cooperative diversity techniques to design a wireless communication technique capable of improving the error performance and the data rate has been proposed. The idea of this strategy is to have the relays apply a simple operation on their received information signal such that the received signal at the destination terminal exhibits similar characteristics as in conventional STC.

In the subsequent section, the state of the art multiple-antenna and cooperative diversity techniques are described in more detail.

1.2 Motivation and Preliminary Works

While many of the demands of new wireless communication systems, for example the need for high data rates, quality of service, small latencies, and others, increase rapidly, the available resources such as bandwidth, power, and processing capacity are limited. Therefore, several spatial diversity techniques using multiple antennas are proposed to improve the spectral efficiency and combat the effects of multi-path fading. Multiple-antenna techniques are applied to provide more reliable communication and offer improvements in the data rate and throughput [22] which have led to multiple-antenna techniques being considered as one of the efficient wireless technologies considered in current and future wireless communication standards [8, 19]. Studies by Foschini and Gans [1] and Telatar [2] have shown that wireless communication systems with multiple transmit and receive antennas have generally a higher capacity than single-antenna systems [1, 2].

Several forms of spatial diversity techniques, e.g., transmit and receive diversity have also been studied extensively to combat the multi-path effects in wireless channels where many efficient transmit and receive diversity techniques have been recently proposed in [10–20, 23–34, 95].

In the last decade, many works have been proposed to generalize and improve multiple-antenna techniques. Some works are proposed based on unrealistic assumptions such as perfect CSI at both the transmitter and the receiver. Other works are proposed based on more realistic assumptions of perfect or partial CSI at the transmitter side only. Recent contributions have also considered the more realistic case of no CSI available at either transmitter or receiver for which several theoretic capacity results have been obtained, e.g., in [35–38].

In 1998, the idea of STC has been proposed by Tarokh, Seshadri and Calderbank in [9]. In STC, the encoding process at the transmitter is carried out not only in the time dimension, but also in the space dimension. By distributing the transmitted information symbols to both time and space dimension, both the error performance and the data rate are improved by many orders of magnitude without requiring multiple receive antennas and CSI at the transmitter [8–13]. This is an important observation ignited great interest in these techniques and attracted much attention from academic and industrial researchers.

Later, several STC techniques suitable for transmission through wireless communication networks have been proposed [9, 10, 39, 40] such as *space-time trellis codes* [9], *space-time block codes* [10, 11], and *unitary space-time codes* (USTCs) [40]. Space-time trellis coding is a technique that operates on one input information symbol at a time generating a vector of symbols whose length represents the number of transmit antennas. STTCs designed for two to four transmit antennas are well established in slow fading channels. However, their decoding complexity for a fixed number of transmit antennas increases exponentially with the transmission rate. There has also much effort been made in trying to improve the coding gain by merging STC techniques with other error correcting codes or modulation techniques [41–52].

STBCs for several transmit antennas which operate on a stream of input symbols generating a matrix output whose columns represent transmit antennas and rows represent time are proposed in [9–13]. The design of STBCs concerns about find a constellation of matrices that satisfies specific optimality criteria and provides a good tradeoff among three conflicting goals of offering a low decoding complexity, maximizing the error performance and maximizing the data rate.

In [12], Alamouti proposed a powerful STBC technique for two transmit antennas which improves the quality of the received signal by applying a simple encoding scheme at the transmitter and linear decoding at the receiver [12]. The complexity of the Alamouti technique is much less than that of STTCs, however, at a loss in the BER performance. The Alamouti technique is still appealing in terms of simplicity and it ignited a great search for similar techniques using more than two transmit antennas.

The Alamouti technique has been a basis to create the so called *orthogonal space-time block codes* (OSTBCs) for more than two transmit antennas. In order to ensure full diversity and to simplify decoding at the receiver, the STBC techniques used to distribute the transmitted data streams over the space and time need to exhibit the orthogonality property [19]. Extending Alamouti's work, the authors in [10] proposed OSTBCs which use the orthogonal design technique at the transmitter side to ensure full diversity and achieve a linear decoding complexity at the receiver side. Although OSTBCs provide full diversity and enjoy low decoding complexity, full transmission rate is not possible for more than two transmit antennas.

In [53], Jafarkhani proposed a *quasi-orthogonal space-time block code* (QOSTBC) to overcome the low transmission rate limitation of OSTBCs. The QOSTBC provides full-rate for four transmit antennas while having a pair-wise decoding complexity with partial diversity. In [54–56], it is shown that the full-diversity property can be recovered using constellation rotation.

In [57], another design was proposed which also provides full-rate STBC for an even number of transmit antennas. In [58], a general design technique to generate maximal data rate codes with full diversity OSTBCs was proposed.

Other STC techniques for certain number of transmit antennas were presented in [59–61], in which they enjoy high code rates and minimal decoding delay. Comprehensive surveys of coding and modulation approaches for multiple-antenna wireless communication systems can be found in [62] and [63].

The STBCs require coherent receiver in the sense that CSI is required only at the receiver. Differential distributed space-time coding techniques which do not require CSI either at the transmitter or at the receiver to decode the transmitted symbols have been introduced in [19, 64–67]. Since these techniques can overcome the overhead involved with the channel estimation and reduce the overall system complexity, they have recently received much attention.

Due to hardware constraints of the real wireless communication networks, the use of multiple-antennas may not always be practical for certain applications especially in small compact devices. As an alternative way to achieve transmit diversity in face of these limitations, another spatial diversity approach for the relay channel has been proposed where, e.g., the antennas of multiple cooperating terminals are used to combat the multi-path fading [68]. Later, an extension of the relay channel for multiple-hop wireless communication networks has been proposed [14, 17]. In this context, the concept of *cooperative diversity* has been established.

In cooperative diversity, which can be considered as a specific type of spatial diversity technique, the main idea is to exploit the broadcast nature of wireless media where the signal transmitted by the source node is retransmitted by other cooperating relay nodes. The source node and the relays can jointly process and send their information creating a *virtual antenna array* and, therefore, exploiting transmit diversity. In the considered setup, each cooperating user transmits not only its own information, but also forwards its own received data. This means that in this diversity scheme, the users cooperate in share the common resources time, bandwidth, and power. The conventional source-destination communication, as in point-to-point multiple-antenna systems, is extended to source-relay-destination communication which offers significant performance gain in wireless

communication networks by enabling, e.g., two single-antenna terminals to transmit and receive their information signals using multiple single-antenna relays.

In specific, cooperation among relays in a wireless communication network has been proved to be very useful to reduce multi-path effects [26] and to increase the data rate of the wireless communication networks [27]. Therefore, relay cooperation can improve the overall error performance and the data rate of wireless communication networks [14, 16, 29, 68–70].

Since the work of [14, 15], different cooperative transmission protocols have been proposed in [16, 17, 29, 71–73]. Based on the function of the relays, two principal classes can be distinguished: the *amplify-and-forward* (AF) and the *decode-and-forwards* (DF) protocols where the requirements on the functionality of the relay are either low as in the AF protocol [17] or high as in the DF protocol. In the former protocol, the AF relay simply forwards a (complex) weighted version of its received signal and in the latter protocol, the DF relay decodes, re-encodes, and forwards the received signal [16, 17].

A difficulty arising in the context of the AF protocol is that each cooperating relay receives a noisy version of the signal which is then amplified and retransmitted. Although, in this scheme, the noise received at the relays is amplified, the destination node can still benefit from relaying as it receives several independently faded copies of the source signal.

In the DF protocol, each cooperating relay detects the source's bits and then resends an estimate of the detected bits. The cooperating relays provide significant diversity gain in the wireless communication networks. Therefore, cooperative diversity is emerging as a powerful technique in wireless communication systems which allows single-antenna relays to improve reliability and throughput of wireless networks and achieve some of the benefits of the conventional multiple-antenna techniques.

In [22, 28, 29], different cooperative diversity techniques are compared. The techniques presented in [22, 28] are essentially based on time repetition coding which suffer from a reduced transmission rate. Therefore, several works have been proposed to find codes that are optimal with respect to the so-called *diversity-*

multiplexing gain tradeoff [71, 74]. The *distributed space-time coding* (DSTC) approach has been proposed for relaying systems to achieve the maximum diversity gain without suffering from the rate loss of repetition coding. It allows multiple relays to share their antennas to create a virtual transmit array and then implement DSTC over the virtual array. In other words, this powerful technique merges ideas from STC and multiple-relay cooperative networks to design a wireless communication network capable of improving reliability and throughput of the wireless network by taking advantage of the spatial diversity available in cooperative networks in a bandwidth efficient manner.

In [29], Laneman and Wornell used orthogonal STBCs to design a DSTC technique where each relay sends a different column of the STBC matrix. Since the design of orthogonal STBCs for a large number of transmit antennas is difficult and the full transmission rate code is unachievable, the straightforward application of orthogonal STBCs is limited to wireless networks with a small number of relays. On the other hand, using non-orthogonal full-rate STBCs [75], which are available for any number of transmit antennas, is a solution, however, their decoding complexity increases rapidly with the increase of number of relays.

The distributed STBCs require CSI only at the receiver. To overcome the overhead involved with the channel estimation, differential DSTC techniques which do not require CSI either at the transmitter or at the receiver to successfully decode the transmitted symbols have been introduced in [76–90].

In the next section, a detailed overview of the contributions and organization of the thesis is provided.

1.3 Thesis Contributions

In the design of new STC and cooperative diversity schemes, certain optimality criteria need to be guaranteed. The STC has to provide a good tradeoff among three conflicting goals of allowing simple decoding, maximizing the overall BER performance and maximizing the data rate. Therefore, the aim of the

research activities carried out under this thesis is to design multiple-antenna and cooperative diversity techniques for wireless communication networks with a good rate-diversity-complexity tradeoff. At high SNR, the measure of reliability is the diversity gain which describes how fast the probability of error decreases with the increase of SNR. On the other hand, the multiplexing gain shows the rate at which the actual transmission rate of the system increases with SNR.

In chapter three of this thesis, we introduce an efficient coherent and non-coherent quasi-orthogonal STBC that offers a reduced decoding complexity. In this work, *coherent* techniques consider the case of perfect CSI available at the receiver only while *non-coherent or differential* ones are based on more realistic assumption of no CSI available at both the receiver and the transmitter which avoid overhead involved with channel estimation in order to decode the information symbols.

In chapter four, five, and six, we design several different coherent and non-coherent AF and DF transmission strategies for two-way relay networks with a single source-destination pair and multiple relays, each relay equipped with a single antenna. In chapter four, we design coherent and non-coherent DSTC transmission strategies for two-way relay networks using the DF protocol. In chapter five, we propose non-coherent DSTC strategies for two-way relay networks using the AF protocol. In the last chapter, we design a non-coherent distributed beamforming strategy for two-way relay networks using the AF protocol.

The outline of the thesis is as follows:

Chapter 2: *Wireless Communication in Multi-antenna Systems and Cooperative Relay Networks.*

In this chapter, a general overview about the basic models of the wireless channel and fundamental concepts of multiple-antenna systems and wireless relay networks is provided.

Chapter 3: *Quasi-Orthogonal Space-Time Block Coding in Multiple-Antenna systems.*

This chapter covers the first part of this thesis that is dealing with full-rate full diversity STBC design and low complexity decoding for QOSTBCs. The main contribution is that we propose a decoder that enjoys a nearly linear complexity and approximately the same BER performance as the optimal maximum-likelihood decoder which, however, exhibits exponential complexity. We also extend our proposed decoder to the non-coherent case where no CSI is available at both the receiver and the transmitter. The results of this chapter have also been published in [91].

Chapter 4: *Distributed Space-Time Block Coding in Decode and Forward Relay Networks.*

In this chapter, we consider the extension of the concept of STBC in multiple-antenna systems to distributed relay networks. While this chapter is emphasizing the decode-and-forward relaying protocol, the amplify-and-forward relaying protocol is covered in the following chapters. For the case of full CSI available at the receiver, we propose a novel DSTC transmission strategy for TWRNs that provides a higher coding gain and enjoys a substantially lower relay decoding complexity than the state-of-the art methods. Furthermore, our transmission strategy allows the communicating terminals to use the direct link between them to improve the diversity which is not valid for other simultaneous bidirectional DF transmission strategies. We present the analysis of the combination functions and propose a new one that uses directly the symbols rather than the bits to generate the superimposed symbol. Finally, we extend our results to the case where no CSI is available at the relay nodes, where we propose a new non-coherent DF transmission strategy for TWRNs. The results of this chapter have also been published in [92].

Chapter 5: *Distributed Differential Space-Time Block Coding in Amplify and Forward Relay Networks.*

In this chapter, we consider differential DSTC in AF relay networks. Unlike the DF relay networks discussed in the previous chapter, the difficulty arising in AF relaying consists in the inevitable noise amplification. The simultaneous bidirectional AF protocol using differential DSTC has been shown to outperform the conventional four-phase differential DSTC strategy in the low to medium SNR region, however, there are mainly three disadvantages associated with it: i) the relay power wasted for transmitting information known at either side, ii) the difficulty to incorporate the direct link between the communicating terminals and iii) the considerable bias at high SNR. In this chapter, we propose two non-coherent DSTC strategies for TWRNs using the AF protocol. In our proposed strategies, the relays do not waste power to transmit known information and the direct link between the communicating terminals can be fully exploited. The results of this chapter have also been published in [93].

Chapter 6: *Distributed Differential Beamforming in Amplify and Forward Relay Networks.*

Although differential distributed space-time codes for cooperative relay networks do not require CSI at any of the relay node, they are associated with a low BER performance and a comparably high latency and decoding complexity. In this chapter, we consider distributed beamforming techniques that enjoy a high system performance in terms of BER and low decoding complexity while offering an optimal decoding delay. A common requirement in distributed beamforming is perfect CSI available at both transmitter and receiver. Our proposed differential distributed transmit beamforming strategy combines both techniques, the differential diversity and the distributed beamforming technique while retaining the benefits of both approaches. The novel strategy does not require CSI at any node and enjoys high BER performance, optimal delay, and low decoding complexity. The results of this chapter have also been published in [94].

Chapter 2

Wireless Communication in Multi-antenna Systems and Cooperative Relay Networks

2.1 Wireless Channel Models

In a digital communication system, as shown in Fig. 2.1, a band limited information signal is transmitted from the source to the destination over the communication channel. The information source generates an information signal which is either analog or digital. In the source encoder, the shortest description of the message sequence is found by translating the message into a sequence of codewords where the symbols that occur with higher probabilities are assigned the shorter codewords. Afterwards, the channel encoder adds redundancy in the information sequence that can be used at the channel decoder to detect and correct errors that occurred during the transmission due to noise and fading. Channel coding increases the reliability of the communication and improves the overall error performance. At the output of the channel, the received signal is down-converted and sampled to digital baseband and the errors which occurred during transmission are corrected in the channel decoder.

In wireless communication channel, different phenomena affect the propagation of electromagnetic waves between the transmitter and the receiver such as reflection, diffraction, absorption, refraction, and scattering.

Reflection occurs in the case when the electromagnetic wave impinges on an object with dimensions larger than its wavelength. Due to reflection from different surfaces, the electromagnetic waves may reach the destination through other pathes than the direct link.

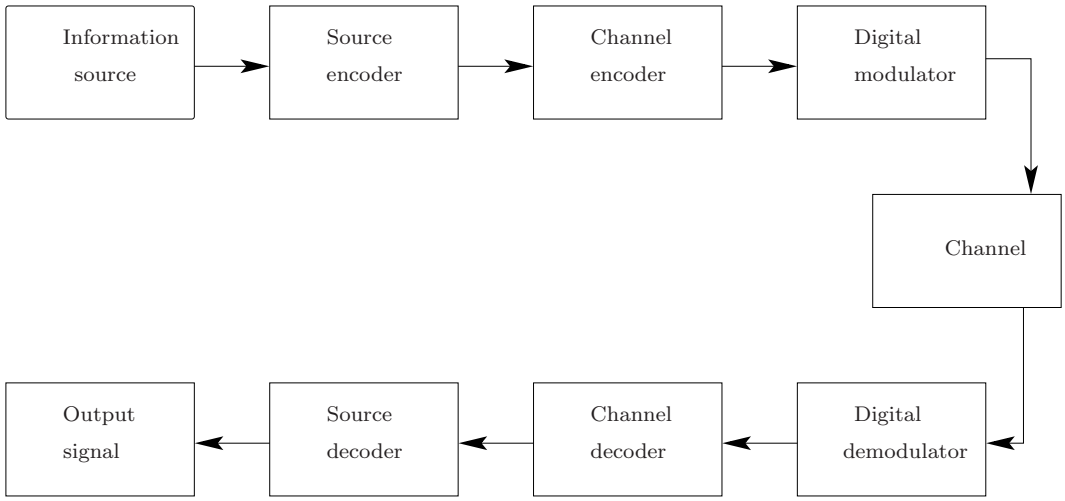

Figure 2.1: Digital communication system.

Diffraction occurs when the electromagnetic wave hits an object smaller than its wavelength while absorption happens when the electromagnetic wave is absorbed rather than being reflected, diffracted, or bent. Refraction describes the bending of the electromagnetic waves as they pass through a medium of different electromagnetic densities. Scattering happens when the electromagnetic wave impinges on an irregular surface where the reflected energy is spread out in diffuse directions.

Due to these phenomena, the destination receives several different copies of the same signal which go through different pathes with different distances larger than that of the direct path resulting in power strengths and phases other than

those of the direct path. The effect of these phenomena changes the power of the received signal in different ways. There are two general aspects of such power variations. The first aspect is the large scale effect known as attenuation or large scale fading. This refers to power reductions which, e.g., depends on the distance between transmitter and receiver.

The other aspect, known as small scale fading or generally fading, is the rapid variation in the power of the signal over short distance due to the interference of the multiple signals from several different pathes between the transmitter and the receiver which arrive at the receiver at slightly different time [95].

In a simplified model, considering a number of L_t dominant discrete scatters, the multi-path channel can be modeled as a linear time varying system with the following analog baseband input-output relation [95]:

$$y(t) = \sum_{l=1}^{L_t} h_l(t)x(t-l) + n(t) \tag{2.1}$$

where $y(t)$, $h_l(t)$, $x(t)$, $n(t)$, L_t and t denote the received signal, the complex channel gain corresponding to the lth propagation path, the transmitted signal, the additive white Gaussian receiver noise, the total number of channel taps, and the continuous time, respectively. Multi-path effects lead to different path delays associated with each propagation path. This causes inter-symbol interference (ISI). Wireless channels are function of frequency, time, and space. Generally, a wireless communication channel is selective when it varies as a function of frequency, time, or space.

- Time selectivity: This effect is referred to the *coherence time*, defined as the duration of time in which the channel impulse response is effectively invariant [19, 95]. Equivalently, it can be characterized by the *Doppler spread*, defined as the inverse of the *coherence time*.

- Frequency selectivity: This effect is referred to the *delay spread*, which is defined as the difference between the longest and shortest path propagation

delay [19, 95]. Equivalently, it can be characterized by the *coherence bandwidth* of the channel, defined as the inverse of the *delay spread*. A fading channel is said to be *frequency selective* when the *coherence bandwidth* of the channel is comparable or less than the bandwidth of the transmitted signal, equivalently, the *delay spread* is comparable or larger than the symbol duration. Otherwise the fading channel is said to be *frequency flat* or just *flat*.

- Spatial selectivity: This effect can be characterized by the *angular spread* and means that the received signal amplitude depends on the spatial location of the antenna. *Angular spread* at the receive antennas refers to the spread of angles of arrival of the multi-paths at the antenna. Spatial selectivity is referred to the *spatial coherence*, defined as the spatial displacement of the receiver in which the channel does not change. The larger the angle spread, the shorter the *spatial coherence*. This means that *spatial coherence* represents the maximum spatial separation for which the channel responses at two antennas remain strongly correlated.

In this work, we model the fading channel as [8, 19, 95]:

- Flat fading: The *coherence bandwidth* of the channel is much larger than the bandwidth of the signal, i.e. there is no interference between symbols transmitted at different time intervals. In contrast, frequency selective channel has ISI and will not be considered in this work.

- Slow fading: The signal duration is much smaller than the *coherence time* of the channel, i.e. the channel response does not vary over one block of communication. This means that during one time interval, the channel can be treated as constant. On other hand, we consider a scattering-rich environment due to a large number of independent reflected and scattered pathes arriving from many different directions.

The input-output relation for a linear flat fading channel is given by [19, 95]:

$$y = hx + n \tag{2.2}$$

where h denotes the channel coefficient between the transmitter and the receiver, n denotes the additive white Gaussian receiver noise with zero mean and with probability density function (pdf) $\mathcal{CN}(0, \sigma^2)$ where σ^2 is the noise variance.

The following simplified fading models are often used in the analysis of wireless communications systems.

- *Rayleigh* fading: The direct link between the transmitter and receiver is known as the line-of-side (LOS) path and does not exist when a large object obstructs the path between them. Usually, the strongest and dominant signal is the one received through the LOS path. In flat fading channel, when there is no LOS path between the transmitter and the receiver, the channel is zero-mean circular symmetric complex Gaussian with the pdf $\mathcal{CN}(0, \sigma_h^2)$. Due to a large number of independent reflected and scattered pathes, each channel coefficient is the sum of two terms, *in phase* and *quadrature*. Those terms denote the real and the imaginary part of the channel coefficient and can be modeled as independent and identical distributed zero-mean Gaussian random variables. In this case, the envelope $|h|$ follows a *Rayleigh* distribution. The probability density function of the *Rayleigh* distribution is given by [8, 19, 95]:

$$f_{|h|}(a) = \begin{cases} \frac{a}{\sigma_h^2} e^{\frac{-a^2}{2\sigma_h^2}}, & a \geq 0 \\ 0, & a < 0 \end{cases} \tag{2.3}$$

  where $|\cdot|$ denotes the absolute value.

- *Rician* fading: In addition to random multi-path components, when the direct link between the transmitter and the receiver is significant, the channel coefficient has the pdf $\mathcal{CN}(\mu_h, \sigma_h^2)$ where μ_h and σ_h denote the channel mean

and the channel variance, respectively. The envelope $|h|$ follows a *Rician* distribution. The probability density function of the *Rician* distribution is given by [8, 19, 95]:

$$f_{|h|}(a) = \begin{cases} \frac{a}{\sigma_h^2} e^{\frac{-\left(|a|^2+|\mu_h|^2\right)}{2\sigma_h^2}} I_o(\frac{|a\mu_h|}{\sigma_h^2}), & a \geq 0 \\ 0, & a < 0 \end{cases} \tag{2.4}$$

2.2 Multi-antenna Communications and Spatial Diversity Techniques

The use of diversity techniques is practical, effective, and widely applied in most scattering environment to improve the reliability and throughput of the wireless networks by receiving more than one independently faded replica of the transmitted signal [8, 19, 95]. The diversity techniques can be classified as frequency diversity, due to transmitting the same signal simultaneously in different frequency bandwidth, time diversity, due to transmitting the same signal repeatedly in different time slots, and spatial diversity, due to transmitting and receiving the same signal using multiple antennas.

Spatial diversity techniques improve the error performance and the data rate of the wireless networks at no additional costs for frequency bandwidth or transmitted power [19, 95]. Basically, these techniques can be classified into *receive and transmit diversity*. *Receive diversity* techniques use several antennas at receiver side [8, 19, 95]. Fig. 2.2 shows a simple scenario, known as *single-input multi-output* (SIMO) system, using one transmitter and M_r receive antennas. These techniques are simple to implement, since they do not require special coding methods where the same information signal transmitted over one antenna is received by M_r antennas. Receiving multiple faded signals from different pathes between the receive and transmit antennas provides a significant diversity gain over conventional single-antenna systems.

Transmit diversity techniques use several antennas at transmitter side [8, 19, 95]. Fig. 2.3 shows a simple scenario, known as *multi-input single-output* (MISO)

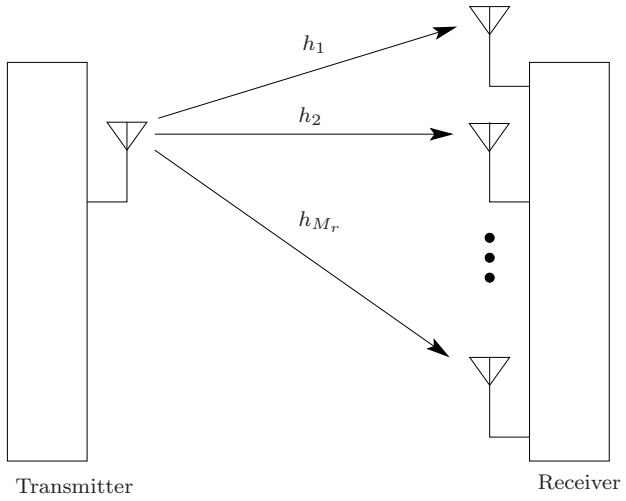

Figure 2.2: SIMO communication system.

system, using M_t transmit antennas and one receiver.

The use of multiple-antenna techniques is an efficient way to make wireless communication systems more robust and increase the achievable data rate at no additional costs for bandwidth or transmitted power. These techniques are mainly based on the theoretical work proposed by Foschini [1] and Teletar [2]. They have proved that multiple-antenna systems have a significantly higher capacity than single-antenna systems.

Consider a *multiple-input multiple-output* (MIMO) system with M_t transmit and M_r receive antennas as shown in Fig. 2.4. For simplicity, we consider only flat fading, i.e., the fading is not frequency selective and the channel coherence time significantly exceeds the symbol duration. A stream of bits is first mapped onto complex symbols. Afterwards, the symbols are passed to the transmitter which encodes them into the transmitted signal vector $\mathbf{x} = [x_1,\ x_2,\ \cdots,\ x_{M_t}]$.

When a signal x_j is transmitted from the jth transmit antenna, each of the M_r receive antennas sees a complex-weighted version of the transmitted signal. The signal at the ith receive antenna is $\sum_{j=1}^{M_t} h_{ij}\ x_j + n_i$ where h_{ij} denotes the CSI between the jth transmit antenna and the ith receive antenna and n_i denotes the

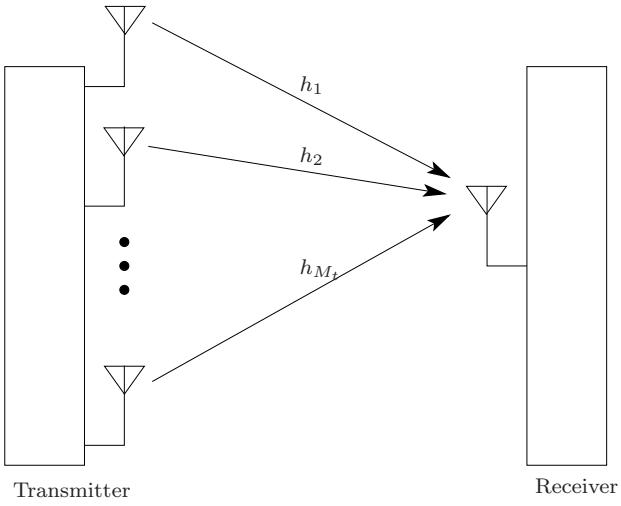

Figure 2.3: MISO communication system.

noise at the ith receive antenna. We denote the MIMO channel which describes the input-output relation of the MIMO system in a matrix notation as:

$$\mathbf{H} = \begin{bmatrix} h_{11} & h_{12} & \cdots & h_{1M_r} \\ h_{21} & h_{22} & \cdots & h_{2M_r} \\ \vdots & \vdots & \ddots & \vdots \\ h_{M_t1} & h_{M_t2} & \cdots & h_{M_tM_r} \end{bmatrix}. \tag{2.5}$$

If a signal vector $\mathbf{x}$ is transmitted from the transmit antenna array where x_j transmitted from the jth transmit antenna, then the signal at the receive antennas can be expressed as:

$$\mathbf{y} = \mathbf{x}\,\mathbf{H} + \mathbf{n} \tag{2.6}$$

where

$$\mathbf{y} = [y_1,\ y_2, \cdots,\ y_{M_r}], \tag{2.7}$$

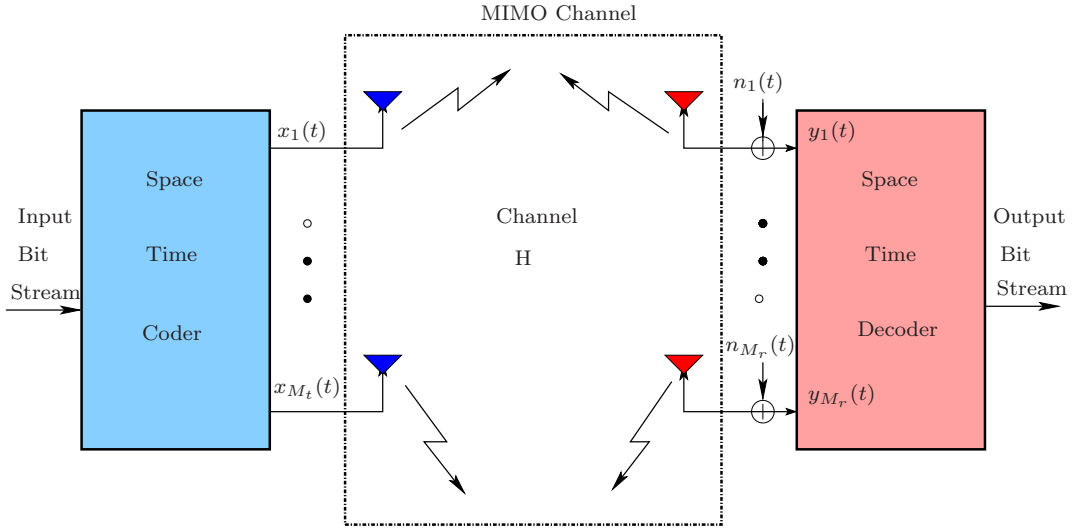

Figure 2.4: MIMO system with M_t transmit antennas and M_r receive antennas.

$$\mathbf{x} = [x_1,\ x_2, \cdots,\ x_{M_t}], \tag{2.8}$$

$$\mathbf{n} = [n_1,\ n_2, \cdots,\ n_{M_r}], \tag{2.9}$$

$(\cdot)^T$ denotes the transpose of a matrix and $\mathbf{n}$ denotes the noise vector which is modeled as independent, zero-mean, complex Gaussian random variables with unit variance. This model is popularly referred to as independent and identical distributed (i.i.d) Gaussian MIMO channel [8, 19, 95]. The channel matrix in (2.5) can be considered as a snapshot of the wireless channel at a certain frequency and at a specific instant of time. When there is a large delay spread, $\mathbf{H}$ is a function of frequency. Similarly, when there is a large Doppler spread caused by mobility, $\mathbf{H}$ is a function of time. When the channel $\mathbf{H}$ is Rayleigh fading and fully known at the receiver, the MIMO channel capacity at high SNRs increases approximately linearly with the minimum number of transmit and receive antennas in the presence of a scattering-rich environment [19, 95].

We can assume that the CSI remains constant during T time slots and change independently afterward where this assumption is known as block fading and used in STC techniques. The input-output relation of the MIMO system, after stacking T subsequent vectors of (2.6) into matrices, can be expressed as [10]:

$$\mathbf{Y} = \mathbf{X}\mathbf{H} + \mathbf{N} \tag{2.10}$$

where

$$\mathbf{Y} = \begin{bmatrix} \mathbf{y}(1) \\ \mathbf{y}(2) \\ \vdots \\ \mathbf{y}(T) \end{bmatrix} \tag{2.11}$$

denotes the $T \times M_r$ complex matrix of the received signals, $\mathbf{y}(i)$ denotes the $1 \times M_r$ signal vector received in the ith time slot,

$$\mathbf{X} = \begin{bmatrix} \mathbf{x}(1) \\ \mathbf{x}(2) \\ \vdots \\ \mathbf{x}(T) \end{bmatrix} \tag{2.12}$$

denotes the $T \times M_t$ complex matrix of the transmitted signals, which is known as the space-time coding matrix, $\mathbf{x}(i)$ denotes the $1 \times M_t$ signal vector transmitted over the ith time slot,

$$\mathbf{N} = \begin{bmatrix} \mathbf{n}(1) \\ \mathbf{n}(2) \\ \vdots \\ \mathbf{n}(T) \end{bmatrix} \tag{2.13}$$

denotes the $T \times M_r$ complex white Gaussian noise matrix, and $\mathbf{n}(i)$ denotes the $1 \times M_r$ received noise vector at the ith time slot.

2.3 Space-Time Block Codes

The first and remarkable STBC scheme for transmission using two transmit antennas was introduced by Alamouti in [12]. This scheme is then generalized for any number of transmit antennas by Tarokh in the form of STBCs [10]. In STBCs, the input data is grouped into blocks, each block is used to produce a space-time coding matrix where its rows represent the time and its columns represent the transmit antennas. This matrix is then transmitted row by row where the M_t signals of each row are simultaneously transmitted using M_t transmit antennas. At the receiver, the received symbols can be decoded using a maximum-likelihood (ML) decoder.

The rate R_d of STBCs, which describes their bandwidth efficiency, is defined as the ratio of the number of transmitted information symbols L in each block to the length of the block T. The length of the block, known as the decoding delay, is defined as the signaling intervals needed to transmit the block.

2.3.1 Alamouti Code

In *Alamouti scheme*, the symbol stream is grouped into blocks of length two, each block is converted from serial to parallel to give two parallel signals, at a given time slot. Two signals are transmitted simultaneously from the two antennas where the first signal x_1 is transmitted from the first antenna and the second signal x_2 is transmitted from the second antenna. In the next time slot, $-{x_2}^*$ is transmitted from the first antenna and ${x_1}^*$ is transmitted from the second antenna where $(\cdot)^*$ denotes the complex conjugate. Let us assume that the CSI is constant during two consecutive time slots. In the first and second time slot, the received signals are given by:

$$y_1 = h_1 x_1 + h_2 x_2 + n_1, \tag{2.14}$$

$$y_2 = -h_1 {x_2}^* + h_2 {x_1}^* + n_2, \tag{2.15}$$

respectively, where h_i, $i = 1, 2$, denotes the channel coefficient from the ith transmit antenna to the receive antenna, and n_1 and n_2 denote the noise signals during the first and second time slot, respectively. In a matrix form, (2.14) and (2.15) can be written as:

$$\mathbf{y} = \mathbf{X}\ \mathbf{h} + \mathbf{n} \tag{2.16}$$

where $\mathbf{y} = [y_1,\ y_2]^T$, $\mathbf{h} = [h_1,\ h_2]^T$, $\mathbf{n} = [n_1,\ n_2]^T$ and $\mathbf{X}$, known as the space-time coding matrix, is given by:

$$\mathbf{X} = \begin{bmatrix} x_1 & x_2 \\ -{x_2}^* & {x_1}^* \end{bmatrix}. \tag{2.17}$$

The rate of this scheme is $R_d = \frac{L}{T} = 1$, where L denotes the number of symbols contained in the space-time coding matrix. Since the columns of $\mathbf{X}$ are orthogonal to each other, this design is called OSTBC. A STBC is said to be a full-diversity OSTBC if

$$\mathbf{X}^H\mathbf{X} = ||\mathbf{x}||^2\mathbf{I}_{M_t} \tag{2.18}$$

where $\mathbf{I}_{M_t}$ and $||\cdot||$ denote the $M_t \times M_t$ identity matrix and the Euclidean norm, respectively.

2.3.2 Orthogonal Space-Time Block Codes

The Alamouti scheme achieves full rate and full diversity using two transmit antennas with a simple ML decoding algorithm [12]. This scheme constructed for two transmit antennas has been a basis to create OSTBCs for more than two transmit antennas. First, a generalization to an arbitrary number of transmit antennas was introduced in [11] where OSTBCs guarantee that the ML detection of the transmitted symbols is decoupled and the transmission scheme achieves a diversity order equal to $M_r \times M_t$ (full diversity). In other words, these schemes achieve full diversity and at the same time enjoy a low decoding complexity.

OSTBCs can be classified into real and complex OSTBCs constructed from

real and complex orthogonal design, respectively [58]. In the real orthogonal design, the transmitted symbols are taken from a real signal constellation such as pulse amplitude modulation (PAM) while the transmitted symbols in the complex orthogonal design are taken from a complex signal constellation such as phase shift keying (PSK) or quadrature amplitude modulation (QAM).

2.3.2.1 Real Orthogonal Codes

Any full-rate full-diversity OSTBC using M_t transmit antennas and T symbol periods is described by a $T \times M_t$ orthogonal transmission matrix $\mathbf{X}$ with real entries which are linear functions of the symbols $x_i,\ i = 1, ..., L$. The transmission matrix $\mathbf{X}$ has the following unitarity property:

$$\mathbf{X}^T\mathbf{X} = (x_1^2 + x_2^2 + \cdots + x_L^2)\ \mathbf{I}_{M_t}. \tag{2.19}$$

The jth column of $\mathbf{X}$ represents the symbols transmitted from the jth transmit antenna while the ith row of $\mathbf{X}$ represents the symbols transmitted in the ith time slot. The transmission rate of a STBC is defined to be the average number of data symbols transmitted per time slot, or simply $R_d = L/T$. A STBC is full rate if $L = T$. For an arbitrary real signal constellation, it has been shown in [11] that a full-rate full-diversity real OSTBC exists for more than one transmit antenna. An example of the real orthogonal designs for two and four transmit antennas is given by:

$$\mathbf{X}_2 = \begin{bmatrix} x_1 & x_2 \\ -x_2 & x_1 \end{bmatrix}, \tag{2.20}$$

$$\mathbf{X}_4 = \begin{bmatrix} x_1 & x_2 & x_3 & x_4 \\ -x_2 & x_1 & -x_4 & x_3 \\ -x_3 & x_4 & x_1 & -x_2 \\ -x_4 & -x_3 & x_2 & x_1 \end{bmatrix}, \tag{2.21}$$

respectively. Clearly from (2.21), the columns of the matrix $\mathbf{X}_4$ are orthogonal to each other which enables us to achieve full diversity and at the same time to use a low complexity decoder at the receiver side. The decoding delay T represents

the memory requirements which should be minimized. In [11], a generalized real orthogonal delay-optimal design with full rate and full diversity was introduced. An example of this design for three transmit antennas ($M_t = 3$) is given by:

$$\mathbf{X}_3 = \begin{bmatrix} x_1 & x_2 & x_3 \\ -x_2 & x_1 & -x_4 \\ -x_3 & x_4 & x_1 \\ -x_4 & -x_3 & x_2 \end{bmatrix}. \tag{2.22}$$

2.3.2.2 Complex Orthogonal Codes

A full-rate full-diversity complex orthogonal design using M_t transmit antennas is described by a $T \times M_t$ orthogonal matrix $\mathbf{X}$ with complex entries which are linear functions of the symbols $x_i,\ i = 1, \cdots, L$ and their conjugates $x_i^*,\ i = 1, \cdots, L$ such that

$$\mathbf{X}^H\mathbf{X} = \left(|x_1|^2 + |x_2|^2 + \cdots + |x_L|^2\right) \mathbf{I}_{M_t} \tag{2.23}$$

where $(\cdot)^H$ denotes the Hermitian transpose. A full-rate full-diversity complex orthogonal design using M_t transmit antennas exists if and only if $M_t = 2$ [11]. An example for this design is given by:

$$\mathbf{X}_2 = \begin{bmatrix} x_1 & x_2 \\ -x_2^* & x_1^* \end{bmatrix} \tag{2.24}$$

which is the same matrix used in the Alamouti scheme. For an arbitrary number of transmit antennas and any complex signal constellation, there are OSTBCs that can achieve a rate of $\frac{1}{2}$ with a non-square transmission matrix. Any of these OSTBCs is a $T \times M_t$ matrix with complex entries which are linear functions of the symbols x_i, x_i^*, $i = 1, \ldots, L$, and 0 such that

$$\mathbf{X}^H\mathbf{X} = \left(|x_1|^2 + |x_2|^2 + \cdots + |x_L|^2\right) \mathbf{I}_{M_t}. \tag{2.25}$$

The authors in [11] proved that there is a rate-$\frac{1}{2}$ complex orthogonal design for more than two transmit antennas. For example, OSTBCs with a rate of $\frac{1}{2}$ symbol

per time slot for three and four transmit antennas are given by:

$$\mathbf{X}_3 = \begin{bmatrix} x_1 & x_2 & x_3 \\ -x_2 & x_1 & -x_4 \\ -x_3 & x_4 & x_1 \\ -x_4 & -x_3 & x_2 \\ x_1^* & x_2^* & x_3^* \\ -x_2^* & x_1^* & -x_4^* \\ -x_3^* & x_4^* & x_1^* \\ -x_4^* & -x_3^* & x_2^* \end{bmatrix}, \tag{2.26}$$

$$\mathbf{X}_4 = \begin{bmatrix} x_1 & x_2 & x_3 & x_4 \\ -x_2 & x_1 & -x_4 & x_3 \\ -x_3 & x_4 & x_1 & -x_2 \\ -x_4 & -x_3 & x_2 & x_1 \\ x_1^* & x_2^* & x_3^* & x_4^* \\ -x_2^* & x_1^* & -x_4^* & x_3^* \\ -x_3^* & x_4^* & x_1^* & -x_2^* \\ -x_4^* & -x_3^* & x_2^* & x_1^* \end{bmatrix}, \tag{2.27}$$

respectively. For rates grater than $\frac{1}{2}$, the authors in [11] construct rate-$\frac{3}{4}$ codes for three and four transmit antennas using scaled combinations of the transmitted symbols. For example, rate-$\frac{3}{4}$ full-diversity OSTBCs for three and four transmit antennas are given by:

$$\mathbf{X}_3 = \begin{bmatrix} x_1^* & x_2^* & \frac{x_3}{\sqrt{2}} \\ -x_2^* & x_1^* & \frac{x_3}{\sqrt{2}} \\ \frac{x_3^*}{\sqrt{2}} & \frac{x_3^*}{\sqrt{2}} & \frac{x_1 - x_1^* + x_2 - x_2^*}{2} \\ \frac{x_3^*}{\sqrt{2}} & -\frac{x_3^*}{\sqrt{2}} & \frac{x_1 - x_1^* + x_2 + x_2^*}{2} \end{bmatrix}, \tag{2.28}$$

$$\mathbf{X}_4 = \begin{bmatrix} x_1^* & x_2^* & \frac{x_3}{\sqrt{2}} & \frac{x_3}{\sqrt{2}} \\ -x_2^* & x_1^* & \frac{x_3}{\sqrt{2}} & -\frac{x_3}{\sqrt{2}} \\ \frac{x_3^*}{\sqrt{2}} & \frac{x_3^*}{\sqrt{2}} & \frac{x_1 - x_1^* + x_2 - x_2^*}{2} & \frac{x_1 - x_1^* + x_2 - x_2^*}{2} \\ \frac{x_3^*}{\sqrt{2}} & -\frac{x_3^*}{\sqrt{2}} & \frac{x_1 - x_1^* + x_2 + x_2^*}{2} & -\frac{(x_1 + x_1^* + x_2 - x_2^*)}{2} \end{bmatrix}, \tag{2.29}$$

respectively. In (2.28), three complex symbols are transmitted via three transmit antennas in four time slots resulting in a transmission rate of $\frac{3}{4}$ as shown in the transmission matrix $\mathbf{X}_3$. In (2.29), three complex symbols are transmitted via four transmit antennas in four time slots, therefore, the symbol rate is $\frac{3}{4}$ as well. The designs in (2.28) and (2.29) have been simplified as:

$$\mathbf{X}_3 = \begin{bmatrix} x_1 & x_2 & x_3 \\ -x_2^* & x_1^* & 0 \\ -x_3^* & 0 & x_1^* \\ 0 & x_3^* & -x_2^* \end{bmatrix}, \tag{2.30}$$

$$\mathbf{X}_4 = \begin{bmatrix} x_1 & x_2 & x_3 & 0 \\ -x_2^* & x_1^* & 0 & -x_3 \\ -x_3^* & 0 & x_1^* & x_2 \\ 0 & x_3^* & -x_2^* & x_1 \end{bmatrix}, \tag{2.31}$$

respectively. OSTBCs have been proposed to provide full-diversity with a low (linear) ML decoding complexity [10–12]. Therefore, an efficient choice of $\mathbf{X}$ is the OSTBCs. However, there is no full-rate full-diversity complex OSTBC for more than two transmit antennas. QOSTBCs for more than two transmit antennas have been proposed to overcome the low-rate limitation of OSTBCs [54–56]. Unfortunately, the price for an improved rate is that the QOSTBCs have a substantially higher ML decoding complexity than that of the OSTBCs. The QOSTBCs are described in more detail in chapter three.

In the last decade, several STBCs with a lower ML decoding complexity than that of the standard QOSTBCs have been proposed in [97–100]. However, their improvements in decoding complexity come at the expense of a substantial BER performance loss as compared to the QOSTBCs [98, 100].

In Fig. 2.5, the BER is displayed versus the SNR for different number of transmit antennas and one receive antenna. We have assumed independent Rayleigh flat-fading channels. The OSTBC in (2.27) for four transmit antennas using QPSK modulation is compared with the OSTBC in (2.26) for three transmit antennas using QPSK modulation, the OSTBC in (2.22) for three transmit antennas using BPSK modulation, the OSTBC in (2.21) for four transmit antennas using BPSK modulation, the Alamouti code in (2.20) for two transmit antennas using BPSK modulation, and the conventional single-transmit antenna system using BPSK modulation. From Fig. 2.5, it can be observed that the diversity order increases linearly with the increase of the transmit antennas where the diversity order is given by [108]:

$$-\lim_{\mathrm{SNR}\to\infty}\frac{\log(\mathrm{BER})}{\log(\mathrm{SNR})} \tag{2.32}$$

where the SNR denotes the ratio of the transmitted signal power to the noise power. From Fig. 2.5, the diversity order is almost equal to one using one transmit antenna while the diversity order of two, three, and four can be achieved using two, three, and four transmit antennas, respectively. From Fig. 2.5, it can be observed that for a system with a large number of transmit antennas, a high diversity order can be achieved where the BER curve becomes almost vertical at high SNR. This means that the improvement in the error performance achieved by adding more transmit antennas to a system with a large number of transmit antennas is insignificant.

2.3.3 Differential Space-Time Block Codes

In the non-coherent receiver case, a differential STBC can be employed to transmit the information symbols to the receiver. We illustrate the application of the STC strategy to the non-coherent receiver by means of the following example which describes a differential transmission for two transmit antennas using the distributed Alamouti code [12, 67].

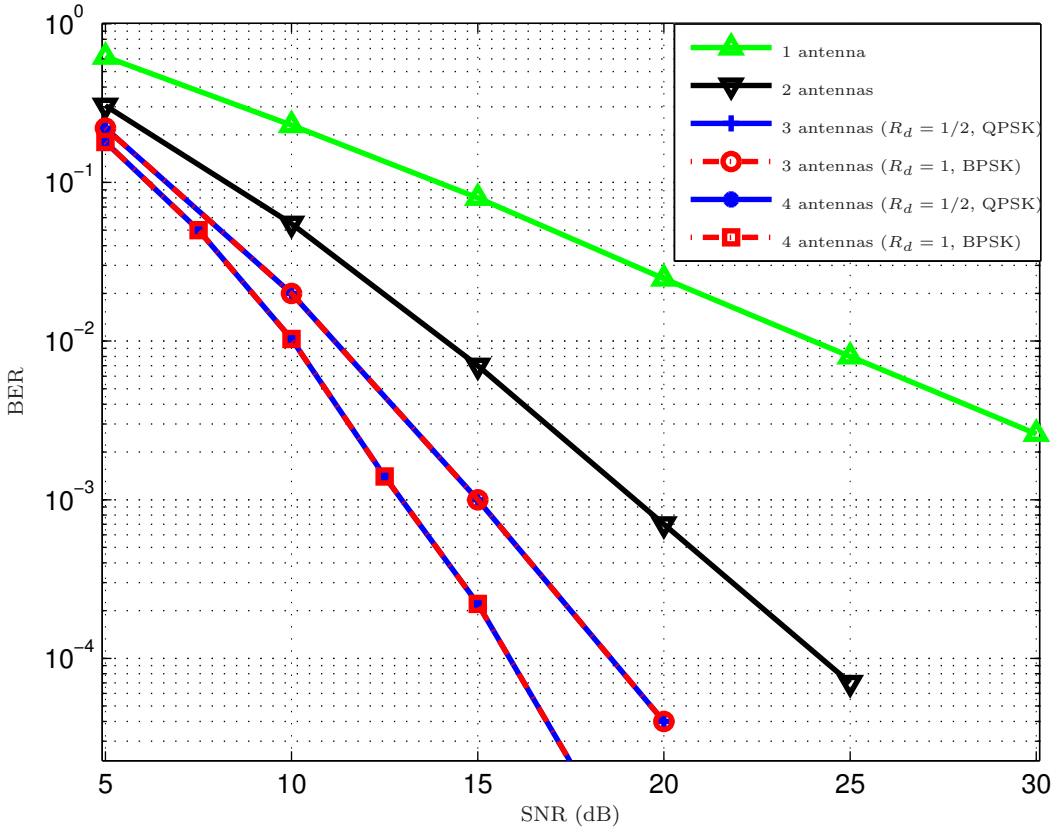

Figure 2.5: BER versus SNR for the coherent OSTBCs using different numbers of transmit antennas and one receive antenna.

Extension to the case of $M_t > 2$ is straightforward where any OSTBC whose transmitted symbols drawn from a M-PSK constellation can be used directly in the differential encoding scheme. We assume that neither the transmitter nor the receiver has CSI. In contrast to (2.16), we consider the transmission of two consecutive blocks, (k) and $(k-1)$, where the $(k-1)$th block is a reference for the decoding of the kth block. The superscripts $(\cdot)^{(k)}$ and $(\cdot)^{(k-1)}$ stand for the block indices. The transmitter sends $\mathbf{X}^{(k)}$ over the kth block where $\mathbf{X}^{(0)} = \mathbf{I}_2$,

$$\mathbf{U}^{(k)} \triangleq \begin{bmatrix} s_1^{(k)} & s_2^{(k)} \\ -\left(s_2^{(k)}\right)^* & \left(s_1^{(k)}\right)^* \end{bmatrix}, \tag{2.33}$$

$$\begin{aligned} \mathbf{X}^{(k)} &\triangleq \mathbf{U}^{(k)}\mathbf{X}^{(k-1)}, \\ &\triangleq \begin{bmatrix} s_1^{(k)}x_1^{(k-1)} - s_2^{(k)}\left(x_2^{(k-1)}\right)^* & s_2^{(k)}\left(x_1^{(k)}\right)^* + s_1^{(k)}x_2^{(k-1)} \\ -\left(s_2^{(k)}\left(x_1^{(k)}\right)^* + s_1^{(k)}x_2^{(k-1)}\right)^* & \left(s_1^{(k)}x_1^{(k-1)} - s_2^{(k)}\left(x_2^{(k-1)}\right)^*\right)^* \end{bmatrix} \\ &\triangleq \begin{bmatrix} x_1^{(k)} & x_2^{(k)} \\ -\left(x_2^{(k)}\right)^* & \left(x_1^{(k)}\right)^* \end{bmatrix} \end{aligned} \tag{2.34}$$

where $s_1^{(k)}$ and $s_2^{(k)}$ denote the information symbols of the kth transmission block which are taken from a M-PSK constellation and $x_1^{(k)}$ and $x_2^{(k)}$ denote the transmitted symbols of the kth transmission block. Throughout this thesis, we assume that $\mathrm{E}\left\{|s_i^{(k)}|^2\right\} = 1$ and $\mathrm{E}\left\{|x_i^{(k)}|^2\right\} = 1$, $\forall i$. From (2.33) and (2.34), it can be observed that $(\mathbf{U}^{(k)})^H\mathbf{U}^{(k)} = (\mathbf{X}^{(k)})^H\mathbf{X}^{(k)}$ where $(\cdot)^H$ stands for the Hermitian transpose. The received signal vectors at the blocks $(k-1)$ and (k) are given by:

$$\mathbf{y}^{(k-1)} = \mathbf{X}^{(k-1)}\mathbf{h} + \mathbf{n}^{(k-1)}, \tag{2.35}$$

$$\begin{aligned} \mathbf{y}^{(k)} &= \mathbf{X}^{(k)}\mathbf{h} + \mathbf{n}^{(k)} \\ &= \mathbf{U}^{(k)}\mathbf{X}^{(k-1)}\mathbf{h} + \mathbf{n}^{(k)} \\ &= \mathbf{U}^{(k)}\mathbf{y}^{(k-1)} - \mathbf{U}^{(k)}\mathbf{n}^{(k-1)} + \mathbf{n}^{(k)} \end{aligned} \tag{2.36}$$

where $\mathbf{y}^{(k)} = [y_1^{(k)},\ y_2^{(k)}]^T$, $\mathbf{h} = [h_1,\ h_2]^T$, and $\mathbf{n}^{(k)} = [n_1^{(k)},\ n_2^{(k)}]^T$, respectively. The ML decoder finds the matrix $\mathbf{U}$ that minimizes the following cost function

$$f_{ML}(\mathbf{U}) = \min \left|\left|\mathbf{y}^{(k)} - \mathbf{U}\mathbf{y}^{(k-1)}\right|\right|^2 \tag{2.37}$$

Due to orthogonality of the OSTBCs, a symbol-wise decoder can be used to decode the symbols at the receiver. The ML decoder is described in more detail in Sec. 2.3.4. The difference in error performance between the coherent and differential schemes is around 3 dB due to the noise term $\mathbf{U}^{(k)}\mathbf{n}^{(k-1)}$ in (2.36). The 3 dB loss in error performance can be explained by the absence of perfect CSI at the receiver [19].

2.3.4 Maximum-likelihood Decoding for Space-Time Block codes

For the sake of simplicity, the case of one receive antenna will be considered. Extension to the case of $M_r > 1$ is straightforward. The coherent ML decoder finds the space-time coding matrix $\mathbf{X}$ that minimizes the following cost function

$$f_{ML}(\mathbf{X}) = \min \left|\left|\mathbf{y} - \mathbf{X}\mathbf{h}\right|\right|^2 \tag{2.38}$$

where $\mathbf{y} = [y_1, \cdots, y_T]^T$, $\mathbf{h} = [h_1, \cdots, h_{M_t}]^T$, and $\mathbf{X}$ denotes the $T \times M_t$ space-time coding matrix of the real transmitted signals. Expanding (2.38), we obtain

$$\begin{aligned} f_{ML}(\mathbf{X}) &= \mathbf{h}^H\mathbf{X}^H\mathbf{X}\mathbf{h} - 2\Re\{\mathbf{y}^H\mathbf{X}\mathbf{h}\} + c \\ &= \mathbf{x}^H\check{\mathbf{H}}^H\check{\mathbf{H}}\mathbf{x} - 2\Re\{\mathbf{r}\mathbf{x}\} + c \end{aligned} \tag{2.39}$$

where c is a constant term that does not depend on the symbols, $\mathbf{r} = \mathbf{y}^H\check{\mathbf{H}} = [r_1, \cdots, r_L]$, $\mathbf{X}\mathbf{h} = \check{\mathbf{H}}\mathbf{x}$, $\mathbf{x} = [x_1, \cdots, x_L]^T$, $\check{\mathbf{H}}$ denotes the $T \times L$ channel matrix, and $\Re\{\cdot\}$ denotes the real part. To decode the STBC symbols, the ML decoder finds the vector $\mathbf{x}$ that minimizes the cost function (2.39) over all possible combinations of symbol vectors. In this context, the concept of the so called *vector-wise-decoder* has been established. The complexity of the *vector-wise-decoder* increases exponentially with the increase of the constellation size or the symbol-vector length.

In the case of OSTBCs, we can consider the fact that $\mathbf{X}^H\mathbf{X} = \sum_{i=1}^{L} |x_i|^2 \mathbf{I}_{M_t}$. Then, (2.39) can be expressed as:

$$f_{ML}(\mathbf{X}) = ||\mathbf{x}||^2||\mathbf{h}||^2 - 2\Re\{\mathbf{rx}\} + c \tag{2.40}$$

The cost function in (2.40), which can be written as $\sum_{i=1}^{L} f(x_i) + c$, is a linear combination of x_i and $|x_i|^2$, $i = 1, \cdots, L$, and equivalent to L independent cost functions where

$$f(x_i) = |x_i|^2||\mathbf{h}||^2 - 2\Re\{x_i r_i\}. \tag{2.41}$$

Therefore, the ML decoder for the OSTBCs operates by separating the symbols and detecting them symbol-by-symbol. In this context, the concept of *symbol-wise-decoder* has been established.

2.3.5 Design Criteria for Space-Time Block Codes

In order to design space-time block codes, there are several different design criteria that guarantee the maximum possible diversity and coding gain at high SNRs. The pair-wise error probability (PEP) of transmitting $\mathbf{X}$ and detecting an erroneous $\tilde{\mathbf{X}}$, $P(\mathbf{X}, \tilde{\mathbf{X}})$, has been studied in [9, 19]. Two different design criteria were proposed at high SNRs:

- Rank criterion: This criterion says that the minimum rank of the error matrix $(\mathbf{X} - \tilde{\mathbf{X}})$ over all pairs of distinct code matrices has to be large [19]. In order to obtain full diversity, the error matrix $(\mathbf{X} - \tilde{\mathbf{X}})$ has to be full rank.

- Determinant criterion: This criterion suggests that the minimum product of the eigenvalues different from zero of the error matrix $(\mathbf{X} - \tilde{\mathbf{X}})$ among all pairs of distinct code matrices has to be as large as possible to obtain high coding gain [19].

To check if the Alamouti scheme achieves full diversity, we need to show that the rank of all possible error matrices $\mathbf{D} = (\mathbf{X} - \tilde{\mathbf{X}})$ is equal to two for every

($\mathbf{X} \neq \tilde{\mathbf{X}}$). The Alamouti transmission matrix is given by:

$$\mathbf{X} = \begin{bmatrix} x_1 & x_2 \\ -x_2^* & x_1^* \end{bmatrix}. \tag{2.42}$$

Let us consider different symbols x_1', x_2' where the corresponding codeword is given by:

$$\tilde{\mathbf{X}} = \begin{bmatrix} x_1' & x_2' \\ -x_2'^* & x_1'^* \end{bmatrix}. \tag{2.43}$$

The error matrix $\mathbf{D}$ is expressed as:

$$\mathbf{D} = \begin{bmatrix} x_1 - x_1' & x_2 - x_2' \\ x_2'^* - x_2^* & x_1^* - x_1'^* \end{bmatrix}. \tag{2.44}$$

As in the rank criterion, the code can achieve full diversity, if the error matrix is full rank. The determinant of the error matrix $\mathbf{D}$ is given by:

$$\det(\mathbf{D}) = |x_1' - x_1|^2 + |x_2' - x_2|^2. \tag{2.45}$$

where $\det(\cdot)$ stands for the determinant. Clearly, $\det(\mathbf{D}) = 0$ if and only if $x_1' = x_1$ and $x_2' = x_2$ where this does not hold when ($\mathbf{X} \neq \tilde{\mathbf{X}}$). Therefore, $\mathbf{D}$ is always full rank and Alamouti scheme achieves full diversity.

2.4 Wireless Relay Networks

The use of multiple-antenna and STC techniques may not always be practical for certain applications due to hardware constraints like size, cost, complexity, and limitation in power. As a solution in face of these limitations, cooperative diversity which is another form of spatial diversity for relay channel has been proposed in [14, 15] as an alternative way to achieve similar diversity gain as in the conventional multiple-antenna systems.

In the last decade, DSTC techniques have received much attention as they can dramatically improve the error performance and the achievable data rate of wireless communication networks with a reasonable level of complexity and can achieve some of the benefits of conventional multi-antenna techniques.

2.4.1 Distributed Space-Time Coding for Wireless Relay Networks

DSTC is a cooperative strategy where one of the STC techniques is implemented using several relays located in a distributed manner between the source and destination as shown in Fig. 2.6. In DSTC techniques, source and relay nodes share their antennas to create a virtual transmit antenna array and then relays cooperate and encode the information signal using a STBC scheme. Each relay then sends a column of the block code towards the destination node. In this case, multiple single-antenna relays between two single-antenna users emulate a virtual array by processing and then retransmitting the information signal sent from source node to the destination node in the form of a space-time codeword. In other words, the idea of the DSTC techniques is to have multiple single-antenna relay nodes apply a simple operation on information signal they receive and implement a DSTC scheme over the virtual multiple-antenna system.

Similar to the conventional STC techniques in MIMO systems where transmit diversity is exploited without the availability of CSI at the transmitter, cooperation among relays in wireless communication system allows the relays to exploit transmit diversity without the need of CSI at the relays.

Consider a half-duplex wireless network, where each node can either transmit or receive but not both at the same time, consisting of one source node (S), one or more relay nodes ($\mathcal{R}_1, \mathcal{R}_2, \cdots, \mathcal{R}_R$), and one destination node (D) where each node is equipped with a single antenna as shown in Fig. 2.7. In this figure, we denote the source-to-rth relay, rth relay-to-destination, and source-to-destination channels by f_r, g_r, and f_o, respectively. We further assume independent flat fading

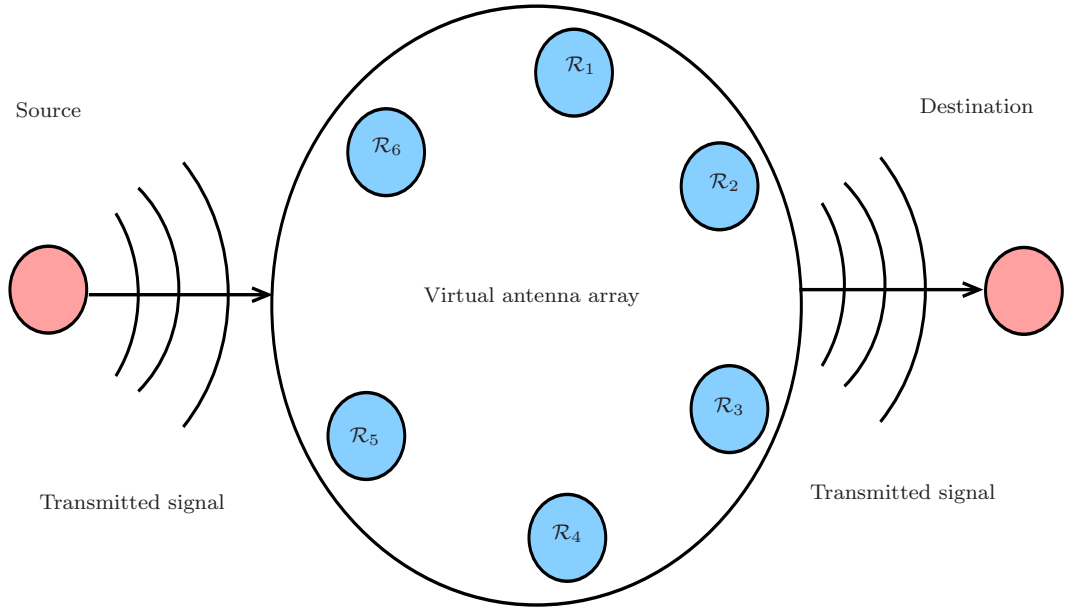

Figure 2.6: Virtual antenna array.

channels. During the first phase of transmission from time slot 1 to T, the source node transmits a vector $\mathbf{x} = [x_1, \cdots, x_T]^T$ to both the relays and destination node. Assuming that the CSI does not vary during $2T$ time slots, the received signal vector at the rth relay is given by:

$$\mathbf{y}_{\mathcal{R},r} = \sqrt{P_1} f_r \mathbf{x} + \mathbf{n}_{\mathcal{R},r} \tag{2.46}$$

and the received signal vector at the destination is given by:

$$\mathbf{y}_{dl} = \sqrt{P_1} f_o \mathbf{x} + \mathbf{n}_{dl} \tag{2.47}$$

where $\mathbf{n}_{\mathcal{R},r}$ and $\mathbf{n}_{dl}$ denote $T \times 1$ complex white Gaussian noise vectors at the rth relay and destination, respectively, and P_1 denote the average transmitted power at the source node. The rth relay then processes its received signal vector $\mathbf{y}_{\mathcal{R},r}$ to obtain the signal vector $\mathbf{x}_{\mathcal{R},r}$. In the second phase of transmission, from time $T+1$ to $2T$, the rth relay precodes the signal vector $\mathbf{x}_{\mathcal{R},r}$ or its conjugate with

the $T \times T$ matrix $\mathbf{A}_r$ and scales it before broadcasting it to the destination node. The received signal vector at the destination node is given by:

$$\mathbf{y} = \sum_{r=1}^{R} \sqrt{P_r} g_r \mathbf{A}_r \breve{\mathbf{x}}_{\mathcal{R},r} + \mathbf{n} \tag{2.48}$$

where either $\breve{\mathbf{x}}_{\mathcal{R},r} = \mathbf{x}_{\mathcal{R},r}$ or $\breve{\mathbf{x}}_{\mathcal{R},r} = \mathbf{x}^*_{\mathcal{R},r}$, $\mathbf{n}$ denotes $T \times 1$ complex white Gaussian noise vector at the destination, and P_r is the average transmitted power at rth relay. The selection of $\breve{\mathbf{x}}_{\mathcal{R},r}$ and $\mathbf{A}_r$ on each relay depends on the used DSTC scheme where any linear STCs can directly be applied to DSTC. For example, in case of the Alamouti code with two relay nodes, $\breve{\mathbf{x}}_{\mathcal{R},r}$ and $\mathbf{A}_r$ can be chosen as follows:

$$\mathbf{A}_1 = \begin{bmatrix} 1 & 0 \\ 0 & 1 \end{bmatrix}, \quad \mathbf{A}_2 = \begin{bmatrix} 0 & 1 \\ -1 & 0 \end{bmatrix},$$

$$\breve{\mathbf{x}}_{\mathcal{R},1} = \mathbf{x}_{\mathcal{R},1}, \quad \breve{\mathbf{x}}_{\mathcal{R},2} = \mathbf{x}^*_{\mathcal{R},2}.$$

Another example, in case of QOSTBCs with four relay nodes, $\breve{\mathbf{x}}_{\mathcal{R},r}$ and $\mathbf{A}_r$ can be chosen as follows:

$$\mathbf{A}_1 = \begin{bmatrix} 1 & 0 & 0 & 0 \\ 0 & 1 & 0 & 0 \\ 0 & 0 & 1 & 0 \\ 0 & 0 & 0 & 1 \end{bmatrix}, \qquad \mathbf{A}_2 = \begin{bmatrix} 0 & 1 & 0 & 0 \\ -1 & 0 & 0 & 0 \\ 0 & 0 & 0 & 1 \\ 0 & 0 & -1 & 0 \end{bmatrix},$$

$$\mathbf{A}_3 = \begin{bmatrix} 0 & 0 & 1 & 0 \\ 0 & 0 & 0 & 1 \\ -1 & 0 & 0 & 0 \\ 0 & -1 & 0 & 0 \end{bmatrix}, \quad \mathbf{A}_4 = \begin{bmatrix} 0 & 0 & 0 & 1 \\ 0 & 0 & -1 & 0 \\ 0 & -1 & 0 & 0 \\ 1 & 0 & 0 & 0 \end{bmatrix},$$

$$\breve{\mathbf{x}}_{\mathcal{R},1} = \mathbf{x}_{\mathcal{R},1}, \quad \breve{\mathbf{x}}_{\mathcal{R},2} = \mathbf{x}^*_{\mathcal{R},2}, \quad \breve{\mathbf{x}}_{\mathcal{R},3} = \mathbf{x}^*_{\mathcal{R},3}, \quad \breve{\mathbf{x}}_{\mathcal{R},4} = \mathbf{x}_{\mathcal{R},4}.$$

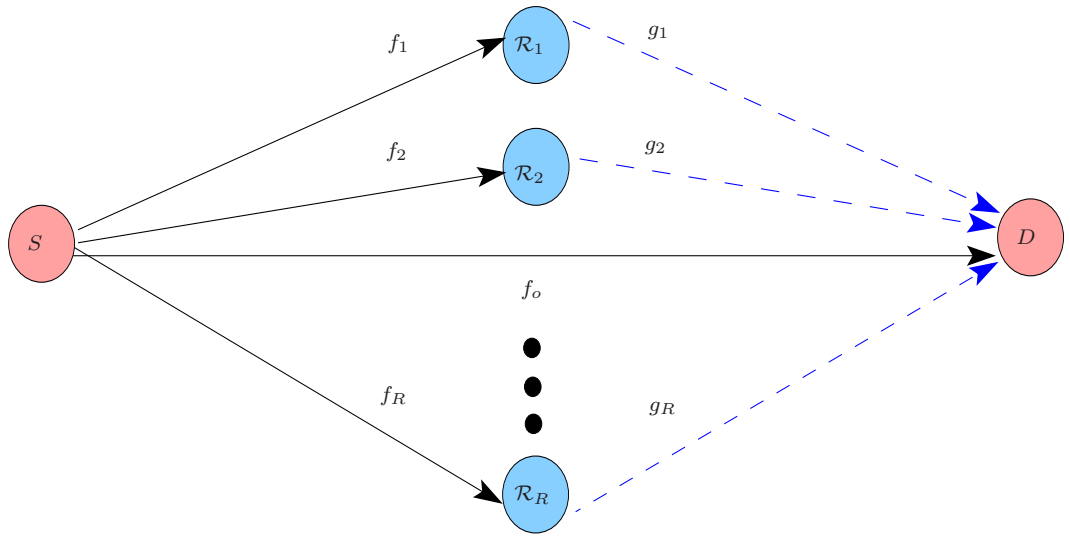

Figure 2.7: Wireless relay network with $R+2$ nodes.

Based on the role of the relays, different cooperative transmission protocols have been proposed to process the signal vector $\mathbf{y}_{\mathcal{R},r}$ at the rth relay [14–16]. Among them, the common protocols are

- The AF protocol: Each relay receives a noisy version of the information signal and then it simply amplifies and retransmits it.
- The DF protocol: Each relay decodes the symbols and then resends the estimates of the detected symbols.

2.4.2 Parallel and Serial Relay Networks

A parallel relay network consists of a source, a destination, and R relays as shown in Fig. 2.8 where f_r and g_r are the channel gains between the source terminal and the rth relay and between the rth relay and the destination terminal, respectively. In the first phase, the source terminal transmits a vector to all relay nodes. Afterwards, each relay processes its received signal vector to obtain the estimated signal vector. In the second phase, each relay

transmits each element of the estimated signal vector to the destination terminal. Clearly, the symbol transmission in this configuration needs only two phases.

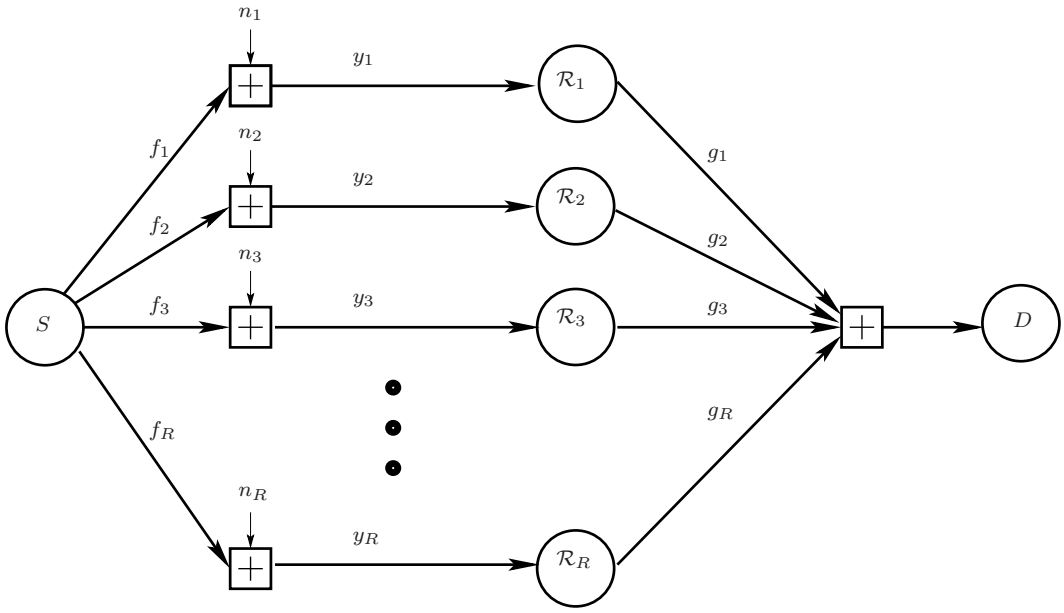

Figure 2.8: Parallel relay network.

On the other hand, a serial relay network consists of a source terminal, a destination terminal, and R relays as shown in Fig. 2.9. In this configuration, the source transmits its information symbol to the first relay and then each relay either amplifies and forwards the received signal or decodes and forwards it to the next relay. In the serial networks, the total transmission requires $(R + 1)$ phases. In case of three relays, a parallel network needs two phases to transmit one symbol while the symbol transmission in a serial network completes in four phases. This means that the rate of the parallel network is twice that of the serial network with three relays.

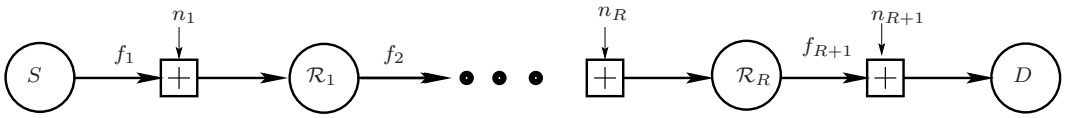

Figure 2.9: Serial relay network.

2.4.3 One and Two Way Relay Networks

Basically, the one-way relay network consists of a source terminal, a destination terminal, and multiple single-antenna relay nodes. This relay network allows the source terminal and the relay nodes to process and send the information signal to the destination node by creating a virtual antenna array, thus emulating transmit diversity. Fig. 2.10 shows a one-way relay network which has R relays where f_r, g_r, and f_0 are the channel gain from the source terminal to the rth relay, from the rth relay to the destination, and from the source terminal to the destination terminal, respectively.

Two-way wireless relay network (TWRN) is another common communication scenario which was first studied by Shannon in [112] where he considered a full-duplex scenario using a direct link between two terminals.

In TWRNs, both terminals transmit and receive information via a group of relays. This relay network can be categorized based on the number of phases needed for information transmission into three principal classes: four-phase TWRNs, three-phase TWRNs, and two-phase TWRNs. Fig. 2.11 shows a four-phase TWRN which basically consists of three single-antenna nodes where two nodes are the terminals that intend to communicate with each other and an assisting node acts as a relay for the transmitted signals from the terminals. In the first phase, the first terminal transmits its information signal to the assisting relay. During the second phase, the relay transmits the received signal to the second terminal. In the third phase, the second terminal transmits its information signal to the relay which then transmits the received signal to the first terminal in the fourth phase.

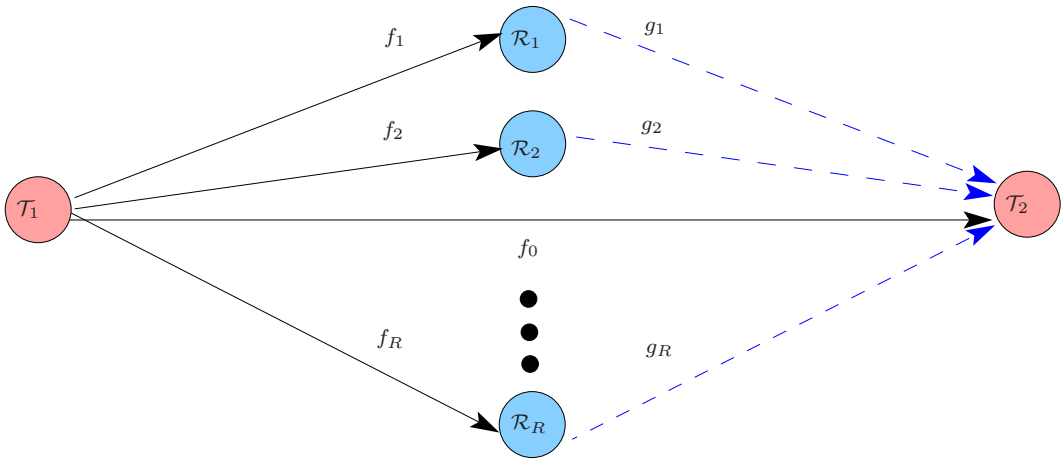

Figure 2.10: One-way wireless relay network.

Two strategies were proposed in the literature to reduce the number of phases needed for information transmission. The first strategy, known as three-phase scheme, reduces the total number of phases from four phases to three. Fig. 2.12 shows a three-phase TWRN which basically consists of two single-antenna terminals and an assisting relay. In the first phase of this scheme, the first terminal transmits its information signal to the assisting relay. During the second phase, the second terminal transmits its information signal to the relay. In the third phase, the relay combines both received signals, $s_{\mathcal{T}_1}$ and $s_{\mathcal{T}_2}$, into one signal $s_{\mathcal{R}} = \mathcal{F}(s_{\mathcal{T}_1}, s_{\mathcal{T}_2})$ using a combination function $\mathcal{F}(\cdot,\cdot)$ and broadcasts it to both terminals. Each terminal then can decode the transmitted symbol of the other terminal using the information of its own transmitted symbol and the inverse of the combination function $\mathcal{F}^{-1}(\cdot,\cdot)$. By doing this, the error performance and the data rate are improved, as the relay does not waste power to transmit redundant information at either side.

In the second strategy, known as two-phase scheme, the total number of phases needed for information transmission is further reduced to two. Fig. 2.13 shows a two-phase TWRN which basically consists of two single-antenna

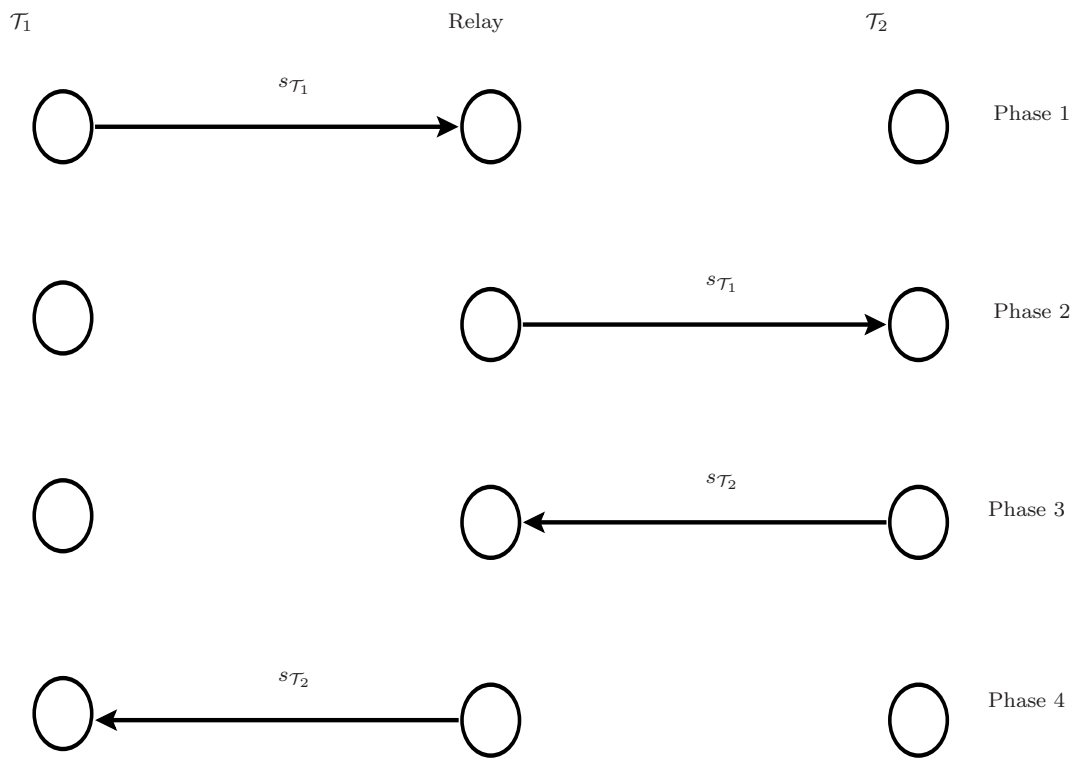

Figure 2.11: Four-phase TWRN.

terminals and a helping relay. In the first phase of this scheme, both terminals transmit simultaneously their information signals to the helping relay. During the second phase, the relay combines the received signals into one signal and broadcasts it to both terminals.

2.4.3.1 System Model for Two Way Wireless Relay Networks

In chapter four, five, and six of this thesis, we consider a half-duplex relay network with $R + 2$ single-antenna nodes where two nodes are the terminals, $\mathcal{T}_1$ and $\mathcal{T}_2$, that intend to communicate with each other and R nodes $(\mathcal{R}_1, \ldots, \mathcal{R}_R)$ act as relays for the signals transmitted from the terminals as shown in Fig. 2.14. We

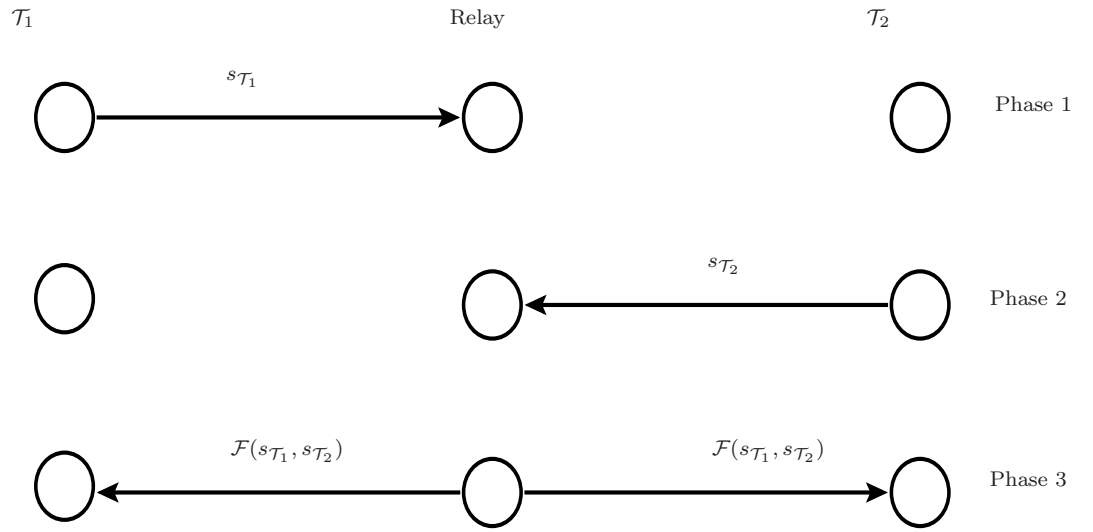

Figure 2.12: Three-phase TWRN.

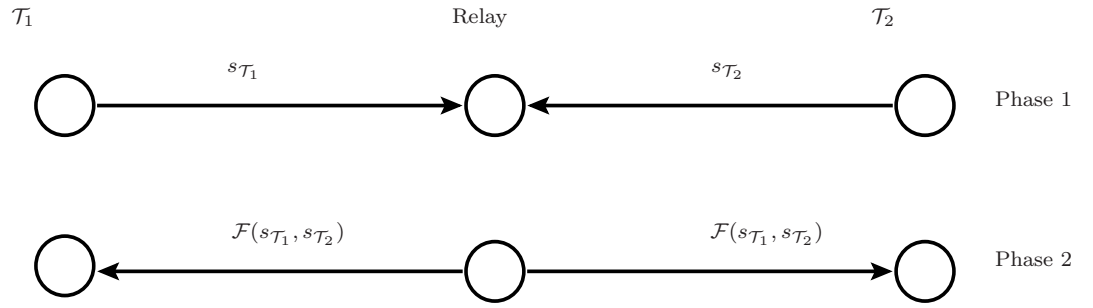

Figure 2.13: Two-phase TWRN.

assume independent Rayleigh flat-fading channels with unit variance and denote the channels from $\mathcal{T}_1$ to $\mathcal{T}_2$, from $\mathcal{T}_1$ to the rth relay, and from $\mathcal{T}_2$ to the rth relay as f_0, f_r, and g_r, respectively.

We assume that the channels are reciprocal for the transmission from $\mathcal{T}_1$ to $\mathcal{T}_2$ and vice versa. In the non-coherent case, we assume that neither the transmitter nor the receiver has any CSI. In the coherent case, perfect CSI is assumed at the receiving node where the coherent decoder is used, however, the CSI is not known

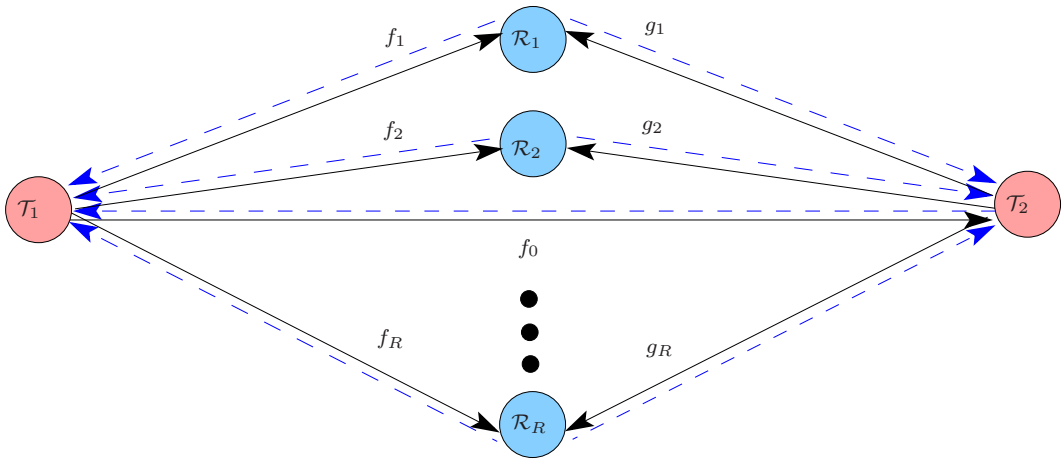

Figure 2.14: TWRN with $R+2$ nodes.

to the transmitting nodes. Furthermore, perfect synchronization is considered. The nodes $\mathcal{T}_1$, $\mathcal{T}_2$, $\mathcal{R}_1, \ldots, \mathcal{R}_R$ have limited average transmit powers $P_{\mathcal{T}_1}$, $P_{\mathcal{T}_2}$, $P_{\mathcal{R}_1}, \ldots, P_{\mathcal{R}_R}$, respectively.

Chapter 3

Quasi-Orthogonal Space-Time Block Coding in Multiple-Antenna systems

In this chapter, a low complexity suboptimal decoder for coherent and non-coherent QOSTBCs is introduced. The proposed decoder enjoys a nearly linear complexity and approximately the same performance as the optimal maximum-likelihood (ML) decoder.

3.1 Introduction

Transmit diversity has been studied extensively as a way to combat detrimental effects in fading channels [10]. Recently, spatial diversity techniques for MIMO systems [1, 2] have gained much interest due to their potential to enhance the error-rate performance of the communication without increasing the bandwidth or transmitted power. OSTBCs have been introduced to provide full diversity with a linear ML decoding complexity [10–12]. However, it is known that there is no rate-one complex OSTBCs except for systems involving two transmit antennas as explained in Sec. 2.3.2. In [53], QOSTBCs for four and three transmit antennas have been proposed to overcome the low-rate limitation of OSTBCs. Unfortu-

nately, the price for an improved rate is that the QOSTBCs do not achieve full diversity and have a substantially higher ML decoding complexity than the OSTBCs. In [54–56], it was shown that the full diversity property can be recovered if specific transmitted symbols in the code matrix are rotated. Recently, several space-time codes with a lower ML decoding complexity than that of the standard QOSTBCs have been proposed [97–100]. However, their improvements in decoding complexity come at the price of a substantial performance loss in comparison to the QOSTBCs [98, 100].

Early transmit diversity schemes were designed for coherent detection [1, 2, 10–12, 53] assuming perfect CSI at the receiver. However, the complexity and overheads for pilot transmission to facilitate channel estimation grow with the number of transmit and receive antennas [64].

As an alternative, differential STC techniques explained in Sec. 2.3.3 have been proposed which do not require any CSI at the transmitter and receiver [64–67]. Similar to their coherent counterpart, rate-one full-diversity differential STBCs have a higher than linear ML decoding complexity for more than two transmit antennas. To reduce the decoding complexity for coherent and non-coherent QOSTBCs, different approaches have been proposed [101–103]. However, as the method of [101] uses two parallel four dimensional real-valued sphere decoders, its complexity is still rather high. In [102], a decoder with a linear complexity has been proposed. Unfortunately, the decoder of [102] can only be used if the number of receive antennas is at least half the number of transmit antennas which limits its applicability in many practical systems. Moreover, this method can have a significant error performance loss when the number of receive antennas is less than the number of transmit antennas. On the other hand, the linear detectors of [103] have a low complexity but achieve this at the price of a substantially reduced error performance.

In this chapter, a low complexity sub-optimal QOSTBC decoder is proposed. Both the coherent and non-coherent implementations of this decoder are developed. Simulations with different signal constellations show that the proposed

QOSTBC decoder enjoys a substantially improved performance-to-complexity tradeoff as compared to the earlier decoding techniques.

3.2 Quasi-Orthogonal Space-Time Codes

The main property of OSTBCs explained in chapter two is the orthogonality of the codes where their transmission matrices have orthogonal columns. OSTBCs enjoy low decoding complexity, however, a full-rate full-diversity complex orthogonal STBC is not possible for more than two transmit antennas.

In an QOSTBC, the columns of the transmission matrix are not all orthogonal to each other, however, they can be partitioned into groups of non-orthogonal columns where the columns of each group are orthogonal to all columns of the respective other groups. In case of three and four transmit antennas, the columns of any QOSTBC matrix are divided into two groups. Therefore, the decoder of a QOSTBC for three and four transmit antennas is performed on pairs of transmitted symbols instead of single symbols. The loss of diversity is due to existence of cross terms between the estimated symbols. QOSTBCs for three and four transmit antennas can be classified into the following three categories:

3.2.1 Jafarkhani's Code

In this code, which was the first QOSTBC introduced in [53], two 2×2 Alamouti codes, $\mathbf{X}_{12}$ and $\mathbf{X}_{34}$, given by:

$$\mathbf{X}_{12} = \begin{bmatrix} x_1 & x_2 \\ -x_2^* & x_1^* \end{bmatrix}, \tag{3.1}$$

$$\mathbf{X}_{34} = \begin{bmatrix} x_3 & x_4 \\ -x_4^* & x_3^* \end{bmatrix} \tag{3.2}$$

are combined in a Alamouti-type manner, resulting in the so called extended Alamouti QOSTBC for four transmit antennas [53], given by:

$$\begin{aligned}\mathbf{X}_J &= \begin{bmatrix} \mathbf{X}_{12} & \mathbf{X}_{34} \\ -\mathbf{X}_{34}^* & \mathbf{X}_{12}^* \end{bmatrix} \\ &= \begin{bmatrix} x_1 & x_2 & x_3 & x_4 \\ -x_2^* & x_1^* & -x_4^* & x_3^* \\ -x_3^* & -x_4^* & x_1^* & x_2^* \\ x_4 & -x_3 & -x_2 & x_1 \end{bmatrix}. \end{aligned} \tag{3.3}$$

The matrix $\mathbf{X}_J$ in (3.3) is the QOSTBC transmission matrix. Clearly from (3.3), its transmission rate is equal to one as four symbols are transmitted in four consecutive time intervals. However, the minimum rank, as explained in Sec. 2.3.5, of this transmission matrix is equal to two. Therefore, a diversity advantage of only two can be achieved instead of four. The columns of the QOSTBC transmission matrix are not fully orthogonal to each other where for the transmission matrix in (3.3)

$$\mathbf{X}_J^H \mathbf{X}_J = \begin{bmatrix} \alpha_1 & 0 & 0 & \alpha_2 \\ 0 & \alpha_1 & \alpha_2 & 0 \\ 0 & \alpha_2 & \alpha_1 & 0 \\ \alpha_2 & 0 & 0 & \alpha_1 \end{bmatrix}.$$

$\alpha_1 = \sum_{i=1}^{4} |x_i|^2$ and $\alpha_2 = 2\Re\{x_1 x_4^* - x_2 x_3^*\}$.

3.2.2 ABBA Code

In this design, two 2×2 Alamouti codes, $\mathbf{X}_{12}$ and $\mathbf{X}_{34}$, given by (3.1) and (3.2) are also used to construct the ABBA code for four transmit antennas [105], given by:

$$\begin{aligned} \mathbf{X}_{ABBA} &= \begin{bmatrix} \mathbf{X}_{12} & \mathbf{X}_{34} \\ \mathbf{X}_{34} & \mathbf{X}_{12} \end{bmatrix} \\ &= \begin{bmatrix} x_1 & x_2 & x_3 & x_4 \\ -x_2^* & x_1^* & -x_4^* & x_3^* \\ x_3 & x_4 & x_1 & x_2 \\ -x_4^* & -x_3^* & -x_2^* & x_1^* \end{bmatrix}. \end{aligned} \tag{3.4}$$

The columns of the QOSTBC transmission matrix in (3.4) are not orthogonal to each other where

$$\mathbf{X}_{ABBA}^H \mathbf{X}_{ABBA} = \begin{bmatrix} \alpha_1 & 0 & \alpha_3 & 0 \\ 0 & \alpha_1 & 0 & \alpha_3 \\ \alpha_3 & 0 & \alpha_1 & 0 \\ 0 & \alpha_3 & 0 & \alpha_1 \end{bmatrix},$$

$\alpha_1 = \sum_{i=1}^{4} |x_i|^2$, and $\alpha_3 = 2\Re\{x_1 x_3^* + x_2 x_4^*\}$.

3.2.3 Papadias's Code

Another proposal for a QOSTBC is introduced by Papadias and Foschini [106], given by:

$$\mathbf{X}_{PF} = \begin{bmatrix} x_1 & x_2 & x_3 & x_4 \\ x_2^* & -x_1^* & x_4^* & -x_3^* \\ x_3 & -x_4 & -x_1 & x_2 \\ x_4^* & x_3^* & -x_2^* & -x_1^* \end{bmatrix}.$$

In this code, the data symbols $x_i,\ i = 1, \cdots, 4$, are arranged in a different way

than the previous QOSTBCs where $\mathbf{X}_{PF}$ can not be expressed as a simple combination of two 2×2 Alamouti codes. The columns of the QOSTBC transmission matrix in (3.5) are not orthogonal to each other where

$$\mathbf{X}_{PF}^{H}\mathbf{X}_{PF} = \begin{bmatrix} \alpha_1 & 0 & \alpha_4 & 0 \\ 0 & \alpha_1 & 0 & \alpha_4 \\ -\alpha_4 & 0 & \alpha_1 & 0 \\ 0 & -\alpha_4 & 0 & \alpha_1 \end{bmatrix},$$

$\alpha_1 = \sum_{i=1}^{4} |x_i|^2$, $\alpha_4 = 2j\Im\{x_1^* x_3 + x_2 x_4^*\}$, $j = \sqrt{-1}$, and $\Im\{\cdot\}$ denotes the imaginary part. Simulation results in [53] show that full transmission rate is of great importance in the low SNR region and high BERs whereas full diversity is more important in high SNR region and low BERs. This is because of the fact that in the high SNR region, the slope of the performance curve is determined by the diversity order.

3.2.4 Quasi-orthogonal Codes for Eight Transmit Antennas

In Sec. (3.2.1) and Sec. (3.2.2), two 2×2 rate-one STC matrices, defined in (3.1) and (3.2), are used to construct a rate-one 4×4 STC matrix. A similar procedure can be performed using two 4×4 rate-$\frac{3}{4}$ STC matrices, given by:

$$\mathbf{X}_{14} = \begin{bmatrix} x_1 & x_2 & x_3 & 0 \\ -x_2^* & x_1^* & 0 & -x_3 \\ -x_3^* & 0 & x_1^* & x_2 \\ 0 & x_3^* & -x_2^* & x_1 \end{bmatrix}, \tag{3.5}$$

$$\mathbf{X}_{58} = \begin{bmatrix} x_4 & x_5 & x_6 & 0 \\ -x_5^* & x_4^* & 0 & -x_6 \\ -x_6^* & 0 & x_4^* & x_5 \\ 0 & x_6^* & -x_5^* & x_4 \end{bmatrix} \tag{3.6}$$

to construct a rate-$\frac{3}{4}$ 8×8 STC matrix, given by:

$$\mathbf{X}_8 = \begin{bmatrix} \mathbf{X}_{14} & \mathbf{X}_{58} \\ -\mathbf{X}_{58}^* & \mathbf{X}_{14}^* \end{bmatrix} \tag{3.7}$$

$$= \begin{bmatrix} x_1 & x_2 & x_3 & 0 & x_4 & x_5 & x_6 & 0 \\ -x_2^* & x_1^* & 0 & -x_3 & -x_5^* & x_4^* & 0 & -x_6 \\ -x_3^* & 0 & x_1^* & x_2 & -x_6^* & 0 & x_4^* & x_5 \\ 0 & x_3^* & -x_2^* & x_1 & 0 & x_6^* & -x_5^* & x_4 \\ -x_4^* & -x_5^* & -{x_6}^* & 0 & x_1^* & x_2^* & {x_3}^* & 0 \\ x_5 & -x_4 & 0 & {x_6}^* & -x_2 & x_1 & 0 & -{x_3}^* \\ x_6 & 0 & -x_4 & -x_5^* & -x_3 & 0 & x_1 & x_2^* \\ 0 & -x_6 & x_5 & -x_4^* & 0 & x_3 & -x_2 & x_1^* \end{bmatrix}. \tag{3.8}$$

Since there is a transmission rate loss (i.e. the rate is less than one), another form of QOSTBC for eight transmit antennas that achieves full rate has been proposed. In this design, eight complex symbols are transmitted during eight time slots where its ML decoder consists in separating the eight symbols into two groups and jointly detecting four complex symbols (quad-symbol-decodable) per group. Similar to Sec. (3.2.1) and Sec. (3.2.2) where two 2×2 rate-one STC matrices, (3.3) and (3.4), are used to construct a rate-one 4×4 STC matrix, one can use four 2×2 rate-one STC matrices given by:

$$\mathbf{X}_{12} = \begin{bmatrix} x_1 & x_2 \\ -x_2^* & x_1^* \end{bmatrix}, \tag{3.9}$$

$$\mathbf{X}_{34} = \begin{bmatrix} x_3 & x_4 \\ -x_4^* & x_3^* \end{bmatrix}, \tag{3.10}$$

$$\mathbf{X}_{56} = \begin{bmatrix} x_5 & x_6 \\ -x_6^* & x_5^* \end{bmatrix}, \tag{3.11}$$

$$\mathbf{X}_{78} = \begin{bmatrix} x_7 & x_8 \\ -x_8^* & x_7^* \end{bmatrix} \tag{3.12}$$

to construct a rate-one 8×8 STC matrix, proposed by Tirkkonen et. at. in [105], given by:

$$\mathbf{X}_T = \begin{bmatrix} \mathbf{X}_{12} & \mathbf{X}_{34} & \mathbf{X}_{56} & \mathbf{X}_{78} \\ \mathbf{X}_{34} & \mathbf{X}_{12} & \mathbf{X}_{78} & \mathbf{X}_{56} \\ \mathbf{X}_{56} & \mathbf{X}_{78} & \mathbf{X}_{12} & \mathbf{X}_{34} \\ \mathbf{X}_{78} & \mathbf{X}_{56} & \mathbf{X}_{34} & \mathbf{X}_{12} \end{bmatrix}$$

$$= \begin{bmatrix} x_1 & x_2 & x_3 & x_4 & x_5 & x_6 & x_7 & x_8 \\ -x_2^* & x_1^* & -x_4^* & x_3^* & -x_6^* & x_5^* & -x_8^* & x_7^* \\ x_3 & x_4 & x_1 & x_2 & x_7 & x_8 & x_5 & x_6 \\ -x_4^* & x_3^* & -x_2^* & x_1^* & -x_8^* & x_7^* & -x_6^* & x_5^* \\ x_5 & x_6 & x_7 & x_8 & x_1 & x_2 & x_3 & x_4 \\ -x_6^* & x_5^* & -x_8^* & x_7^* & -x_2^* & x_1^* & -x_4^* & x_3^* \\ x_7 & x_8 & x_5 & x_6 & x_3 & x_4 & x_1 & x_2 \\ -x_8^* & x_7^* & -x_6^* & x_5^* & -x_4^* & x_3^* & -x_2^* & x_1^* \end{bmatrix}. \quad (3.13)$$

Another form of rate-one 8×8 QOSTBC is proposed by Yuen et. al. in [107].

3.2.5 Full-Diversity Quasi-orthogonal Space-Time Block Codes with Constellation Rotation

Although QOSTBCs enjoy higher transmission rates than OSTBCs, they do not achieve full diversity directly. To achieve full diversity, a constellation rotation method is proposed in [55]. From the rank criterion explained in Sec. 2.3.5, the diversity order of the STBCs is equal to the minimum rank of the error matrix $\mathbf{D} = (\mathbf{X} - \tilde{\mathbf{X}})$. Therefore, to maximize the overall error performance, the minimum rank and minimum determinant of the error matrix over all pairs of distinct code matrices have to be maximized. As an example, we use the QOSTBC given by (3.3) whose error matrix can be expressed as:

$$\mathbf{D} = \mathbf{X} - \tilde{\mathbf{X}} = \begin{bmatrix} d_1 & d_2 & d_3 & d_4 \\ -d_2^* & d_1^* & -d_4^* & d_3^* \\ -d_3^* & -d_4^* & d_1^* & d_2^* \\ d_4 & -d_3 & -d_2 & d_1 \end{bmatrix} \tag{3.14}$$

where $d_i = x_i - \tilde{x}_i,\ i = 1, \cdots, 4$. From the rank criterion explained in Sec. 2.3.5, the matrix $\mathbf{D}$ has to be full rank. The determinant of the matrix $\mathbf{D}$ can be written as:

$$\det(\mathbf{D}) = \left[\left(|d_1 + d_4|^2 + |d_2 - d_3|^2\right)\left(|d_1 - d_4|^2 + |d_2 + d_3|^2\right)\right] \tag{3.15}$$

Clearly from (3.15), the matrix $\mathbf{D}$ is singular when ($d_1 = -d_4$ and $d_2 = d_3$) or ($d_1 = d_4$ and $d_2 = -d_3$). Due to the symmetry of the constellation sets such as QAM and PSK, this case can easily happen. Thus, the matrix $\mathbf{D}$ generally does not exhibit the full rank property and thus the QOSTBC given by (3.3) can not achieve full transmit diversity. Therefore, to achieve a non singular $\mathbf{D}$, we need to ensure that $d_1 \neq -d_4$, $d_2 \neq d_3$, $d_1 \neq d_4$ and $d_2 \neq -d_3$. This can be achieved by, e.g., rotating the symbols x_3 and x_4 to $x_3 e^{j\phi}$ and $x_4 e^{j\phi}$, respectively, where ϕ is the rotation angle that is selected as in [55].

3.2.6 The Pair-wise Maximum Likelihood Decoder

For the three QOSTBCs in Sec. 3.2.1, Sec. 3.2.2, and Sec. 3.2.3, their ML decoders consist in separating the four symbols into two groups and jointly detecting two complex symbols (*pair-wise-symbol-decodable*) per group. As an example, let us use the QOSTBC given by (3.3) for four transmit antennas ($M_t = 4$) [53] to show the pair-wise ML decoding of QOSTBCs. In the case of one receive antenna, the coherent ML decoder can be written as:

$$\min_{x_1,x_2,x_3,x_4} \left|\left|\mathbf{Y} - \mathbf{XH}\right|\right|^2 \;=\; \min_{x_1,x_4} f_{14}(x_1, x_4) + \min_{x_2,x_3} f_{23}(x_2, x_3) \tag{3.16}$$

where

$$\begin{aligned} f_{14}(x_1, x_4) &= \left(|x_1|^2 + |x_4|^2\right)\left(|h_1|^2 + |h_2|^2 + |h_3|^2 + |h_4|^2\right) \\ &+ 2\mathrm{Re}\left\{\left(-h_1 y_1^* - h_2^* y_2 - h_3^* y_3 - h_4 y_4^*\right)(x_1)\right\} \\ &+ 2\mathrm{Re}\left\{\left(-h_4 y_1^* + h_3^* y_2 + h_2^* y_3 - h_1 y_4^*\right)(x_4)\right\} \\ &+ 4\mathrm{Re}\left\{h_1 h_4^* - h_2 h_3^*\right\}\mathrm{Re}\left\{x_1 x_4^*\right\}, \end{aligned} \tag{3.17}$$

$$\begin{aligned} f_{23}(x_2, x_3) &= \left(|x_2|^2 + |x_3|^2\right)\left(|h_1|^2 + |h_2|^2 + |h_3|^2 + |h_4|^2\right) \\ &+ 2\mathrm{Re}\left\{\left(-h_2 y_1^* + h_1^* y_2 - h_4^* y_3 + h_3 y_4^*\right)(x_2)\right\} \\ &+ 2\mathrm{Re}\left\{\left(-h_3 y_1^* - h_4^* y_2 + h_1^* y_3 + h_2 y_4^*\right)(x_3)\right\} \\ &+ 4\mathrm{Re}\left\{-h_1 h_4^* + h_2 h_3^*\right\}\mathrm{Re}\left\{x_2 x_3^*\right\}, \end{aligned} \tag{3.18}$$

$\|\cdot\|$ stands for the Frobenious norm. From (3.17) and (3.18), we note that x_1 and x_4 can be decoded independently of x_2 and x_3 and vice versa. The subscripts of the functions denote the unknown symbols used in their respective arguments. As the pairs (x_1, x_4) and (x_2, x_3) can be detected independently of each other, a pair-wise complex symbol decoder can be used instead of the full ML decoder. However, such decoding can be still prohibitively expensive when the signal constellation size is high.

3.3 The Proposed Low Complexity Decoder for Three Transmit Antennas

Similar to Sec. 2.2, we consider, in this chapter, a MIMO system with M_t transmit and M_r receive antennas and assume a flat block fading channel with the block length T. The input-output relation for such a MIMO system can be expressed as in (2.10):

$$\mathbf{Y} = \mathbf{X}\mathbf{H} + \mathbf{N} \tag{3.19}$$

where $\mathbf{Y}$ is the $T \times M_r$ complex matrix of received signals, $\mathbf{X}$ is the $T \times M_t$

complex matrix of transmitted signals, $\mathbf{H}$ is the $M_t \times M_r$ complex channel matrix and $\mathbf{N}$ is the $T \times M_r$ complex white Gaussian noise matrix. The entries of $\mathbf{H}$ and $\mathbf{N}$ are assumed to be modeled as statistically independent, zero-mean, complex Gaussian random variables.

Let us assume that there are L information symbols s_i transmitted per block $\mathbf{X}$ from some given constellation $\mathcal{S}$ of size M. Then, the full ML decoder requires a M^L size search whereas the complex symbol pair-wise and complex symbol-wise decoders need $\lceil L/2 \rceil M^2$ and LM size searches, respectively, where the operator $\lceil \cdot \rceil$ maps its argument to the next largest integer.

For the sake of simplicity, the case of one receive antenna will be considered. Extension of our results to the case of $M_r > 1$ is straightforward. To derive our low complexity decoder, let us use the following QOSTBC for $M_t = 3$ [104] [1]

$$\mathbf{X} = \begin{bmatrix} x_1 & x_2 & 0 \\ -x_2^* & x_1^* & 0 \\ 0 & x_3 & x_4 \\ 0 & -x_4^* & x_3^* \end{bmatrix} \tag{3.20}$$

where $(\cdot)^*$ denotes the complex conjugate and x_i are the transmitted signals that depend on s_i. If $x_i = s_i$ $(i = 1, 2, 3, 4)$, then (3.20) can be partitioned into two separated Alamouti systems and only the diversity order of two can be achieved. To achieve the full diversity, the following mapping can be used [104]:

$$\begin{aligned} x_1 &= s_1 + \tilde{s}_3, \quad x_2 = s_2 + \tilde{s}_4, \\ x_3 &= s_1 - \tilde{s}_3, \quad x_4 = s_2 - \tilde{s}_4 \end{aligned} \tag{3.21}$$

where

$$\tilde{s}_3 \triangleq s_3 e^{j\phi}, \tag{3.22}$$

$$\tilde{s}_4 \triangleq s_4 e^{j\phi}, \tag{3.23}$$

[1] We discuss later in Sec. 3.4 the extension to $M_t = 4$.

and ϕ is the rotation angle that is selected as in [55]. Using (3.20) and (3.21), (3.19) can be partitioned into two equations as:

$$\mathbf{y}_1 = \mathbf{X}_1\mathbf{h}_1 + \mathbf{n}_1, \tag{3.24}$$

$$\mathbf{y}_2 = \mathbf{X}_2\mathbf{h}_2 + \mathbf{n}_2 \tag{3.25}$$

where

$$\mathbf{y}_1 \triangleq \begin{bmatrix} y_1 \\ y_2 \end{bmatrix}, \quad \mathbf{h}_1 \triangleq \begin{bmatrix} h_1 \\ h_2 \end{bmatrix}, \quad \mathbf{n}_1 \triangleq \begin{bmatrix} n_1 \\ n_2 \end{bmatrix}, \quad \mathbf{X}_1 \triangleq \begin{bmatrix} s_1 + \tilde{s}_3 & s_2 + \tilde{s}_4 \\ -(s_2 + \tilde{s}_4)^* & (s_1 + \tilde{s}_3)^* \end{bmatrix},$$

$$\mathbf{y}_2 \triangleq \begin{bmatrix} y_3 \\ y_4 \end{bmatrix}, \quad \mathbf{h}_2 \triangleq \begin{bmatrix} h_2 \\ h_3 \end{bmatrix}, \quad \mathbf{n}_2 \triangleq \begin{bmatrix} n_3 \\ n_4 \end{bmatrix}, \quad \mathbf{X}_2 \triangleq \begin{bmatrix} s_1 - \tilde{s}_3 & s_2 - \tilde{s}_4 \\ -(s_2 - \tilde{s}_4)^* & (s_1 - \tilde{s}_3)^* \end{bmatrix}.$$

3.3.1 The Coherent Quasi-orthogonal Space-Time Codes

Using (3.24) and (3.25) and assuming the perfect CSI at the receiver, the coherent ML decoder of (3.20) can be written as:

$$\min_{s_1,s_2,\tilde{s}_3,\tilde{s}_4} \left|\left|\mathbf{Y} - \mathbf{XH}\right|\right|^2 = \min_{s_1,s_2,\tilde{s}_3,\tilde{s}_4} \left|\left|\mathbf{y}_1 - \mathbf{X}_1\mathbf{h}_1\right|\right|^2 + \left|\left|\mathbf{y}_2 - \mathbf{X}_2\mathbf{h}_2\right|\right|^2. \tag{3.26}$$

Expanding the first and second term at the right hand side of (3.26), we obtain

$$\begin{aligned} \left|\left|\mathbf{y}_1 - \mathbf{X}_1\mathbf{h}_1\right|\right|^2 &= c_1 + \left(|s_1 + \tilde{s}_3|^2 + |s_2 + \tilde{s}_4|^2\right)\left(|h_1|^2 + |h_2|^2\right) \\ &- 2\mathrm{Re}\left\{(h_1 y_1^* + h_2^* y_2)(s_1 + \tilde{s}_3) - (h_2 y_1^* - h_1^* y_2)(s_2 + \tilde{s}_4)\right\}, \end{aligned} \tag{3.27}$$

$$\begin{aligned} \left|\left|\mathbf{y}_2 - \mathbf{X}_2\mathbf{h}_2\right|\right|^2 &= c_2 + \left(|s_1 - \tilde{s}_3|^2 + |s_2 - \tilde{s}_4|^2\right)\left(|h_2|^2 + |h_3|^2\right) \\ &- 2\mathrm{Re}\left\{(h_2 y_3^* + h_3^* y_4)(s_1 - \tilde{s}_3) - (h_3 y_3^* - h_2^* y_4)(s_2 - \tilde{s}_4)\right\}, \end{aligned} \tag{3.28}$$

respectively, where c_1 and c_2 are constant terms that do not depend on the symbols. Using (3.27) and (3.28) in (3.26), we note that s_1 and $\tilde{s}_3$ can be decoded independently of s_2 and $\tilde{s}_4$. Therefore, (3.26) can be rewritten as:

$$\min_{s_1,s_2,\tilde{s}_3,\tilde{s}_4} \left|\left|\mathbf{Y}-\mathbf{XH}\right|\right|^2 = \min_{s_1,\tilde{s}_3} f_{13}(s_1,\tilde{s}_3) + \min_{s_2,\tilde{s}_4} f_{24}(s_2,\tilde{s}_4) \tag{3.29}$$

where

$$\begin{aligned} f_{13}(s_1,\tilde{s}_3) &= |s_1+\tilde{s}_3|^2\left(|h_1|^2+|h_2|^2\right)+|s_1-\tilde{s}_3|^2\left(|h_2|^2+|h_3|^2\right) \\ &- 2\mathrm{Re}\left\{\left(h_1y_1^*+h_2^*y_2\right)\left(s_1+\tilde{s}_3\right)-\left(h_2y_3^*+h_3^*y_4\right)\left(s_1-\tilde{s}_3\right)\right\}, \end{aligned} \tag{3.30}$$

$$\begin{aligned} f_{24}(s_2,\tilde{s}_4) &= |s_2+\tilde{s}_4|^2\left(|h_1|^2+|h_2|^2\right)+|s_2-\tilde{s}_4|^2\left(|h_2|^2+|h_3|^2\right) \\ &- 2\mathrm{Re}\left\{\left(h_2y_1^*-h_1^*y_2\right)\left(s_2+\tilde{s}_4\right)-\left(h_3y_3^*-h_2^*y_4\right)\left(s_2-\tilde{s}_4\right)\right\} \end{aligned} \tag{3.31}$$

and the subscripts of the functions denote the unknown symbols used in their respective arguments. As the pairs (s_1,$\tilde{s}_3$) and (s_2,$\tilde{s}_4$) can be detected independently of each other, we can use a pair-wise complex symbol decoder instead of the full ML decoder. However, such decoding can be still prohibitively expensive when the signal constellation size is high.

Let us now develop our suboptimal decoder for s_1 and $\tilde{s}_3$. The decoding procedure for s_2 and $\tilde{s}_4$ follows similar steps. We can express $f_{13}(s_1,\tilde{s}_3)$ in (3.30) as:

$$\begin{aligned} f_{13}(s_1,\tilde{s}_3) &= |s_1|^2(|h_1|^2+2|h_2|^2+|h_3|^2)-2\,\mathrm{Re}\{(h_1y_1^*+h_2^*y_2+h_2y_3^*+h_3^*y_4)s_1\} \\ &+ |\tilde{s}_3|^2(|h_1|^2+2|h_2|^2+|h_3|^2)-2\,\mathrm{Re}\{(h_1y_1^*+h_2^*y_2-h_2y_3^*-h_3^*y_4)\tilde{s}_3\} \\ &+ 2(|h_1|^2-|h_3|^2)\mathrm{Re}\{s_1\tilde{s}_3^*\}. \end{aligned} \tag{3.32}$$

If the decoder knows s_3, then (3.32) can be reduced to

$$\begin{aligned} f_1(s_1,\tilde{s}_3) &= |s_1|^2(|h_1|^2+2|h_2|^2+|h_3|^2)-2\,\mathrm{Re}\{(h_1y_1^*+h_2^*y_2+h_2y_3^*+h_3^*y_4)s_1\} \\ &+ 2(|h_1|^2-|h_3|^2)\mathrm{Re}\{s_1\tilde{s}_3^*\} \end{aligned} \tag{3.33}$$

to detect s_1. Similarly, if the decoder knows s_1, then we can reduce (3.32) to

$$\begin{aligned} f_3(s_1, \tilde{s}_3) &= |\tilde{s}_3|^2(|h_1|^2 + 2|h_2|^2 + |h_3|^2) - 2\,\mathrm{Re}\{(h_1 y_1^* + h_2^* y_2 - h_2 y_3^* - h_3^* y_4)\tilde{s}_3\} \\ &+ 2(|h_1|^2 - |h_3|^2)\mathrm{Re}\{s_1 \tilde{s}_3^*\} \end{aligned} \tag{3.34}$$

to detect s_3. To decode s_3 using (3.34), we can obtain an initial value for s_1 as $\breve{s}_1(1) = \mathrm{rnd}(s_1', 1)$ where the operator $\mathrm{rnd}(s, n)$ returns the symbol which is the nth closest to s in the constellation $\mathcal{S}$. From (3.24), it can be observed that the columns of the STC matrix $\mathbf{X}_1$ in the first subsystem are orthogonal to each other with respect to the symbols x_1 and x_2 where (3.24) can be rewritten as:

$$\tilde{\mathbf{y}}_1 = \mathbf{H}_1 \mathbf{x}_1 + \tilde{\mathbf{n}}_1 \tag{3.35}$$

where $\tilde{\mathbf{y}}_1 = [y_1, y_2^*]^T$, $\mathbf{x}_1 = [x_1, x_2]^T$, $\tilde{\mathbf{n}}_1 = [n_1, n_2^*]^T$, and

$$\mathbf{H}_1 = \begin{bmatrix} h_1 & h_2 \\ h_2^* & -h_1^* \end{bmatrix}. \tag{3.36}$$

To decode the symbols x_1 and x_2, we can use the following zero-forcing decoder

$$\hat{\mathbf{x}}_1 = \frac{\mathbf{H}_1^H \tilde{\mathbf{y}}_1}{|h_1|^2 + |h_2|^2} \tag{3.37}$$

where $\hat{\mathbf{x}}_1 = [\hat{x}_1, \hat{x}_2]^T$. A similar procedure can be performed on the second subsystem to decode the symbols x_3 and x_4 where the columns of the STC matrix $\mathbf{X}_2$ in the second subsystem given by (3.25) are also orthogonal to each other with respect to the symbols x_3 and x_4. (3.25) can be rewritten as:

$$\tilde{\mathbf{y}}_2 = \mathbf{H}_2 \mathbf{x}_2 + \tilde{\mathbf{n}}_2 \tag{3.38}$$

where $\tilde{\mathbf{y}}_2 = [y_3, y_4^*]^T$, $\mathbf{x}_2 = [x_3, x_4]^T$, $\tilde{\mathbf{n}}_2 = [n_3, n_4^*]^T$, and

$$\mathbf{H}_2 = \begin{bmatrix} h_3 & h_4 \\ h_4^* & -h_3^* \end{bmatrix}. \tag{3.39}$$

To decode the symbols x_3 and x_4, we can use the following zero-forcing decoder

$$\hat{\mathbf{x}}_2 = \frac{\mathbf{H}_2^H \tilde{\mathbf{y}}_2}{|h_2|^2 + |h_3|^2} \tag{3.40}$$

where $\hat{\mathbf{x}}_2 = [\hat{x}_3, \hat{x}_4]^T$. Therefore, s_1' can be expressed as:

$$\begin{aligned} s_1' &\triangleq \frac{\hat{x}_1 + \hat{x}_3}{2} \\ &\triangleq \frac{h_1^* y_1 + h_2 y_2^*}{2(|h_1|^2 + |h_2|^2)} + \frac{h_2^* y_3 + h_3 y_4^*}{2(|h_2|^2 + |h_3|^2)}. \end{aligned} \tag{3.41}$$

$\breve{s}_1(1)$ can be considered as the zero-forcing estimate of s_1, as s_1' is computed by neglecting the noise and relaxing the finite alphabet constraint. The value of s_3 can be estimated by minimizing (3.34) using $\breve{s}_1(1)$ and then, the so-obtained initial estimate of s_3, $\hat{s}_3(1)$, can be inserted in (3.33) to estimate $\hat{s}_1(1)$ by minimizing $f_1(s_1, \tilde{s}_3 = \hat{s}_3(1)e^{j\phi})$. The quality of $\hat{s}_1(1)$ and $\hat{s}_3(1)$ depends on the initial suboptimal choice $\breve{s}_1(1)$ and therefore, the resulting decoding performance can be very poor.

The probability that $\breve{s}_1(1)$ is the correct symbol is inverse proportional to the distance from $\breve{s}_1(1)$ to s_1'. That is, the closer $\breve{s}_1(1)$ to s_1', the more likely $\breve{s}_1(1)$ is the correct symbol. To decide if $\breve{s}_1(1)$ has a low probability of being the correct symbol, we check whether the inverse of the distance is smaller than a given threshold, i.e. $d < \alpha$ where

$$d \triangleq \frac{c_0}{|\breve{s}_1(1) - s_1'|} \tag{3.42}$$

is the inverse of the normalized distance, c_0 is the minimum distance between two constellation points in $\mathcal{S}$, α is a threshold that depends non-linearly on the SNR as:

$$\alpha \triangleq K \left(\frac{\text{SNR(dB)}}{10} \right)^{\gamma} \tag{3.43}$$

and K and γ are two constants. The selection of α is empirical and is based on extensive simulations. Note, however, that it is expected that the higher the SNR, the closer is s_1' to $\breve{s}_1(1)$.

If $\breve{s}_1(1)$ has a low probability of being the correct symbol, we can improve the probability of choosing the correct estimates of s_1 and s_3 by inspecting the next closest symbols to s_1' in $\mathcal{S}$ to generate new possible estimates of s_1 and s_3 that can be compared using the ML metric in (3.32).

To limit the complexity, we restrict the decoder to obtain these new estimates of s_1 and s_3 based only on the second and third closest symbols to s_1', i.e., $\breve{s}_1(2) = \text{rnd}(s_1', 2)$ and $\breve{s}_1(3) = \text{rnd}(s_1', 3)$, respectively. Using the value of $f_{13}(s_1, \tilde{s}_3)$, the three pairs of estimates of s_1 and s_3 are compared and the pair with the lowest value of $f_{13}(s_1, \tilde{s}_3)$ is selected as final output of the decoder.

In the case when $d \geq \alpha$, the decoder returns the estimates based on $\breve{s}_1(1)$ as the final output. Clearly, the latter case has a complexity similar to the symbol-wise decoder while the case $d < \alpha$ has a complexity which lies in between that of the symbol-wise and symbol pair-wise decoders.

From our simulations, it follows that the case $d \geq \alpha$ is the most frequent. This results in an average decoding complexity which is nearly similar to the symbol-wise decoder. The decoding procedure can be summarized as follows.

Decoding Algorithm

1. Set $m = 1$.

2. Compute $\breve{s}_1(m) = \text{rnd}(s_1', m)$. Substitute $\breve{s}_1(m)$ in (3.34) and find

$$\hat{s}_3(m) = \arg\min_{s_3 \in \mathcal{S}} f_3(\breve{s}_1(m), \tilde{s}_3 = s_3 e^{j\phi}).$$

   Substitute $\hat{s}_3(m)$ in (3.33) and find

$$\hat{s}_1(m) = \arg\min_{s_1 \in \mathcal{S}} f_1(s_1, \hat{s}_3(m) e^{j\phi}).$$

3. If $d > \alpha$, set $\hat{s}_1(m)$ and $\hat{s}_3(m)$ as the final output estimates and terminate. Otherwise go to Step 4.

4. Repeat Step 2 for $m = 2, 3$ and find

$$\tilde{m} = \arg \min_{m=1,2,3} f_{13}(\hat{s}_1(m), \hat{s}_3(m)e^{j\phi}).$$

Set $\hat{s}_1(\tilde{m})$ and $\hat{s}_3(\tilde{m})$ as the final output estimates.

3.3.2 The Non-coherent Quasi-orthogonal Space-Time Codes

Let us develop a suboptimal decoder for the differential version of the QOSTBC [67]. Similar to differential STBC techniques explained in Sec. 2.3.3, we assume in this section that neither the transmitter nor the receiver has any CSI. In contrast to (3.19), we consider the transmission of two consecutive blocks, (k) and $(k-1)$, where the $(k-1)$th block is a reference for the decoding of the kth block. Using (3.24) and (3.25), the transmitter sends $\mathbf{X}_1^{(k)}$ and $\mathbf{X}_2^{(k)}$ for the kth block where $\mathbf{X}_1^{(0)} = \mathbf{X}_2^{(0)} = \mathbf{I}_2$,

$$\mathbf{X}_1^{(k)} \triangleq \frac{\mathbf{U}_1^{(k)}\mathbf{X}_1^{(k-1)}}{d_1^{(k-1)}}, \qquad \mathbf{X}_2^{(k)} \triangleq \frac{\mathbf{U}_2^{(k)}\mathbf{X}_2^{(k-1)}}{d_2^{(k-1)}}, \tag{3.44}$$

$$d_1^{(k-1)} \triangleq \sqrt{\left|s_1^{(k-1)} + \tilde{s}_3^{(k-1)}\right|^2 + \left|s_2^{(k-1)} + \tilde{s}_4^{(k-1)}\right|^2}, \tag{3.45}$$

$$d_2^{(k-1)} \triangleq \sqrt{\left|s_1^{(k-1)} - \tilde{s}_3^{(k-1)}\right|^2 + \left|s_2^{(k-1)} - \tilde{s}_4^{(k-1)}\right|^2}, \tag{3.46}$$

$$\mathbf{U}_1^{(k)} \triangleq \begin{bmatrix} s_1^{(k)} + \tilde{s}_3^{(k)} & s_2^{(k)} + \tilde{s}_4^{(k)} \\ -\left(s_2^{(k)} + \tilde{s}_4^{(k)}\right)^* & \left(s_1^{(k)} + \tilde{s}_3^{(k)}\right)^* \end{bmatrix}, \tag{3.47}$$

$$\mathbf{U}_2^{(k)} \triangleq \begin{bmatrix} s_1^{(k)} - \tilde{s}_3^{(k)} & s_2^{(k)} - \tilde{s}_4^{(k)} \\ -\left(s_2^{(k)} - \tilde{s}_4^{(k)}\right)^* & \left(s_1^{(k)} - \tilde{s}_3^{(k)}\right)^* \end{bmatrix}. \tag{3.48}$$

From (3.44)-(3.48), it can be seen that $\mathbf{U}_1^{(k)}(\mathbf{U}_1^{(k)})^H = \mathbf{X}_1^{(k)}(\mathbf{X}_1^{(k)})^H = \left|d_1^{(k)}\right|^2 \mathbf{I}_2$ and $\mathbf{U}_2^{(k)}(\mathbf{U}_2^{(k)})^H = \mathbf{X}_2^{(k)}(\mathbf{X}_2^{(k)})^H = \left|d_2^{(k)}\right|^2 \mathbf{I}_2$. From (3.24) and (3.44), the received signal vectors for the first sub-system at the blocks $(k-1)$ and (k) are given by:

$$\mathbf{y}_1^{(k-1)} = \mathbf{X}_1^{(k-1)}\mathbf{h}_1 + \mathbf{n}_1^{(k-1)}, \tag{3.49}$$

$$\mathbf{y}_1^{(k)} = \mathbf{X}_1^{(k)}\mathbf{h}_1 + \mathbf{n}_1^{(k)} = \frac{\mathbf{U}_1^{(k)}\mathbf{X}_1^{(k-1)}\mathbf{h}_1}{d_1^{(k-1)}} + \mathbf{n}_1^{(k)}, \tag{3.50}$$

respectively. From (3.25) and (3.44), the received signal vectors for the second sub-system at the blocks $(k-1)$ and (k) are given by:

$$\mathbf{y}_2^{(k-1)} = \mathbf{X}_2^{(k-1)}\mathbf{h}_2 + \mathbf{n}_2^{(k-1)}, \tag{3.51}$$

$$\mathbf{y}_2^{(k)} = \mathbf{X}_2^{(k)}\mathbf{h}_2 + \mathbf{n}_2^{(k)} = \frac{\mathbf{U}_2^{(k)}\mathbf{X}_2^{(k-1)}\mathbf{h}_2}{d_2^{(k-1)}} + \mathbf{n}_2^{(k)}, \tag{3.52}$$

respectively. The ML detector for the first subsystem is expressed as:

$$\begin{aligned}
&\min_{s_1^{(k)},s_2^{(k)},\tilde{s}_3^{(k)},\tilde{s}_4^{(k)}} \left|\left|\mathbf{y}_1^{(k)} - \frac{\mathbf{U}_1^{(k)}\mathbf{y}_1^{(k-1)}}{d_1^{(k-1)}}\right|\right|^2 = \min_{s_1^{(k)},s_2^{(k)},\tilde{s}_3^{(k)},\tilde{s}_4^{(k)}} \left\{ \frac{\left|s_1^k + \tilde{s}_3^k\right|^2}{d_1^{k-1}} \left(\left|y_1^{k-1}\right|^2 + \left|y_2^{k-1}\right|^2\right) \right. \\
&+ \frac{\left|s_2^k + \tilde{s}_4^k\right|^2}{d_1^{k-1}} \left(\left|y_1^{k-1}\right|^2 + \left|y_2^{k-1}\right|^2\right) - 2\mathrm{Re}\left\{\left(y_1^{k-1}\left(y_1^k\right)^* + \left(y_2^{k-1}\right)^* y_2^k\right)\left(s_1^k + \tilde{s}_3^k\right)\right\} \\
&\left. - 2\mathrm{Re}\left\{\left(y_2^{k-1}\left(y_1^k\right)^* - \left(y_1^{k-1}\right)^* y_2^k\right)\left(s_2^k + \tilde{s}_4^k\right)\right\}\right\}.
\end{aligned} \tag{3.53}$$

The ML detector for the second subsystem is expressed as:

$$\begin{aligned}
&\min_{s_1^{(k)},s_2^{(k)},\tilde{s}_3^{(k)},\tilde{s}_4^{(k)}} \left|\left|\mathbf{y}_2^{(k)} - \frac{\mathbf{U}_2^{(k)}\mathbf{y}_2^{(k-1)}}{d_2^{(k-1)}}\right|\right|^2 = \min_{s_1^{(k)},s_2^{(k)},\tilde{s}_3^{(k)},\tilde{s}_4^{(k)}} \left\{ \frac{\left|s_1^k - \tilde{s}_3^k\right|^2}{d_2^{k-1}} \left(\left|y_3^{k-1}\right|^2 + \left|y_4^{k-1}\right|^2\right) \right. \\
&+ \frac{\left|s_2^k - \tilde{s}_4^k\right|^2}{d_2^{k-1}} \left(\left|y_3^{k-1}\right|^2 + \left|y_4^{k-1}\right|^2\right) - 2\mathrm{Re}\left\{\left(y_3^{k-1}\left(y_3^k\right)^* + \left(y_4^{k-1}\right)^* y_4^k\right)\left(s_1^k - \tilde{s}_3^k\right)\right\} \\
&\left. - 2\mathrm{Re}\left\{\left(y_4^{k-1}\left(y_3^k\right)^* - \left(y_3^{k-1}\right)^* y_4^k\right)\left(s_2^k - \tilde{s}_4^k\right)\right\}\right\}.
\end{aligned} \tag{3.54}$$

The ML detector for the whole system is the sum of the ML detectors of the first and second subsystem, given by:

$$\begin{aligned}\min_{s_1^{(k)},s_2^{(k)},\tilde{s}_3^{(k)},\tilde{s}_4^{(k)}} \quad & \Bigg\{ \frac{\left|s_1^k+\tilde{s}_3^k\right|^2}{d_1^{k-1}}\left(\left|y_1^{k-1}\right|^2+\left|y_2^{k-1}\right|^2\right)+\frac{\left|s_1^k-\tilde{s}_3^k\right|^2}{d_2^{k-1}}\left(\left|y_3^{k-1}\right|^2+\left|y_4^{k-1}\right|^2\right) \\ & + \frac{\left|s_2^k+\tilde{s}_4^k\right|^2}{d_1^{k-1}}\left(\left|y_1^{k-1}\right|^2+\left|y_2^{k-1}\right|^2\right)+\frac{\left|s_2^k-\tilde{s}_4^k\right|^2}{d_2^{k-1}}\left(\left|y_3^{k-1}\right|^2+\left|y_4^{k-1}\right|^2\right) \\ & -2\mathrm{Re}\left\{\left(y_1^{k-1}\left(y_1^k\right)^*+\left(y_2^{k-1}\right)^* y_2^k\right)\left(s_1^k+\tilde{s}_3^k\right)\right\} \\ & -2\mathrm{Re}\left\{\left(y_3^{k-1}\left(y_3^k\right)^*+\left(y_4^{k-1}\right)^* y_4^k\right)\left(s_1^k-\tilde{s}_3^k\right)\right\} \\ & -2\mathrm{Re}\left\{\left(y_2^{k-1}\left(y_1^k\right)^*-\left(y_1^{k-1}\right)^* y_2^k\right)\left(s_2^k+\tilde{s}_4^k\right)\right\} \\ & -2\mathrm{Re}\left\{\left(y_4^{k-1}\left(y_3^k\right)^*-\left(y_3^{k-1}\right)^* y_4^k\right)\left(s_2^k-\tilde{s}_4^k\right)\right\}\Bigg\}. \end{aligned} \tag{3.55}$$

To decode the signals, the following pair-wise decoder for the differential QOST-BCs proposed in [67] can be used

$$\min_{s_1^{(k)},\tilde{s}_3^{(k)}} g_{13}(s_1^{(k)},\tilde{s}_3^{(k)})+\min_{s_2^{(k)},\tilde{s}_4^{(k)}} g_{24}(s_2^{(k)},\tilde{s}_4^{(k)}) \tag{3.56}$$

where

$$\begin{aligned} g_{13}(s_1^k,\tilde{s}_3^k) &= \frac{\left|s_1^k+\tilde{s}_3^k\right|^2}{d_1^{k-1}}\left(\left|y_1^{k-1}\right|^2+\left|y_2^{k-1}\right|^2\right)+\frac{\left|s_1^k-\tilde{s}_3^k\right|^2}{d_2^{k-1}}\left(\left|y_3^{k-1}\right|^2+\left|y_4^{k-1}\right|^2\right) \\ &- 2\mathrm{Re}\left\{\left(y_1^{k-1}\left(y_1^k\right)^*+\left(y_2^{k-1}\right)^* y_2^k\right)\left(s_1^k+\tilde{s}_3^k\right)\right. \\ &- \left.\left(y_3^{k-1}\left(y_3^k\right)^*+\left(y_4^{k-1}\right)^* y_4^k\right)\left(s_1^k-\tilde{s}_3^k\right)\right\}, \end{aligned} \tag{3.57}$$

$$\begin{aligned} g_{24}(s_2^k,\tilde{s}_4^k) &= \frac{\left|s_2^k+\tilde{s}_4^k\right|^2}{d_1^{k-1}}\left(\left|y_1^{k-1}\right|^2+\left|y_2^{k-1}\right|^2\right)+\frac{\left|s_2^k-\tilde{s}_4^k\right|^2}{d_2^{k-1}}\left(\left|y_3^{k-1}\right|^2+\left|y_4^{k-1}\right|^2\right) \\ &- 2\mathrm{Re}\left\{\left(y_2^{k-1}\left(y_1^k\right)^*-\left(y_1^{k-1}\right)^* y_2^k\right)\left(s_2^k+\tilde{s}_4^k\right)\right. \\ &- \left.\left(y_4^{k-1}\left(y_3^k\right)^*-\left(y_3^{k-1}\right)^* y_4^k\right)\left(s_2^k-\tilde{s}_4^k\right)\right\}. \end{aligned} \tag{3.58}$$

Following the idea of the coherent case, let us develop the suboptimal decoder of $s_1^{(k)}$ and $\tilde{s}_3^{(k)}$. The decoding procedure for $s_2^{(k)}$ and $\tilde{s}_4^{(k)}$ follows similar steps. By simple manipulation, the metric function for $s_1^{(k)}$ and $\tilde{s}_3^{(k)}$ in (3.57) can be expressed as:

$$\begin{aligned}
g_{13}(s_1^{(k)}, \tilde{s}_3^{(k)}) = & \frac{\left|s_1^{(k)}\right|^2}{d_1^{(k-1)}} \left(\left|y_1^{(k-1)}\right|^2 + \left|y_2^{(k-1)}\right|^2 \right) + \frac{\left|s_1^{(k)}\right|^2}{d_2^{(k-1)}} \left(\left|y_3^{(k-1)}\right|^2 + \left|y_4^{(k-1)}\right|^2 \right) \\
& - 2\mathrm{Re}\left\{ \left(y_1^{(k-1)} \left(y_1^{(k)}\right)^* + \left(y_2^{(k-1)}\right)^* y_2^{(k)} + y_3^{(k-1)} \left(y_3^{(k)}\right)^* + \left(y_4^{(k-1)}\right)^* y_4^{(k)} \right) s_1^{(k)} \right\} \\
& + \frac{\left|\tilde{s}_3^{(k)}\right|^2}{d_1^{(k-1)}} \left(\left|y_1^{(k-1)}\right|^2 + \left|y_2^{(k-1)}\right|^2 \right) + \frac{\left|\tilde{s}_3^{(k)}\right|^2}{d_2^{(k-1)}} \left(\left|y_3^{(k-1)}\right|^2 + \left|y_4^{(k-1)}\right|^2 \right) \\
& - 2\mathrm{Re}\left\{ \left(y_1^{(k-1)} \left(y_1^{(k)}\right)^* + \left(y_2^{(k-1)}\right)^* y_2^{(k)} - y_3^{(k-1)} \left(y_3^{(k)}\right)^* - \left(y_4^{(k-1)}\right)^* y_4^{(k)} \right) \tilde{s}_3^{(k)} \right\} \\
& + 2 \left(\frac{|y_1^{(k-1)}|^2 + |y_2^{(k-1)}|^2}{d_1^{(k-1)}} - \frac{|y_3^{(k-1)}|^2 + |y_4^{(k-1)}|^2}{d_2^{(k-1)}} \right) \mathrm{Re}\left\{ s_1^{(k)} \left(\tilde{s}_3^{(k)}\right)^* \right\}. \qquad (3.59)
\end{aligned}$$

If the decoder knows $s_3^{(k)}$, then (3.59) can be reduced to

$$\begin{aligned}
g_1(s_1^{(k)}, \tilde{s}_3^{(k)}) = & \frac{\left|s_1^{(k)}\right|^2}{d_1^{(k-1)}} \left(\left|y_1^{(k-1)}\right|^2 + \left|y_2^{(k-1)}\right|^2 \right) + \frac{\left|s_1^{(k)}\right|^2}{d_2^{(k-1)}} \left(\left|y_3^{(k-1)}\right|^2 + \left|y_4^{(k-1)}\right|^2 \right) \\
& - 2\mathrm{Re}\left\{ \left(y_1^{(k-1)} \left(y_1^{(k)}\right)^* + \left(y_2^{(k-1)}\right)^* y_2^{(k)} + y_3^{(k-1)} \left(y_3^{(k)}\right)^* + \left(y_4^{(k-1)}\right)^* y_4^{(k)} \right) s_1^{(k)} \right\} \\
& + 2 \left(\frac{|y_1^{(k-1)}|^2 + |y_2^{(k-1)}|^2}{d_1^{(k-1)}} - \frac{|y_3^{(k-1)}|^2 + |y_4^{(k-1)}|^2}{d_2^{(k-1)}} \right) \mathrm{Re}\left\{ s_1^{(k)} \left(\tilde{s}_3^{(k)}\right)^* \right\} \qquad (3.60)
\end{aligned}$$

to decode $s_1^{(k)}$. Similarly, if the decoder knows $s_1^{(k)}$, then (3.59) can be reduced to

$$\begin{aligned}
g_3(s_1^{(k)}, \tilde{s}_3^{(k)}) = & \frac{\left|\tilde{s}_3^{(k)}\right|^2}{d_1^{(k-1)}} \left(\left|y_1^{(k-1)}\right|^2 + \left|y_2^{(k-1)}\right|^2 \right) + \frac{\left|\tilde{s}_3^{(k)}\right|^2}{d_2^{(k-1)}} \left(\left|y_3^{(k-1)}\right|^2 + \left|y_4^{(k-1)}\right|^2 \right) \\
& - 2\mathrm{Re}\left\{ \left(y_1^{(k-1)} \left(y_1^{(k)}\right)^* + \left(y_2^{(k-1)}\right)^* y_2^{(k)} - y_3^{(k-1)} \left(y_3^{(k)}\right)^* - \left(y_4^{(k-1)}\right)^* y_4^{(k)} \right) \tilde{s}_3^{(k)} \right\} \\
& + 2 \left(\frac{|y_1^{(k-1)}|^2 + |y_2^{(k-1)}|^2}{d_1^{(k-1)}} - \frac{|y_3^{(k-1)}|^2 + |y_4^{(k-1)}|^2}{d_2^{(k-1)}} \right) \mathrm{Re}\left\{ s_1^{(k)} \left(\tilde{s}_3^{(k)}\right)^* \right\} \qquad (3.61)
\end{aligned}$$

to decode $s_3^{(k)}$. Similar to Sec. 3.3.1, we use (3.61) to obtain a first estimate of $s_3^{(k)}$ ($\hat{s}_3^{(k)}(1)$) with the initial value $\breve{s}_1^{(k)}(1) = \text{rnd}({s'_1}^{(k)}, 1)$ where

$${s'_1}^{(k)} \triangleq \frac{\left(y_1^{(k-1)}\right)^* y_1^{(k)} + y_2^{(k-1)} \left(y_2^{(k)}\right)^*}{2\left(\left|y_1^{(k-1)}\right|^2 + \left|y_2^{(k-1)}\right|^2\right)} + \frac{\left(y_3^{(k-1)}\right)^* y_3^{(k)} + y_4^{(k-1)} \left(y_4^{(k)}\right)^*}{2\left(\left|y_3^{(k-1)}\right|^2 + \left|y_4^{(k-1)}\right|^2\right)}.$$

The value of ${s'_1}^{(k)}$ is computed by neglecting the noise and relaxing the finite alphabet constraint. The rest of the decoding procedure follows same steps of the one presented in Sec. 3.3.1, but using (3.60) and (3.61) instead of (3.33) and (3.34), respectively. The decoding algorithm is summarized as follows.

Decoding Algorithm

1. Set $m = 1$.

2. Compute $\breve{s}_1^{(k)}(m) = \text{rnd}({s'_1}^{(k)}, m)$. Substitute $\breve{s}_1^{(k)}(m)$ in (3.61) and find

$$\hat{s}_3^{(k)}(m) = \arg \min_{s_3^{(k)} \in \mathcal{S}} g_3(\breve{s}_1^{(k)}(m), \tilde{s}_3^{(k)} = s_3^{(k)} e^{j\phi}).$$

   Substitute $\hat{s}_3^{(k)}(m)$ in (3.60) and find

$$\hat{s}_1^{(k)}(m) = \arg \min_{s_1^{(k)} \in \mathcal{S}} g_1(s_1^{(k)}, \hat{s}_3^{(k)}(m) e^{j\phi})$$

3. If $d^{(k)} \triangleq \frac{c_0}{|s_1^{(k)}(1) - {s'_1}^{(k)}|} > \alpha$, then set $\hat{s}_1^{(k)}(m)$ and $\hat{s}_3^{(k)}(m)$ as the final output estimates and terminate. Otherwise go to Step 4.

4. Repeat Step 2 for $m = 2, 3$ and find

$$\tilde{m} = \arg \min_{m=1,2,3} g_{13}(\hat{s}_1^{(k)}(m), \hat{s}_3^{(k)}(m) e^{j\phi}).$$

   Set $\hat{s}_1^{(k)}(\tilde{m})$ and $\hat{s}_3^{(k)}(\tilde{m})$ as the final output estimates.

3.4 The Proposed Low Complexity Decoder for Four Transmit Antennas

In this section, we extend the results obtained in the previous sections, Sec. 3.3.1 and Sec. 3.3.2, for the case of four transmit antennas where we consider the following QOSTBC

$$\mathbf{X} = \begin{bmatrix} x_1 & x_2 & 0 & 0 \\ -x_2^* & x_1^* & 0 & 0 \\ 0 & 0 & x_3 & x_4 \\ 0 & 0 & -x_4^* & x_3^* \end{bmatrix} \tag{3.62}$$

and the symbols are chosen according to (3.22) and (3.23). Using (3.22), (3.23) and (3.62) in (3.19), then we can express (3.19) as:

$$\begin{bmatrix} y_1 \\ y_2 \\ y_3 \\ y_4 \end{bmatrix} = \begin{bmatrix} s_1 + \tilde{s}_3 & s_2 + \tilde{s}_4 & 0 & 0 \\ -(s_2 + \tilde{s}_4)^* & (s_1 + \tilde{s}_3)^* & 0 & 0 \\ 0 & 0 & s_1 - \tilde{s}_3 & s_2 - \tilde{s}_4 \\ 0 & 0 & -(s_2 - \tilde{s}_4)^* & (s_1 - \tilde{s}_3)^* \end{bmatrix} \begin{bmatrix} h_1 \\ h_2 \\ h_3 \\ h_4 \end{bmatrix} \tag{3.63}$$

where h_4 is the channel between the fourth transmit antenna and the receiver. Let us define $\tilde{h}_1 = (h_1 + h_3)$, $\tilde{h}_2 = (h_1 - h_3)$, $\tilde{h}_3 = (h_2 + h_4)$, and $\tilde{h}_4 = (h_2 - h_4)$, then we can rewrite (3.63) as:

$$\underbrace{\begin{bmatrix} y_1 + y_3 \\ y_1 - y_3 \\ y_2 + y_4 \\ y_2 - y_4 \end{bmatrix}}_{\tilde{\mathbf{y}}} = \underbrace{\begin{bmatrix} s_1 & \tilde{s}_3 & s_2 & \tilde{s}_4 \\ \tilde{s}_3 & s_1 & \tilde{s}_4 & s_2 \\ -(s_2)^* & -(\tilde{s}_4)^* & (s_1)^* & (\tilde{s}_3)^* \\ -(\tilde{s}_4)^* & -(s_2)^* & (\tilde{s}_3)^* & (s_1)^* \end{bmatrix}}_{\mathbf{S}} \underbrace{\begin{bmatrix} \tilde{h}_1 \\ \tilde{h}_2 \\ \tilde{h}_3 \\ \tilde{h}_4 \end{bmatrix}}_{\tilde{\mathbf{h}}} \tag{3.64}$$

The columns of the QOSTBC matrix in (3.64) are not orthogonal to each other

with respect to the symbols $s_i, i = 1, \cdots, 4$ where

$$\mathbf{S}^H\mathbf{S} = \begin{bmatrix} \alpha_1 & \alpha_5 & 0 & 0 \\ \alpha_5 & \alpha_1 & 0 & 0 \\ 0 & 0 & \alpha_1 & \alpha_5 \\ 0 & 0 & \alpha_5 & \alpha_1 \end{bmatrix},$$

$\alpha_1 = \sum_{i=1}^{4} |s_i|^2$ and $\alpha_5 = 2\Re\{s_1^* s_3 + s_2^* s_4\}$. As in the case of $M_t = 3$, we can obtain two equations similar to (3.24) and (3.25) from the system model in (3.19) and derive f_{13}, f_1, f_3 and s_1'. After using this procedure, we can redefine them for the case of $M_t = 4$ as:

$$\begin{aligned} f_{13}(s_1, \tilde{s}_3) &= |s_1|^2(|h_1|^2 + |h_2|^2 + |h_3|^2 + |h_4|^2) \\ &- 2\,\mathrm{Re}\{(h_1 y_1^* + h_2^* y_2 + h_3 y_3^* + h_4^* y_4)s_1\} \\ &+ |\tilde{s}_3|^2(|h_1|^2 + |h_2|^2 + |h_3|^2 + |h_4|^2) \\ &- 2\,\mathrm{Re}\{(h_1 y_1^* + h_2^* y_2 - h_3 y_3^* - h_4^* y_4)\tilde{s}_3\} \\ &+ 2(|h_1|^2 + |h_2|^2 - |h_3|^2 - |h_4|^2)\mathrm{Re}\{s_1 \tilde{s}_3^*\}, \end{aligned} \tag{3.65}$$

$$\begin{aligned} f_1(s_1, \tilde{s}_3) &= |s_1|^2(|h_1|^2 + |h_2|^2 + |h_3|^2 + |h_4|^2) \\ &- 2\,\mathrm{Re}\{(h_1 y_1^* + h_2^* y_2 + h_3 y_3^* + h_4^* y_4)s_1\} \\ &+ 2(|h_1|^2 + |h_2|^2 - |h_3|^2 - |h_4|^2)\mathrm{Re}\{s_1 \tilde{s}_3^*\}, \end{aligned} \tag{3.66}$$

$$\begin{aligned} f_3(s_1, \tilde{s}_3) &= |\tilde{s}_3|^2(|h_1|^2 + |h_2|^2 + |h_3|^2 + |h_4|^2) \\ &- 2\,\mathrm{Re}\{(h_1 y_1^* + h_2^* y_2 - h_3 y_3^* - h_4^* y_4)\tilde{s}_3\} \\ &+ 2(|h_1|^2 + |h_2|^2 - |h_3|^2 - |h_4|^2)\mathrm{Re}\{s_1 \tilde{s}_3^*\}, \end{aligned} \tag{3.67}$$

$$s_1' = \frac{h_1^* y_1 + h_2 y_2^*}{2(|h_1|^2 + |h_2|^2)} + \frac{h_3^* y_3 + h_4 y_4^*}{2(|h_3|^2 + |h_4|^2)}. \tag{3.68}$$

In the non-coherent case, all the equations in Sec. 3.3.2 are also valid for four transmit antennas $M_t = 4$.

3.5 Simulations

In this section, the performance and complexity of the proposed decoder are evaluated and compared with several other popular schemes known from the literature. The nearly optimal value of $\gamma = 4$ has been chosen to compute α in (3.43). The value of K is selected based on simulations and depends on the constellation type and the receiver used. Note that the larger the value of K, the higher the complexity and the closer the performance of the proposed algorithm to that of the ML decoder. Therefore, a tradeoff between the performance and complexity should be taken into account when selecting K.

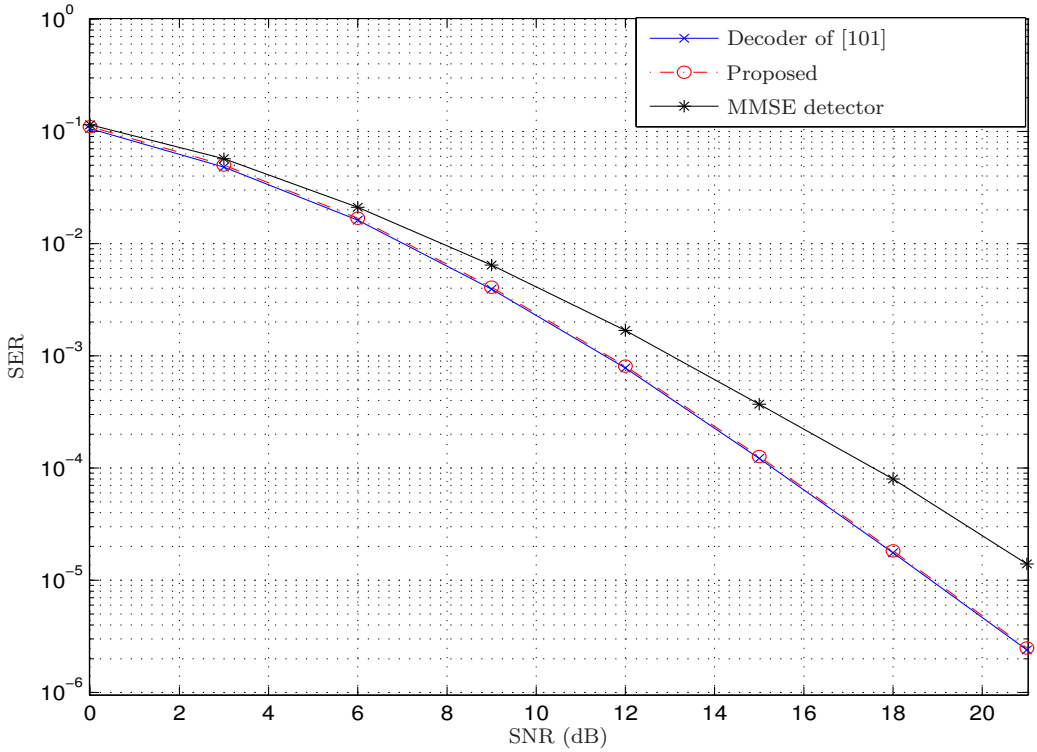

Figure 3.1: SER versus SNR for the coherent QOSTBC using different decoders and BPSK modulation.

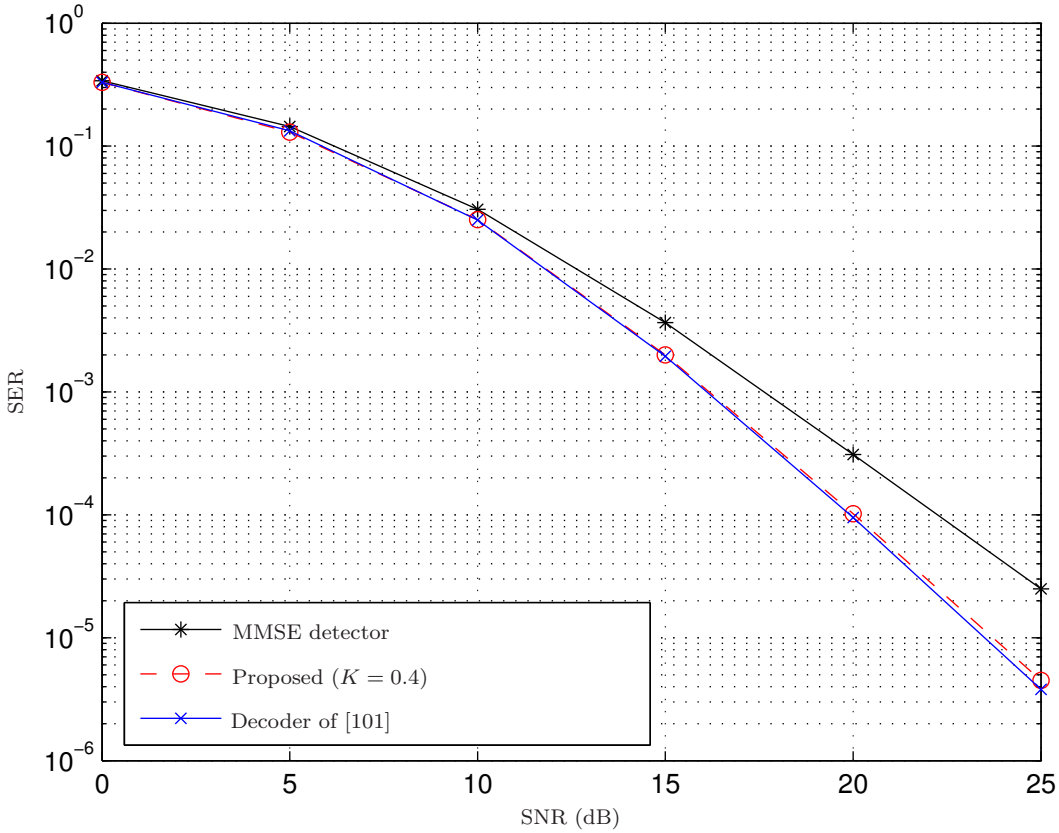

Figure 3.2: SER versus SNR for the coherent QOSTBC using different decoders and QPSK modulation.

We have assumed independent quasi-static Rayleigh flat-fading channels. First, we compare the performance of the coherent QOSTBC using the linear minimum mean squared error (MMSE) detector [103] and the decoders of [101] and of Sec. 3.3.1. Throughout the simulations, we have assumed a system with three transmit antennas ($M_t = 3$) and one receive antenna ($M_r = 1$). In the approach of [101], we have used the sphere decoder of [109] modified for a finite alphabet. In Figs. 3.1, 3.2 and 3.3, the symbol error rate (SER) is shown versus SNR for the BPSK, QPSK and 16-QAM constellations, respectively. From

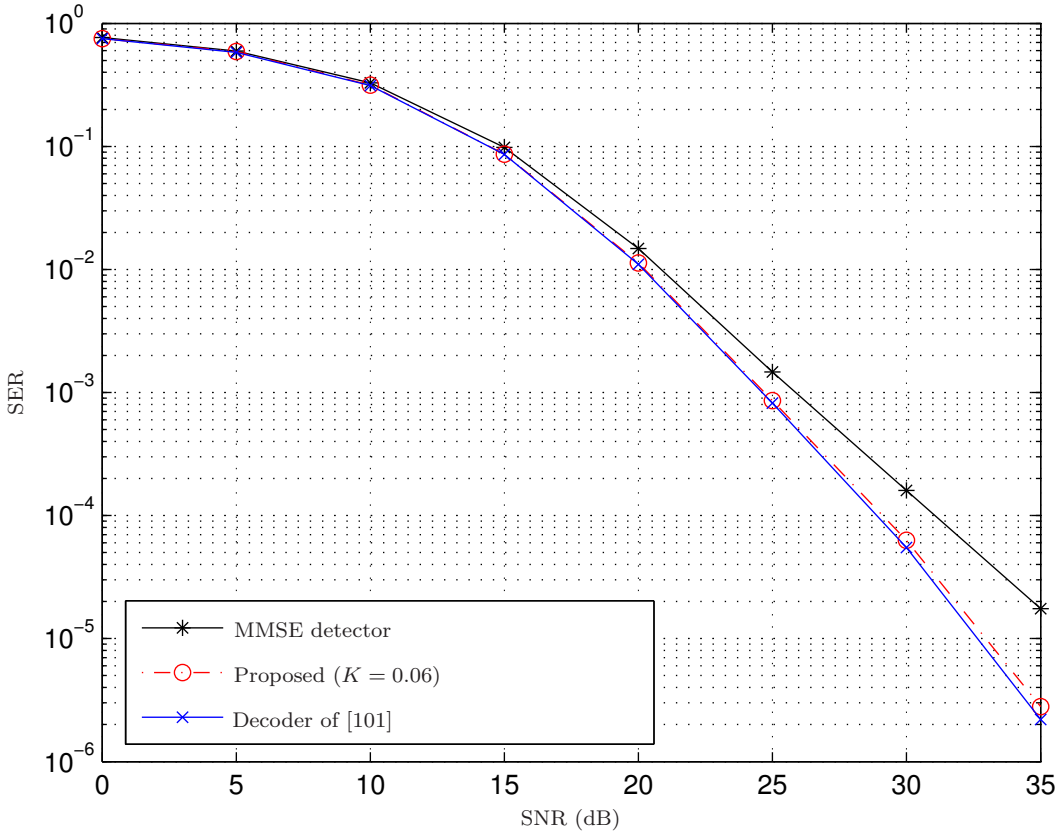

Figure 3.3: SER versus SNR for the coherent QOSTBC using different decoders and 16-QAM modulation.

Figs. 3.1, 3.2 and 3.3, it can be observed that the proposed decoder outperforms the linear MMSE detector and has a very close performance to the approach of [101]. Next, we compare the complexity in terms of the average number of operations for decoding the coherent QOSTBC for the 16-QAM modulation using the linear MMSE detector, the full-search pair-wise decoder and the methods of [101] and of Sec. 3.3.1. Fig. 3.4 shows the number of real-valued arithmetic operations (addition, subtraction, multiplication and division) per symbol versus SNR for all decoders. It can be observed that the proposed decoder has a

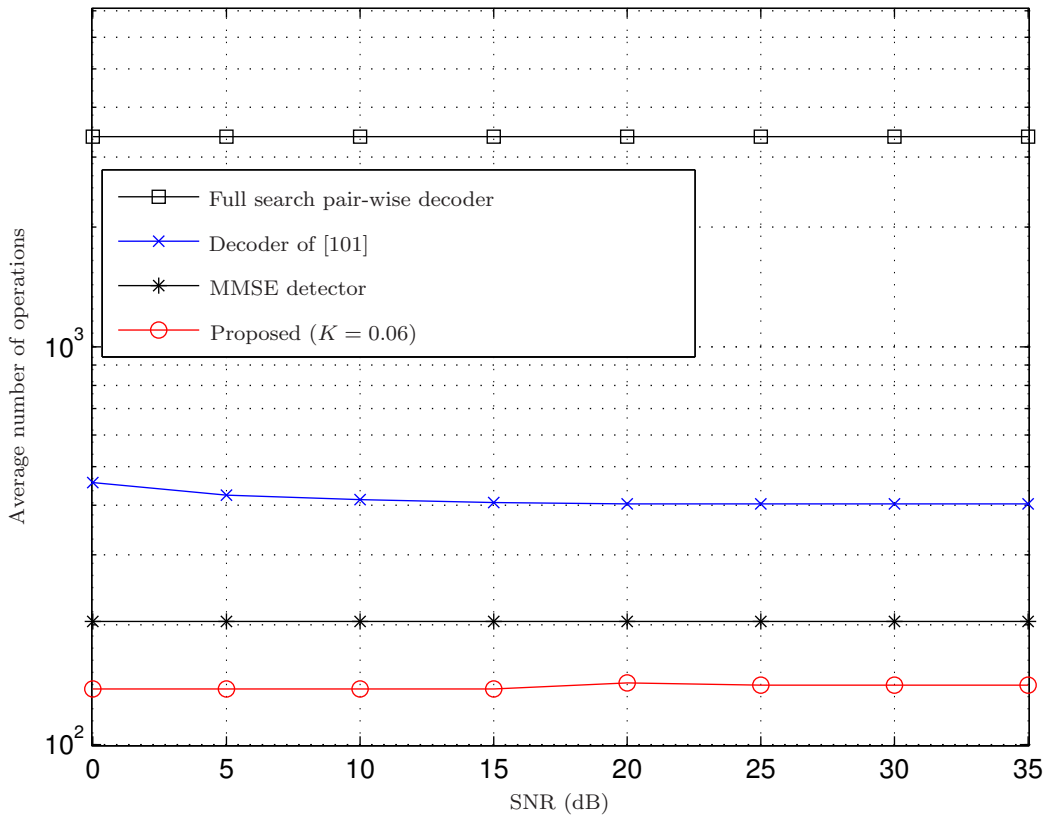

Figure 3.4: The average number of operations per symbol versus SNR for the coherent QOSTBC using different decoders and 16-QAM modulation.

substantially reduced number of operations. Note, however, that the number of operations for the linear MMSE detector does not depend on the constellation size. Figs. 3.5 and 3.6 display the SER versus SNR for the non-coherent QOSTBC using the proposed and the full-search pair-wise decoders for the BPSK and QPSK constellations, respectively. It can be seen that the proposed decoder has a very close performance to that of the ML decoder. Table 3.1 shows the number of symbols that were decoded using the case $d < \alpha$ (i.e., Step 4 of the proposed algorithms) as percentage of the total number of transmitted symbols

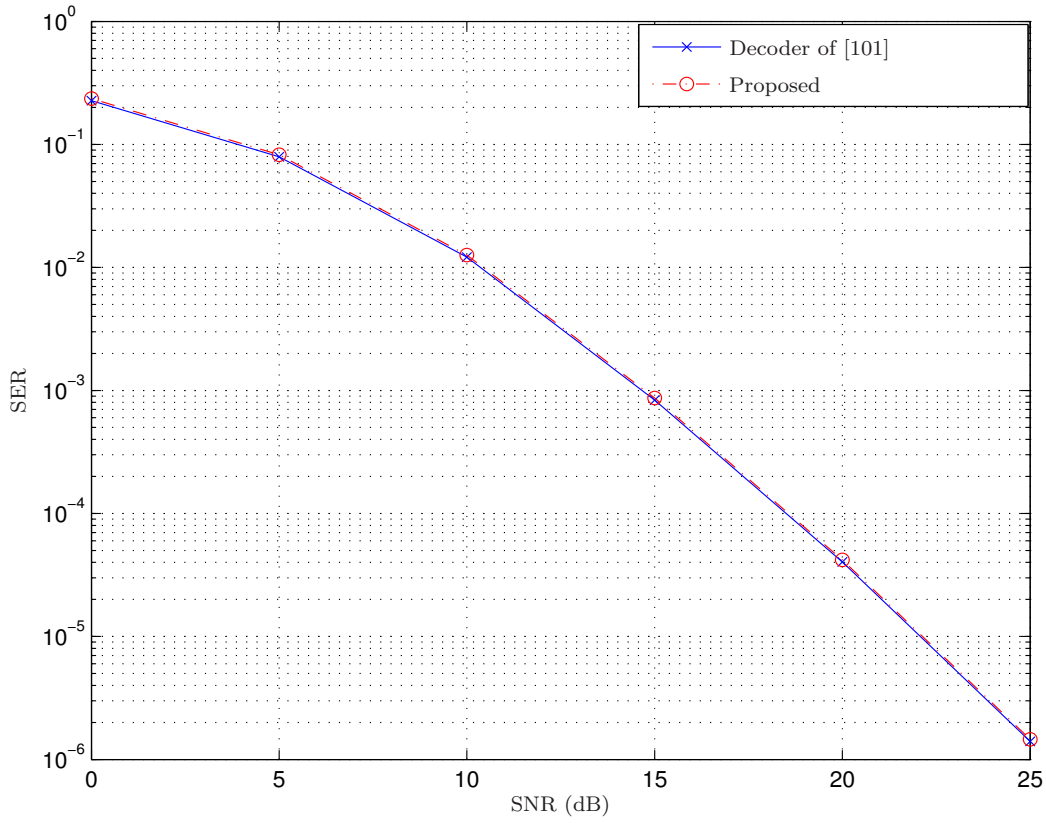

Figure 3.5: SER versus SNR for the differential QOSTBC using different decoders and BPSK modulation.

Table 3.1: Percentage of symbols decoded using Step 4 of the proposed algorithms.

Decoder	$\mathcal{S}$, K	SNR(dB)					
		0-10	15	20	25	30	35
Coherent	QPSK, $K = 0.4$	0%	1.6%	0.74%	0.29%	0.095%	0.028%
	16-QAM, $K = 0.06$	0%	0%	2.58%	0.67%	0.16%	0.035%
Non-coherent	QPSK, $K = 0.24$	0%	4.75%	2.41%	0.86%	0.31%	0.092%

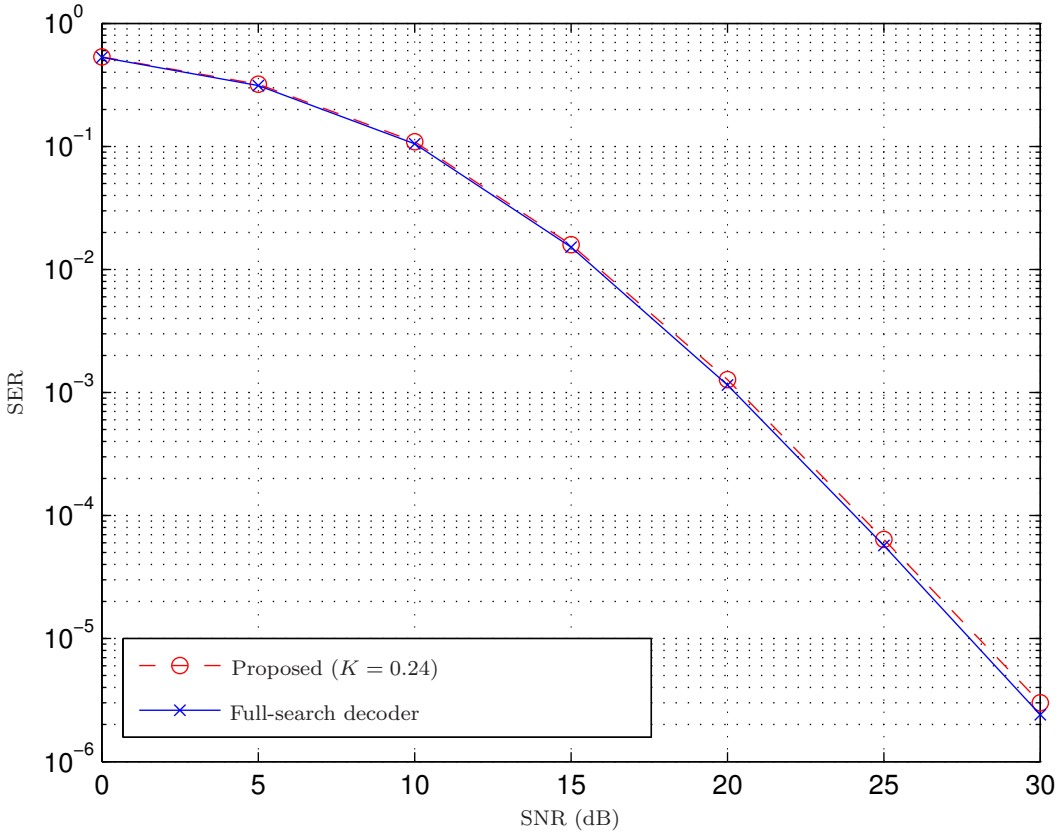

Figure 3.6: SER versus SNR for the differential QOSTBC using different decoders and QPSK modulation.

for different values of SNR. We consider the QPSK and 16-QAM modulations for the coherent case and the QPSK modulation for the non-coherent case. As discussed in Sec. 3.3.1, the decoding complexity when $d \geq \alpha$ is comparable to that of the symbol-wise decoder. It can be seen from Table 3.1 that a very low percentage of the decoded symbols needs to resort to Step 4 of the proposed algorithms. Therefore, the complexity of the proposed decoders is nearly similar to the symbol-wise decoder. Finally, we show in Table 3.2 the percentage of symbols decoded using Step 4 of our algorithm, and in Fig. 3.7, the SER perfor-

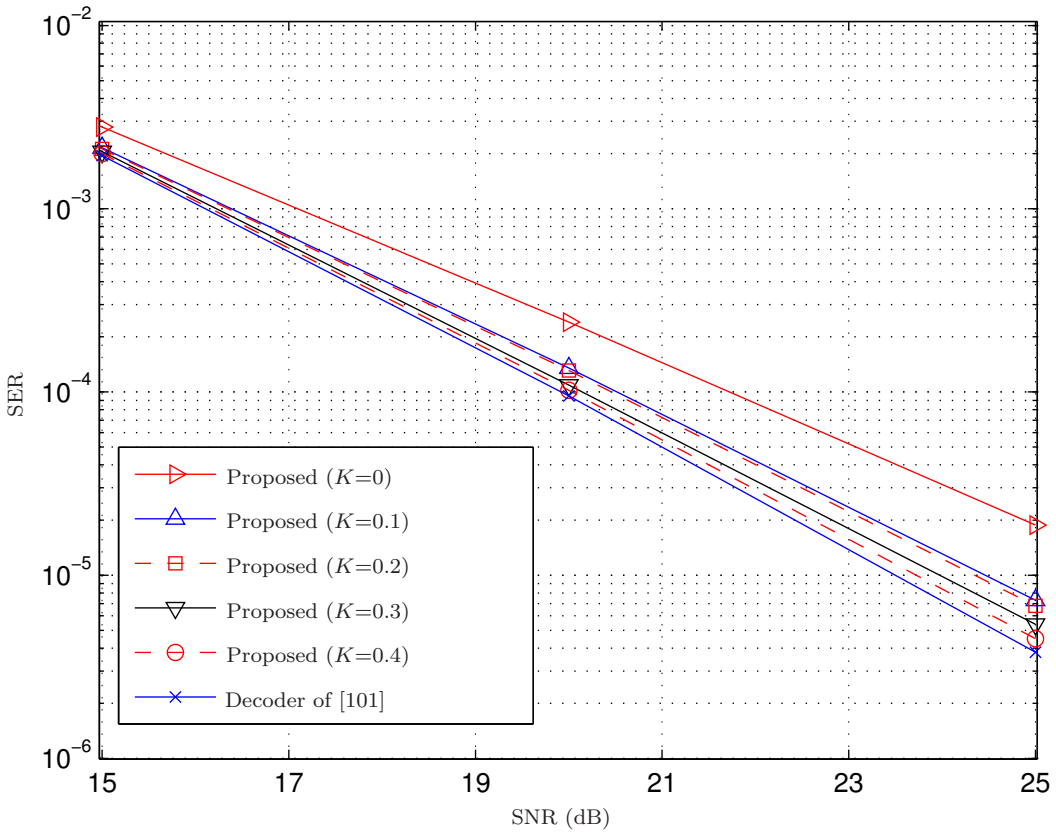

Figure 3.7: SER versus SNR for the coherent QOSTBC with QPSK using different K's.

Table 3.2: Percentage of symbols decoded using Step 4 of the proposed algorithm.

SNR(dB)	K			
	0.1	0.2	0.3	0.4
0-10	0%	0%	0%	0%
15	0.45%	0.84%	1.24%	1.60%
20	0.13%	0.29%	0.49%	0.74%
25	0.035%	0.094%	0.185%	0.29%

mance versus SNR for different values of K using QPSK to illustrate the tradeoff between the complexity and performance when selecting K. It can be observed that the larger the value of K, the better the performance and the higher the computational complexity.

3.6 Conclusion

A low complexity suboptimal decoder for the coherent and non-coherent QOST-BCs is proposed. Numerical results have shown that the proposed decoder can provide a substantially improved tradeoff between the complexity and performance in comparison to current known decoding schemes.

Chapter 4

Distributed Space-Time Block Coding in Decode and Forward Relay Networks

For TWRNs, the simultaneous bidirectional transmission has been shown to outperform other strategies using DF-DSTC, thanks to its high spectral efficiency. However, it has a rather high relay decoding complexity and cannot use the direct link between the communicating terminals.

In this chapter, we propose a novel DSTC transmission scheme for TWRNs which avoids the latter disadvantages at the same symbol rate and with a performance advantage at high powers. Furthermore, the proposed strategy allows the communicating terminals to use the direct link between them to achieve a higher diversity gain. An extension of the proposed strategy to the differential case is also discussed.

4.1 Introduction

The use of MIMO techniques in ad-hoc networks may not be feasible due to their size, cost, or hardware constraints. As an alternative, cooperative communica-

tions have been proposed to achieve gains similar to that of MIMO systems. In this form of spatial diversity, the cooperating nodes retransmit the signal received from the source node through multiple available channel pathes. Several cooperative transmission protocols have been proposed [14–16, 29]. These protocols can be divided into two principal classes: the AF and the DF protocols.

In [110, 111, 113–120] and references therein, the case of two-way communication between two terminals with multiple relays in between has been studied. The bidirectional simultaneous data transmission approach has been proposed in these works to increase the spectral efficiency with respect to the conventional unidirectional relaying schemes.

Recently, DSTC techniques have been introduced as they can improve the performance of wireless networks without using CSI at the transmitter. In other words, these techniques combine both STC and cooperative communication techniques to design a communication system capable of improving the reliability and throughput of the wireless networks. Several distributed space-time coded modulation techniques and their performance analyses can be found in [18,78,113,121].

In [113], different protocols for TWRNs using DSTC have been considered. The authors in [113] have shown that the so-called two-phase partial decode-and-forward II (2-phase PDF) protocol outperforms all other strategies. However, the relay decoding complexity of 2-phase PDF is rather high, as the under-determined ML decoder, which has more symbols to detect than received, used in it is based on a full search over the symbols that are simultaneously transmitted from both terminals.

Taking into account the computational limitations that apply to the relay nodes, we propose a simple protocol to achieve the same symbol rate as 2-phase PDF but with a substantially lower relay decoding complexity. Moreover, the proposed protocol outperforms the previously proposed protocols and can additionally use the direct link between the two communicating terminals. We also develop an extension of our protocol to networks without CSI using differential DSTC. Simulations show substantial performance advantages of the proposed schemes as compared to the earlier methods.

4.2 Wireless Relay Network Model

We consider a half-duplex TWRN with $R + 2$ single-antenna nodes as in Sec. 2.4.3.1 where the two terminals, $\mathcal{T}_1$ and $\mathcal{T}_2$, intend to communicate with each other via R relay nodes, $(\mathcal{R}_1, \ldots, \mathcal{R}_R)$, as shown in Fig. 2.14. In this chapter, similar assumptions as in Sec. 2.4.3.1 are considered. We further assume extended block fading channel model where the channels remain constant during $2T$ time slots and change to an independent realization afterwards.

4.3 Two-Phase Two-Way Distributed Space-Time Coding Protocol

We consider here briefly the 2-phase PDF protocol proposed in [113], as it has been shown to achieve the best error rate performance [113]. In the first phase of this protocol, from time slot 1 to T, $\mathcal{T}_1$ and $\mathcal{T}_2$ transmit simultaneously the $T \times 1$ information symbol vectors $\mathbf{s}_{\mathcal{T}_1}$ and $\mathbf{s}_{\mathcal{T}_2}$, respectively, to the relays where $[\mathbf{s}_{\mathcal{T}_1}]_i \in \mathcal{S}_{\mathcal{T}_1}$, $[\mathbf{s}_{\mathcal{T}_2}]_i \in \mathcal{S}_{\mathcal{T}_2}$, $[\mathbf{s}_{\mathcal{T}_t}]_i$ denotes the ith entry of a vector $\mathbf{s}_{\mathcal{T}_1}$, and $\mathcal{S}_{\mathcal{T}_1}$ and $\mathcal{S}_{\mathcal{T}_2}$ are two, possibly different, symbol constellations.

Each relay decodes the received symbols of the first and second terminal using the ML decoder. Note that there are more symbols to detect than received where two symbols are obtained in the first time slot and thus, the decoder suffers from a high complexity and can have a poor performance. To achieve the full diversity, the authors in [113] proposed the use of cyclic redundancy check (CRC) in the first phase, at the cost of reducing the spectral efficiency.

After decoding, the information symbols of the first and the second terminals at the rth relay, $\tilde{\mathbf{s}}_{\mathcal{T}_1,r}$ and $\tilde{\mathbf{s}}_{\mathcal{T}_2,r}$, respectively, are combined into one single symbol vector as $\mathbf{s}_{\mathcal{R},r} = \mathcal{F}(\tilde{\mathbf{s}}_{\mathcal{T}_1,r}, \tilde{\mathbf{s}}_{\mathcal{T}_2,r})$ where $\mathcal{F}(\cdot,\cdot)$ is a combination function that avoids the transmission of redundant information to the destination terminals as explained in Sec. 2.4.3. In [113], modular arithmetic was proposed to superimpose the symbols. Notice that $\mathbf{s}_{\mathcal{R},r} \in \mathcal{S}_{\mathcal{R}}$ where $\mathcal{S}_{\mathcal{R}}$ is the constellation of the

transmitted symbols from the relays and $|\mathcal{S}_{\mathcal{R}}| = \max\{|\mathcal{S}_{\mathcal{T}_1}|, |\mathcal{S}_{\mathcal{T}_2}|\}$.

Let us denote the ith element s of a constellation set $\mathcal{S}$ as $\mathcal{S}(i)$ where $i \in \{0, 1, \ldots, |\mathcal{S}| - 1\}$ and denote the inverse as $\mathcal{S}^{-1}(s) = i$. Defining $\mathbf{l}_{\mathcal{T}_1}$ and $\mathbf{l}_{\mathcal{T}_2}$ such that $\mathcal{S}_{\mathcal{T}_1}(\mathbf{l}_{\mathcal{T}_1}) = \mathbf{s}_{\mathcal{T}_1}$ and $\mathcal{S}_{\mathcal{T}_2}(\mathbf{l}_{\mathcal{T}_2}) = \mathbf{s}_{\mathcal{T}_2}$, the modular arithmetic function can be expressed as $\mathcal{F}_{\mathrm{m}}(\mathbf{s}_{\mathcal{T}_1}, \mathbf{s}_{\mathcal{T}_2}) = \mathcal{S}_{\mathcal{R}}(\mathrm{mod}(\mathcal{S}_{\mathcal{T}_1}^{-1}(\mathbf{s}_{\mathcal{T}_1}) + \mathcal{S}_{\mathcal{T}_2}^{-1}(\mathbf{s}_{\mathcal{T}_2}), |\mathcal{S}_{\mathcal{R}}|)) = \mathcal{S}_{\mathcal{R}}(\mathrm{mod}(\mathbf{l}_{\mathcal{T}_1} + \mathbf{l}_{\mathcal{T}_2}, |\mathcal{S}_{\mathcal{R}}|))$ where $\mathrm{mod}(a, b)$ denotes the remainder of the division of a by b.

In the second phase, the rth relay precodes $\mathbf{s}_{\mathcal{R},r}$ or its conjugate with the $T \times T$ matrix $\mathbf{A}_r$ before broadcasting the signal to both terminals from the time slot $T + 1$ to $2T$ as explained in Sec. 2.4.1. Finally, both terminals decode the received signal to obtain $\hat{\mathbf{s}}_{\mathcal{R},\mathcal{T}_1}$ at $\mathcal{T}_1$ and $\hat{\mathbf{s}}_{\mathcal{R},\mathcal{T}_2}$ at $\mathcal{T}_2$.

Using the knowledge of their own transmitted symbols, they can obtain their respective information symbol vector. For example, if $\hat{\mathbf{l}}_{\mathcal{R},\mathcal{T}_2}$ is defined such that $\mathcal{S}_{\mathcal{R}}(\hat{\mathbf{l}}_{\mathcal{R},\mathcal{T}_2}) = \hat{\mathbf{s}}_{\mathcal{R},\mathcal{T}_2}$, then the resulting decoded information vector is $\hat{\mathbf{s}}_{\mathcal{T}_1} = \mathcal{F}_{\mathrm{m},\mathcal{T}_2}^{-1}(\hat{\mathbf{s}}_{\mathcal{R},\mathcal{T}_2}, \mathbf{s}_{\mathcal{T}_2}) = \mathcal{S}_{\mathcal{T}_1}(\mathrm{mod}(\hat{\mathbf{l}}_{\mathcal{R},\mathcal{T}_2} - \mathbf{l}_{\mathcal{T}_2}, |\mathcal{S}_{\mathcal{T}_1}|))$ at $\mathcal{T}_2$ where $\mathcal{F}_{\mathrm{m},\mathcal{T}_2}^{-1}$ is the inverse of the modular arithmetic function at $\mathcal{T}_2$.

4.4 The Proposed Two-Way Distributed Space-Time Coding Protocol

Although the protocol presented in Sec. 4.3 allows cooperation in two phases, it has mainly two disadvantages: a computationally demanding ML decoder at the relays and the impossibility to use the direct link between the two terminals. In [113], a three-phase PDF-II protocol (3-phase PDF) was proposed to extend 2-phase PDF and mitigate its drawbacks.

In 3-phase PDF, as shown in Fig. 2.12, first $\mathcal{T}_1$ transmits while $\mathcal{T}_2$ remains silent, then $\mathcal{T}_2$ transmits while $\mathcal{T}_1$ remains silent, and finally, the relays encode and broadcast the signal to the terminals as in the second phase of 2-phase PDF. However, it was shown in [113] that two-phase protocols perform better than three-phase protocols for a large constellation size due to the higher symbol rate.

In this chapter, we propose a modification to the three-phase protocol that results in a symbol rate equivalent to that of the two-phase protocol. The proposed strategy achieves better performance and low decoding complexity. Moreover, the proposed strategy is also able to use the direct link between the two destination terminals.

Let us assume that $T \geq 2$ is an even number. In the first phase, from time slot 1 to $T/2$, $\mathcal{T}_1$ and $\mathcal{T}_2$ transmit simultaneously $\sqrt{P_{\mathcal{T}_1}}\mathbf{x}_{\mathcal{T}_1}$ and $\sqrt{P_{\mathcal{T}_2}}\mathbf{x}_{\mathcal{T}_2}$, respectively, where $\mathbf{x}_{\mathcal{T}_1}$ and $\mathbf{x}_{\mathcal{T}_2}$ are two $T/2 \times 1$ vectors of transmitted signals, $[\mathbf{x}_{\mathcal{T}_1}]_i \in \mathcal{X}_{\mathcal{T}_1}$, $[\mathbf{x}_{\mathcal{T}_2}]_i \in \mathcal{X}_{\mathcal{T}_2}$, $|\mathcal{X}_{\mathcal{T}_1}| = |\mathcal{S}_{\mathcal{T}_1}|^2$ and $|\mathcal{X}_{\mathcal{T}_2}| = |\mathcal{S}_{\mathcal{T}_2}|^2$. Here,

$$\mathbf{x}_{\mathcal{T}_1} = \mathcal{G}_{\mathcal{T}_1}(\mathbf{s}_{\mathcal{T}_1}), \tag{4.1}$$

where $\mathcal{G}_{\mathcal{T}_1}(\cdot)$ is a function that maps the entries $[\mathbf{s}_{\mathcal{T}_1}]_{2i-1}$ and $[\mathbf{s}_{\mathcal{T}_1}]_{2i}$ onto $[\mathbf{x}_{\mathcal{T}_1}]_i$ resulting in a constellation with the square of the size of $\mathcal{S}_{\mathcal{T}_1}$. The symbol $[\mathbf{x}_{\mathcal{T}_2}]_i$ is the respective combination of the symbols $[\mathbf{s}_{\mathcal{T}_2}]_{2i-1}$ and $[\mathbf{s}_{\mathcal{T}_2}]_{2i}$ of $\mathcal{T}_2$ with the function $\mathcal{G}_{\mathcal{T}_2}(\cdot)$. The received signal at the rth relay is given by:

$$\mathbf{y}_{\mathcal{R}1,r} = \sqrt{P_{\mathcal{T}_1}} f_r \mathbf{x}_{\mathcal{T}_1} + \sqrt{P_{\mathcal{T}_2}} g_r \mathbf{x}_{\mathcal{T}_2} + \mathbf{n}_{\mathcal{R}1,r} \tag{4.2}$$

where $\mathbf{n}_{\mathcal{R}1,r}$ is the noise vector at the rth relay in the first phase. In the second phase, from time slot $T/2+1$ to T, $\mathcal{T}_1$ and $\mathcal{T}_2$ transmit simultaneously $\sqrt{P_{\mathcal{T}_1}}\mathbf{x}_{\mathcal{T}_1}$ and $-\sqrt{P_{\mathcal{T}_2}}\mathbf{x}_{\mathcal{T}_2}$, respectively. The only difference with the first phase is that $\mathcal{T}_2$ transmits the same symbols multiplied by -1. The received signal at the rth relay during the second phase is given by:

$$\mathbf{y}_{\mathcal{R}2,r} = \sqrt{P_{\mathcal{T}_1}} f_r \mathbf{x}_{\mathcal{T}_1} - \sqrt{P_{\mathcal{T}_2}} g_r \mathbf{x}_{\mathcal{T}_2} + \mathbf{n}_{\mathcal{R}2,r} \tag{4.3}$$

where $\mathbf{n}_{\mathcal{R}2,r}$ is the noise vector at the rth relay in the second phase. We assume that the entries of all noise vectors can be modeled as independent and identically distributed Gaussian random variables with zero mean and variance $\sigma^2 = 1$.

4.4.1 Decoding Procedure at the Relays

Using (4.2) and (4.3), the rth relay can decode the symbols as:

$$\hat{\mathbf{x}}_{\mathcal{T}_1,r} = \arg\min_{\mathbf{x}_{\mathcal{T}_1}} \left\| \mathbf{y}_{\mathcal{R}1,r} + \mathbf{y}_{\mathcal{R}2,r} - 2\sqrt{P_{\mathcal{T}_1}} f_r \mathbf{x}_{\mathcal{T}_1} \right\|, \tag{4.4}$$

$$\hat{\mathbf{x}}_{\mathcal{T}_2,r} = \arg\min_{\mathbf{x}_{\mathcal{T}_2}} \left\| \mathbf{y}_{\mathcal{R}1,r} - \mathbf{y}_{\mathcal{R}2,r} - 2\sqrt{P_{\mathcal{T}_2}} g_r \mathbf{x}_{\mathcal{T}_2} \right\|. \tag{4.5}$$

Let us explain in detail the decoding procedure at the relays. The rth relay receives the signals given by (4.2) and (4.3) during the first two phases. Using the received signals, the rth relay finds $\tilde{\mathbf{x}}_{\mathcal{T}_1,r}$ and $\tilde{\mathbf{x}}_{\mathcal{T}_2,r}$ as follows:

$$\tilde{\mathbf{x}}_{\mathcal{T}_1,r} = \text{round}\left(\frac{(\mathbf{y}_{\mathcal{R}1,r} + \mathbf{y}_{\mathcal{R}2,r}) f_r^*}{2\sqrt{P_{\mathcal{T}_1}} |f_r|^2} \right), \tag{4.6}$$

$$\tilde{\mathbf{x}}_{\mathcal{T}_2,r} = \text{round}\left(\frac{(\mathbf{y}_{\mathcal{R}1,r} - \mathbf{y}_{\mathcal{R}2,r}) g_r^*}{2\sqrt{P_{\mathcal{T}_2}} |g_r|^2} \right) \tag{4.7}$$

where round$(\cdot)$ rounds the argument to the nearest constellation point. In case of an integer constellation, this can be carried out with just a hard decision in the real and imaginary parts. Using $\hat{\mathbf{x}}_{\mathcal{T}_1,r}$ and $\hat{\mathbf{x}}_{\mathcal{T}_2,r}$, the rth relay can obtain $\tilde{\mathbf{s}}_{\mathcal{T}_1,r}$ and $\tilde{\mathbf{s}}_{\mathcal{T}_2,r}$ by performing the inverse operation of $\mathcal{G}_{\mathcal{T}_1}(\cdot)$ and $\mathcal{G}_{\mathcal{T}_2}(\cdot)$, i.e.,

$$\tilde{\mathbf{s}}_{\mathcal{T}_1,r} = \mathcal{G}_{\mathcal{T}_1}^{-1}(\hat{\mathbf{x}}_{\mathcal{T}_1,r}), \tag{4.8}$$

$$\tilde{\mathbf{s}}_{\mathcal{T}_2,r} = \mathcal{G}_{\mathcal{T}_2}^{-1}(\hat{\mathbf{x}}_{\mathcal{T}_2,r}). \tag{4.9}$$

The $\mathcal{G}_{\mathcal{T}_t}$ and $\mathcal{G}_{\mathcal{T}_t}^{-1}$ operations can be implemented by merging and splitting the bits that represent each symbol, respectively. Note that the relay decoding, given by (4.6) and (4.7), rounds simply the real and imaginary parts to the nearest constellation point in case of an integer constellation. Furthermore, the use of $\mathcal{G}_{\mathcal{T}_t}$ and $\mathcal{G}_{\mathcal{T}_t}^{-1}$ in the proposed scheme has a negligible complexity. On the other hand, the relay decoding complexity of 2-phase PDF explained in Sec. 4.3 [113] has the order of $|\mathcal{S}_{\mathcal{T}_1}||\mathcal{S}_{\mathcal{T}_2}|$, since its system is under-determined and an exhaustive search should be performed. For example,

if $\mathbf{s}_{\mathcal{T}_1}$ and $\mathbf{s}_{\mathcal{T}_2}$ are drawn from M-QAM, then the ML decoder of 2-phase PDF has the order of M^2 in this case. Hence, the relay decoding complexity of our proposed method is much lower than that of the 2-phase PDF which is quadratic.

An equivalent transmission to the previous two phases can be performed if $\mathcal{T}_1$ transmits $\sqrt{2P_{\mathcal{T}_1}}\mathbf{x}_{\mathcal{T}_1}$ while $\mathcal{T}_2$ remains silent from 1 to $T/2$, and then $\mathcal{T}_2$ transmits $\sqrt{2P_{\mathcal{T}_2}}\mathbf{x}_{\mathcal{T}_2}$ while $\mathcal{T}_1$ remains silent from $T/2+1$ to T. In this case, the direct link can be used as the terminal that remains silent can listen to the transmission of the other one. Since one terminal is off at a certain time slot, the other terminal uses the double power. After decoding the received symbols, the relay combines the decoded symbols from the two terminals into one symbol as

$$\mathbf{s}_{\mathcal{R},r} = \mathcal{F}(\tilde{\mathbf{s}}_{\mathcal{T}_1,r}, \tilde{\mathbf{s}}_{\mathcal{T}_2,r}) \tag{4.10}$$

where $\mathbf{s}_{\mathcal{R},r}$ is a $T \times 1$ vector. The selection of $\mathcal{F}(\cdot,\cdot)$ for our protocol is discussed in the next section. The third and final phase of the proposed protocol, from time slot $T+1$ to $2T$, is exactly the same as the second phase of the protocol described in Sec. 4.3. The relay precodes the symbol vector or its conjugate and scales it before broadcasting it to the terminals. The received signals at $\mathcal{T}_1$ and $\mathcal{T}_2$ are given by:

$$\mathbf{y}_{\mathcal{T}_1} = \sum_{r=1}^{R} \sqrt{P_{\mathcal{R}_r}} f_r \mathbf{A}_r \breve{\mathbf{s}}_{\mathcal{R},r} + \mathbf{n}_{\mathcal{T}_1}, \tag{4.11}$$

$$\mathbf{y}_{\mathcal{T}_2} = \sum_{r=1}^{R} \sqrt{P_{\mathcal{R}_r}} g_r \mathbf{A}_r \breve{\mathbf{s}}_{\mathcal{R},r} + \mathbf{n}_{\mathcal{T}_2}, \tag{4.12}$$

respectively, where either $\breve{\mathbf{s}}_{\mathcal{R},r} = \mathbf{s}_{\mathcal{R},r}$ or $\breve{\mathbf{s}}_{\mathcal{R},r} = \mathbf{s}^*_{\mathcal{R},r}$, and $\mathbf{n}_{\mathcal{T}_1}$ and $\mathbf{n}_{\mathcal{T}_2}$ are the noise vectors at $\mathcal{T}_1$ and $\mathcal{T}_2$, respectively. The selection of $\breve{\mathbf{s}}_{\mathcal{R},r}$ and $\mathbf{A}_r$ on each relay depends on the used DSTC scheme as explained in Sec. 2.4.1. Any linear space-time codes can be applied to the proposed technique directly. For example, in case of the Alamouti code with two relay nodes used in the simulation part,

$\breve{\mathbf{s}}_{\mathcal{R},r}$ and $\mathbf{A}_r$ are chosen as follows:

$$\mathbf{A}_1 = \begin{bmatrix} 1 & 0 \\ 0 & 1 \end{bmatrix}, \quad \mathbf{A}_2 = \begin{bmatrix} 0 & 1 \\ -1 & 0 \end{bmatrix},$$

$$\breve{\mathbf{s}}_{\mathcal{R},1} = \mathbf{s}_{\mathcal{R},1}, \quad \breve{\mathbf{s}}_{\mathcal{R},2} = \mathbf{s}^*_{\mathcal{R},2}.$$

4.4.2 Decoding Procedure at the Communicating Terminals without Direct Link

The ML decoding problem at $\mathcal{T}_2$ without considering the direct link between the communicating terminals can be expressed as:

$$\arg\min_{\mathbf{S}\in\mathbb{S}} \|\mathbf{y}_{\mathcal{T}_2} - \mathbf{S}\ \mathbf{g}\|^2 \tag{4.13}$$

where $\mathbf{g} = [\sqrt{P_{\mathcal{R}_1}}g_1, \cdots, \sqrt{P_{\mathcal{R}_R}}g_R]^T$, $\mathbf{S} = [\tilde{\mathbf{s}}_{\mathcal{R},1}, \tilde{\mathbf{s}}_{\mathcal{R},2}, \ldots, \tilde{\mathbf{s}}_{\mathcal{R},R}] \in \mathbb{S}$, $\mathbb{S}$ is the set containing the L_T possible combinations of the symbol matrices and $L_T = (|\mathcal{S}_{\mathcal{T}_1}||\mathcal{S}_{\mathcal{T}_2}|)^{RT}$. As it can be observed from (4.13), the ML decoding is quite complex even for moderate numbers of relays and small constellation sizes. Therefore, the ML decoder is approximated by considering an error free decoding at the relays. This also means that $\mathbf{s}_{\mathcal{R},1} = \cdots = \mathbf{s}_{\mathcal{R},R} = \mathbf{s}_{\mathcal{R}}$ and, therefore, the decoder can be expressed as:

$$\hat{\mathbf{s}}_{\mathcal{R},\mathcal{T}_2} = \arg\min_{\mathbf{s}_{\mathcal{R}}} \left\| \mathbf{y}_{\mathcal{T}_2} - \sum_{r=1}^{R} \sqrt{P_{\mathcal{R}_r}} g_r \mathbf{A}_r \breve{\mathbf{s}}_{\mathcal{R}} \right\|^2. \tag{4.14}$$

To find $\hat{\mathbf{s}}_{\mathcal{T}_1}$ at $\mathcal{T}_2$, the decoder uses the inverse of $\mathcal{F}(\cdot,\cdot)$ (denoted as $\mathcal{F}^{-1}(\cdot,\cdot)$) with the knowledge of $\mathbf{s}_{\mathcal{T}_2}$, i.e.,

$$\hat{\mathbf{s}}_{\mathcal{T}_1} = \mathcal{F}^{-1}(\hat{\mathbf{s}}_{\mathcal{R},\mathcal{T}_2}, \mathbf{s}_{\mathcal{T}_2}). \tag{4.15}$$

Similar procedure can be carried out at $\mathcal{T}_1$.

4.4.3 Decoding Procedure at the Communicating Terminals with Direct Link

In case of using the direct link with the alternative transmission, the decoder at $\mathcal{T}_2$ finds

$$\hat{\mathbf{s}}_{\mathcal{T}_1} = \arg\min_{\mathbf{s}_{\mathcal{T}_1}} \left\| \mathbf{y}_{\mathcal{T}_2} - \sum_{r=1}^{R} \sqrt{P_{\mathcal{R}_r}} g_r \mathbf{A}_r \breve{\mathcal{F}}(\mathbf{s}_{\mathcal{T}_1}, \mathbf{s}_{\mathcal{T}_2}) \right\|^2 + \left\| \mathbf{y}_{\mathcal{T}_2,\mathrm{dl}} - \sqrt{2P_{\mathcal{T}_1}} f_0 \mathcal{G}_{\mathcal{T}_1}(\mathbf{s}_{\mathcal{T}_1}) \right\|^2 \tag{4.16}$$

where $\mathbf{y}_{\mathcal{T}_2,\mathrm{dl}}$ is the received signal at $\mathcal{T}_2$ during the first phase and either $\breve{\mathcal{F}}(\cdot,\cdot) = \mathcal{F}(\cdot,\cdot)$ or $\breve{\mathcal{F}}(\cdot,\cdot) = \mathcal{F}(\cdot,\cdot)^*$, depending on the DSTC scheme. Note that the direct link case can have a significantly more complex decoder, as a full search over $\mathbf{s}_{\mathcal{T}_1}$ is required. In contrast to (5.24), the decoder of (4.14) can be implemented using the sphere decoder, or in case of using orthogonal DSTCs, it can be simplified to the symbol-by-symbol decoder. However, the use of the direct link can provide a higher diversity order.

It can be observed that the total symbol rate of the 2-phase PDF protocol in Sec. 4.3 [113] and the proposed protocol is the same. However, the relay decoding complexity in the proposed protocol is lower than that of 2-phase PDF protocol [113]. Moreover, the proposed protocol can use the direct link and, as shown later in the simulations, it achieves better performance than 2-phase PDF and 3-phase PDF.

4.5 Combination Function at the Relays

The purpose of $\mathcal{F}(\cdot,\cdot)$ is to combine the received symbols from both terminals at the relays into one symbol so that each terminal can decode the transmitted symbol from the other terminal using the information of its own transmitted symbol as explained in Sec. 2.4.3 and Sec. 4.3. In this way, the performance is improved, as the relay does not waste power to transmit known information at either side. However, mapping functions can not obtain the same performance

in terms of the BER, as it can be observed from the following two examples.

Example 1: Let us consider the modular arithmetic function $\mathcal{F}_{\mathrm{m}}(\cdot,\cdot)$ [113], explained in Sec. 4.3, using 4-QAM for both directions. Assume that the binary symbols $[\mathbf{s}_{\mathcal{T}_1}]_i = 11$ and $[\mathbf{s}_{\mathcal{T}_2}]_i = 01$ are chosen using Gray encoding, i.e., $\mathcal{S}_{\mathcal{T}_1}(2) = [\mathbf{s}_{\mathcal{T}_1}]_i = 11$ and $\mathcal{S}_{\mathcal{T}_2}(1) = [\mathbf{s}_{\mathcal{T}_2}]_i = 01$. Applying the modular function to these symbols we obtain $\mathcal{F}_{\mathrm{m}}([\mathbf{s}_{\mathcal{T}_1}]_i, [\mathbf{s}_{\mathcal{T}_2}]_i) = \mathcal{S}_{\mathcal{R}}(0) = 00$. Now, let us assume that one-bit error occurred in the second received bit at the second terminal, i.e., $[\hat{\mathbf{s}}_{\mathcal{R},\mathcal{T}_2}]_i = 01$. Using the inverse of the modular function, the decoded information bits are $[\hat{\mathbf{s}}_{\mathcal{T}_1}]_i = \mathcal{F}^{-1}_{\mathrm{m},\mathcal{T}_2}([\hat{\mathbf{s}}_{\mathcal{R},\mathcal{T}_2}]_i, [\mathbf{s}_{\mathcal{T}_2}]_i) = 00$. This means that a two-bit error has occurred in the decoded information bits of the first terminal at the second terminal. In general, if the scheme uses $\mathcal{F}_{\mathrm{m}}(\cdot,\cdot)$ and one-bit error has occurred in the received symbol, then, *at least*, one-bit error occurs in the decoded information bits.

Example 2: Let us consider now the XOR function proposed in [114] that uses the bits representing each symbol to compute the superimposed symbol. Using the same symbols of Example 1, we obtain $\mathcal{F}_{\mathrm{xor}}([\mathbf{s}_{\mathcal{T}_1}]_i, [\mathbf{s}_{\mathcal{T}_2}]_i) = 11 \oplus 01 = 10$ where $\mathcal{F}_{\mathrm{xor}}(\cdot,\cdot)$ is the XOR combination function and $\oplus$ denotes the exclusive OR (XOR) operation. Applying the same error of the previous example we have $[\hat{\mathbf{s}}_{\mathcal{R},\mathcal{T}_2}]_i = 11$. The resulting decoded bits at the second terminal are $[\hat{\mathbf{s}}_{\mathcal{T}_1}]_i = \mathcal{F}^{-1}_{\mathrm{xor},\mathcal{T}_2}([\hat{\mathbf{s}}_{\mathcal{R},\mathcal{T}_2}]_i, [\mathbf{s}_{\mathcal{T}_2}]_i) = 11 \oplus 01 = 10$, yielding only one erroneous bit. For $\mathcal{F}_{\mathrm{xor}}(\cdot,\cdot)$, it can be shown that the number of erroneous bits in the information word are the same as the number of erroneous bits in the received symbol.

From the previous examples, it can be observed that the use of $\mathcal{F}_{\mathrm{xor}}(\cdot,\cdot)$ is expected to yield a better BER performance than the use of $\mathcal{F}_{\mathrm{m}}(\cdot,\cdot)$. This means that $\mathcal{F}(\cdot,\cdot)$ is preferable as for this combination function the number of erroneous bits in the received symbol are the same as in the decoded information symbol.

4.5.1 The Proposed Combination Function

In [113], the modular arithmetic function $\mathcal{F}_{\mathrm{m}}(\cdot,\cdot)$, explained in Sec. 4.3 [113], using directly the symbols rather than the bits was proposed. However, its performance is lower than that of $\mathcal{F}_{\mathrm{xor}}(\cdot,\cdot)$ which uses the bits to obtain the

superimposed symbol.

In the following, we proposed another combination function $\mathcal{F}_{\mathrm{s}}(\cdot,\cdot)$ to compete with $\mathcal{F}_{\mathrm{m}}$ as it also uses directly the symbols instead of the bit representation to generate the superimposed symbol. The proposed function can be used with M-QAM and yields almost the same BER performance as $\mathcal{F}_{\mathrm{xor}}(\cdot,\cdot)$ as shown in the simulation part. The function can be expressed as:

$$\mathcal{F}_{\mathrm{s}}([\mathbf{s}_{\mathcal{T}_1}]_i,[\mathbf{s}_{\mathcal{T}_2}]_i)=\tilde{\mathcal{F}}_{\mathrm{s}}\left(\Re([\mathbf{s}_{\mathcal{T}_1}]_i),\Re([\mathbf{s}_{\mathcal{T}_2}]_i)\right)+j\tilde{\mathcal{F}}_{\mathrm{s}}\left(\Im([\mathbf{s}_{\mathcal{T}_1}]_i),\Im([\mathbf{s}_{\mathcal{T}_2}]_i)\right) \tag{4.17}$$

where

$$\tilde{\mathcal{F}}_{\mathrm{s}}(\tilde{p},\tilde{q})=\begin{cases}|\tilde{p}+\tilde{q}|\operatorname{sgn}(\tilde{p}\tilde{q})-1, & \text{if } |\tilde{p}+\tilde{q}|\leqslant\sqrt{M}\\ \left|2\sqrt{M}-|\tilde{p}+\tilde{q}|\right|\operatorname{sgn}(\tilde{p}\tilde{q})-1, & \text{otherwise}\end{cases} \tag{4.18}$$

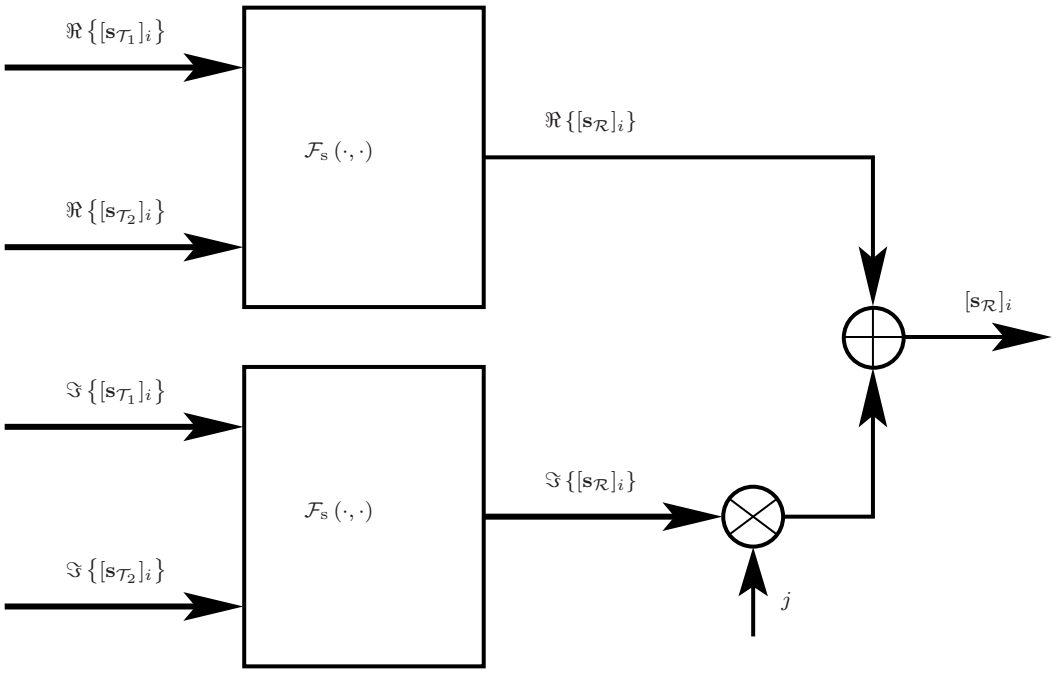

Figure 4.1: The proposed combination function.

$\tilde{p}$ and $\tilde{q}$ are either the real or imaginary part of the symbols, sgn$(\cdot)$ denotes the signum function, and $\Im(\cdot)$ denotes the imaginary part. The function $\mathcal{F}_{\rm s}(\cdot,\cdot)$, as shown in Fig. 4.1, can be described as a permutation of the output of $\mathcal{F}_{\rm xor}(\cdot,\cdot)$ as shown in Table 4.1. To explain the proposed combination function, we provide the following two examples. Let us first assume that the relays decode the symbols correctly and $([\mathbf{s}_{\mathcal{T}_1}]_i, [\mathbf{s}_{\mathcal{T}_2}]_i) \in$ 4-QAM where $[\mathbf{s}_{\mathcal{T}_1}]_i = 1+j$ and $[\mathbf{s}_{\mathcal{T}_2}]_i = 1-j$. From (4.17), the rth relay finds $[\mathbf{s}_{\mathcal{R},r}]_i$ as

$$\begin{aligned}[\mathbf{s}_{\mathcal{R},r}]_i &= \mathcal{F}_{\rm s}([\mathbf{s}_{\mathcal{T}_1}]_i, [\mathbf{s}_{\mathcal{T}_2}]_i) = \tilde{\mathcal{F}}_{\rm s}\left(\Re([\mathbf{s}_{\mathcal{T}_1}]_i), \Re([\mathbf{s}_{\mathcal{T}_2}]_i)\right) + j\tilde{\mathcal{F}}_{\rm s}\left(\Im([\mathbf{s}_{\mathcal{T}_1}]_i), \Im([\mathbf{s}_{\mathcal{T}_2}]_i)\right) \\ &= \tilde{\mathcal{F}}_{\rm s}(1,1) + j\tilde{\mathcal{F}}_{\rm s}(1,-1) = 1-j\end{aligned}$$

Table 4.1 shows the output of the proposed function and the XOR function for all combinations. Due to the symmetry of the real and imaginary part of the symbols, we define $\tilde{p}$ and $\tilde{q}$ in (4.18) as either the real or imaginary part. To produce the output, the function is used once with the real and once with the imaginary parts as shown in the example.

Table 4.1: Input/Output comparison of $\mathcal{F}_{\rm xor}$ and $\mathcal{F}_{\rm s}$ using 4-QAM.

$\tilde{p}$	-1	-1	1	1
$\tilde{q}$	-1	1	-1	1
$\tilde{\mathcal{F}}_{\rm xor}(\tilde{p},\tilde{q})$	-1	1	1	-1
$\tilde{\mathcal{F}}_{\rm s}(\tilde{p},\tilde{q})$	1	-1	-1	1

In case of using 16-QAM, it is assumed that the real or imaginary parts of the symbols $\{-3,-1,1,3\}$ are represented in the binary form using Gray encoding as $\{00,01,11,10\}$, respectively. It can be observed from Tables 4.1 and 4.2 that the output of $\mathcal{F}_{\rm s}$ is a rotated version of the output of $\mathcal{F}_{\rm xor}$ in 4- or 16-QAM.

The inverse of $\mathcal{F}_{\rm s}$ at $\mathcal{T}_2$, as shown in Fig. 4.2, can be defined as:

$$\mathcal{F}_{\rm s}^{-1}([\hat{\mathbf{s}}_{\mathcal{R},\mathcal{T}_2}]_i, [\mathbf{s}_{\mathcal{T}_2}]_i) = \tilde{\mathcal{F}}_{\rm s}^{-1}\left(\Re([\hat{\mathbf{s}}_{\mathcal{R},\mathcal{T}_2}]_i), \Re([\mathbf{s}_{\mathcal{T}_2}]_i)\right) + j\tilde{\mathcal{F}}_{\rm s}^{-1}\left(\Im([\hat{\mathbf{s}}_{\mathcal{R},\mathcal{T}_2}]_i), \Im([\mathbf{s}_{\mathcal{T}_2}]_i)\right) \tag{4.19}$$

where

$$\tilde{\mathcal{F}}_{\mathrm{s}}^{-1}(\tilde{w},\tilde{p}) = \begin{cases} |\phi(\tilde{w}+1,\tilde{p})-\tilde{p}|\,\mathrm{sgn}\left(\phi(\tilde{w}+1,\tilde{p})\tilde{p}\right), & \text{if } \mathrm{sgn}\left((\phi(\tilde{w}+1,\tilde{p})-\tilde{p})\,\tilde{p}\right)=\mathrm{sgn}(\tilde{w}) \\ \phi\left(-\tilde{w}-1,\tilde{p}\right)-\tilde{p}, & \text{otherwise} \end{cases} \tag{4.20}$$

$$\phi(z,\tilde{p}) = \begin{cases} z, & \text{if } |z-\tilde{p}| \leqslant \sqrt{M} \\ \left(|z|-2\sqrt{M}\right)\mathrm{sgn}(z), & \text{otherwise} \end{cases} \tag{4.21}$$

The BER performance of $\mathcal{F}_{\mathrm{s}}$ is close to that of $\mathcal{F}_{\mathrm{xor}}$ as shown later in our simulations.

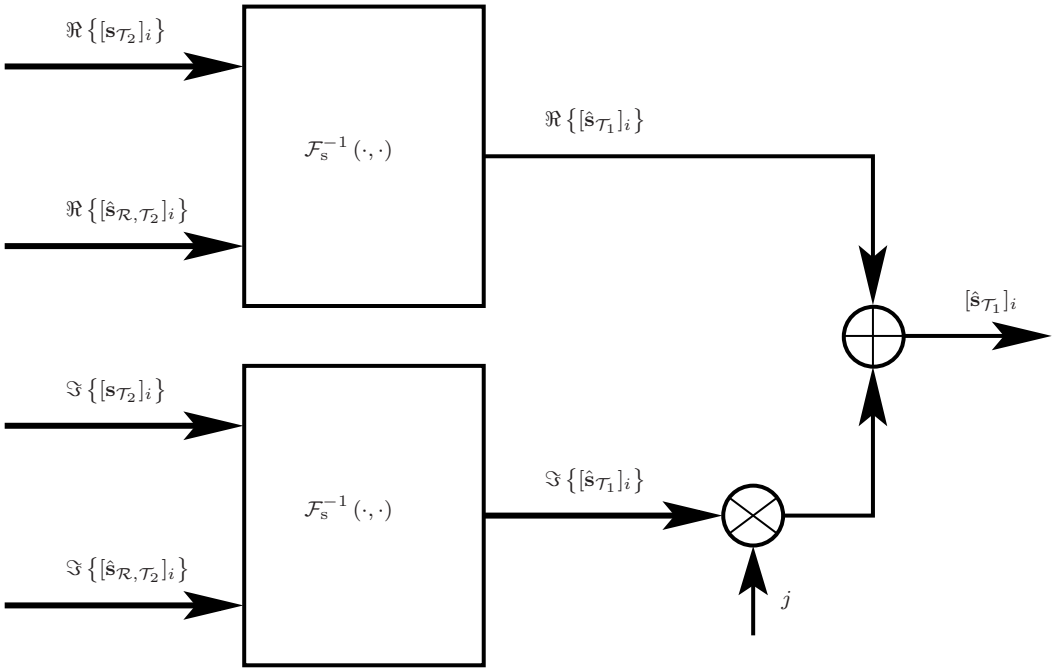

Figure 4.2: The inverse of the proposed combination function at $\mathcal{T}_2$.

Table 4.2: Input/Output comparison of $\mathcal{F}_{\text{xor}}$ and $\mathcal{F}_{\text{s}}$ using 16-QAM.

$\tilde{p}$	-3	-3	-3	-3	-1	-1	-1	-1	1	1	1	1	3	3	3	3
$\tilde{q}$	-3	-1	1	3	-3	-1	1	3	-3	-1	1	3	-3	-1	1	3
$\tilde{\mathcal{F}}_{\text{xor}}(\tilde{p},\tilde{q})$	-3	-1	1	3	-1	-3	3	1	1	3	-3	-1	3	1	-1	-3
$\tilde{\mathcal{F}}_{\text{s}}(\tilde{p},\tilde{q})$	1	3	-3	-1	3	1	-1	-3	-3	-1	1	3	-1	-3	3	1

4.6 Extension to the Non-coherent Receiver Case

In the non-coherent receiver case, the terminals can use differential transmission for each single symbol transmitted from the terminals to the relays during the first and second phase of the protocol proposed in Sec. 4.4 and then, with the decoded symbols at the relays, a differential DSTC can be employed to transmit the information symbols to the respective terminals. We illustrate the application of the protocol to the non-coherent receiver by means of the following example which describes a differential transmission for two relays using the distributed Alamouti code [12]. Extension to the case of $R > 2$ is straightforward. In this case, we adopt a similar differential scheme as the one proposed in [67,122]. Using our scheme, the terminals $\mathcal{T}_1$ and $\mathcal{T}_2$ transmit in the kth block the differential encoded scalars $w_{\mathcal{T}_1}^{(k)}$ and $w_{\mathcal{T}_2}^{(k)}$, respectively, where

$$w_{\mathcal{T}_t}^{(k)} = \frac{w_{\mathcal{T}_t}^{(k-1)} x_{\mathcal{T}_t}^{(k)}}{\left| x_{\mathcal{T}_t}^{(k-1)} \right|}, \tag{4.22}$$

$t = 1, 2$, $x_{\mathcal{T}_1}^{(k)} = \mathcal{G}_{\mathcal{T}_1}(\mathbf{s}_{\mathcal{T}_1}^{(k)})$ as in (4.1), $w_{\mathcal{T}_t}^{(0)} = x_{\mathcal{T}_t}^{(0)} = 1$ and $\left| x_{\mathcal{T}_t}^{(k)} \right| = \left| w_{\mathcal{T}_t}^{(k)} \right|$. The initial symbol $w_{\mathcal{T}_t}^{(0)}$ is transmitted as a reference to start the differential decoding. Note that this symbol is only transmitted at the beginning of the transmission. In the next block of symbols, the last symbol from the previous block can be used as a reference to start the decoding. In the first two phases, the received signals

at the rth relay are given by:

$$y_{\mathcal{R}1,r}^{(k)} = \sqrt{P_{\mathcal{T}_1}} f_r w_{\mathcal{T}_1}^{(k)} + \sqrt{P_{\mathcal{T}_2}} g_r w_{\mathcal{T}_2}^{(k)} + n_{\mathcal{R}1,r}^{(k)}, \tag{4.23}$$

$$y_{\mathcal{R}2,r}^{(k)} = \sqrt{P_{\mathcal{T}_1}} f_r w_{\mathcal{T}_1}^{(k)} - \sqrt{P_{\mathcal{T}_2}} g_r w_{\mathcal{T}_2}^{(k)} + n_{\mathcal{R}2,r}^{(k)}. \tag{4.24}$$

The rth relay decodes the symbols $x_{\mathcal{T}_1}^{(k)}$ and $x_{\mathcal{T}_2}^{(k)}$ as:

$$\hat{x}_{\mathcal{T}_t,r}^{(k)} = \arg\min_{x_{\mathcal{T}_t}^{(k)} \in \mathcal{X}_{\mathcal{T}_t}} \left\| d_{t,r}^{(k)} - \frac{x_{\mathcal{T}_t}^{(k)} \, d_{t,r}^{(k-1)}}{\left| \hat{x}_{\mathcal{T}_t,r}^{(k-1)} \right|} \right\|^2, \tag{4.25}$$

where

$$d_{1,r}^{(k)} = \frac{y_{\mathcal{R}1,r}^{(k)} + y_{\mathcal{R}2,r}^{(k)}}{2}, \tag{4.26}$$

$$d_{2,r}^{(k)} = \frac{y_{\mathcal{R}1,r}^{(k)} - y_{\mathcal{R}2,r}^{(k)}}{2}. \tag{4.27}$$

Similar to Sec. 4.3, the rth relay can obtain $\tilde{\mathbf{s}}_{\mathcal{T}_1,r}^{(k)}$ and $\tilde{\mathbf{s}}_{\mathcal{T}_2,r}^{(k)}$ using $\tilde{\mathbf{s}}_{\mathcal{T}_1,r}^{(k)} = \mathcal{G}_{\mathcal{T}_1}^{-1}(\hat{x}_{\mathcal{T}_1,r}^{(k)})$ and $\tilde{\mathbf{s}}_{\mathcal{T}_2,r}^{(k)} = \mathcal{G}_{\mathcal{T}_2}^{-1}(\hat{x}_{\mathcal{T}_2,r}^{(k)})$ as in (4.8) and (4.9). For the last phase, the rth relay combines the decoded symbols from the two terminals into one symbol as $\mathbf{s}_{\mathcal{R},r}^{(k)} = \mathcal{F}(\tilde{\mathbf{s}}_{\mathcal{T}_1,r}^{(k)}, \tilde{\mathbf{s}}_{\mathcal{T}_2,r}^{(k)})$. Then, the rth relay transmits the 2×1 vector over two consecutive time slots

$$\begin{aligned} \mathbf{v}_{\mathcal{R},r}^{(k)} &= \frac{\mathbf{U}_{\mathcal{R},r}^{(k)} \mathbf{v}_{\mathcal{R},r}^{(k-1)}}{a_{\mathcal{R},r}^{(k-1)}} \\ &= \frac{\mathbf{U}_{\mathcal{R},r}^{(k)} \mathbf{v}_{\mathcal{R},r}^{(k-1)}}{\sqrt{\left| [\mathbf{s}_{\mathcal{R},r}^{(k-1)}]_1 \right|^2 + \left| [\mathbf{s}_{\mathcal{R},r}^{(k-1)}]_2 \right|^2}}, \end{aligned} \tag{4.28}$$

where

$$\mathbf{U}_{\mathcal{R},r}^{(k)} = \begin{bmatrix} [\mathbf{s}_{\mathcal{R},r}^{(k)}]_1 & [\mathbf{s}_{\mathcal{R},r}^{(k)}]_2 \\ -\left([\mathbf{s}_{\mathcal{R},r}^{(k)}]_2\right)^* & \left([\mathbf{s}_{\mathcal{R},r}^{(k)}]_1\right)^* \end{bmatrix}, \tag{4.29}$$

$\mathbf{v}_{\mathcal{R},r}^{(0)} = \mathbf{e}_r$, $a_{\mathcal{R},r}^{(0)} = 1$ and $\mathbf{e}_r$ is the 2×1 vector with the rth entry equal to 1 and the other equal to 0. The received signal vectors at the second terminal for the blocks $(k-1)$ and (k) are given by:

$$\mathbf{y}_{\mathcal{T}_2}^{(k-1)} = \mathbf{V}^{(k-1)}\mathbf{g} + \mathbf{n}_{\mathcal{T}_2}^{(k-1)}, \tag{4.30}$$

$$\mathbf{y}_{\mathcal{T}_2}^{(k)} = \mathbf{V}^{(k)}\mathbf{g} + \mathbf{n}_{\mathcal{T}_2}^{(k)}, \tag{4.31}$$

respectively, where $\mathbf{V}^{(k)} = \left[\mathbf{v}_{\mathcal{R},1}^{(k)},\, \mathbf{v}_{\mathcal{R},2}^{(k)}\right]$ and $\mathbf{g} = [g_1,\, g_2]^T$.

4.6.1 Decoding Procedure at the Communicating Terminals without Direct Link

Assuming that $\mathbf{U}^{(k)} = \mathbf{U}_{\mathcal{R},1}^{(k)} = \mathbf{U}_{\mathcal{R},2}^{(k)}$ (and therefore, $\mathbf{s}_{\mathcal{R},1}^{(k)} = \mathbf{s}_{\mathcal{R},2}^{(k)} = \mathbf{s}_{\mathcal{R}}^{(k)}$), the estimated value of $\mathbf{U}^{(k)}$ at the second terminal is given by:

$$\hat{\mathbf{U}}^{(k)} = \arg\min_{\mathbf{U}^{(k)}} \left\| \mathbf{y}_{\mathcal{T}_2}^{(k)} - \frac{\mathbf{U}^{(k)}\mathbf{y}_{\mathcal{T}_2}^{(k-1)}}{\hat{a}_{\mathcal{T}_2}^{(k-1)}} \right\|^2 \tag{4.32}$$

where

$$\hat{a}_{\mathcal{T}_2}^{(k-1)} = \sqrt{|[\hat{\mathbf{s}}_{\mathcal{R},\mathcal{T}_2}^{(k-1)}]_1|^2 + |[\hat{\mathbf{s}}_{\mathcal{R},\mathcal{T}_2}^{(k-1)}]_2|^2} \tag{4.33}$$

and $\hat{\mathbf{s}}_{\mathcal{R},\mathcal{T}_2}^{(k-1)}$ is the estimated value of $\mathbf{s}_{\mathcal{R}}^{(k-1)}$ at the second terminal. From $\hat{\mathbf{U}}^{(k)}$, $\hat{\mathbf{s}}_{\mathcal{R},\mathcal{T}_2}^{(k)}$ can be obtained and using the inverse of the combination function with $\mathbf{s}_{\mathcal{T}_2}^{(k)}$, the information symbols are finally computed as $\hat{\mathbf{s}}_{\mathcal{T}_1}^{(k)} = \mathcal{F}^{-1}(\hat{\mathbf{s}}_{\mathcal{R},\mathcal{T}_2}^{(k)}, \mathbf{s}_{\mathcal{T}_2}^{(k)})$. The same procedure is applied to decode $\mathbf{U}^{(k)}$ at $\mathcal{T}_1$.

As in the coherent part, an equivalent transmission to the first two phases can be performed if $\mathcal{T}_1$ transmits $\sqrt{2P_{\mathcal{T}_1}}w_{\mathcal{T}_1}^{(k)}$ while $\mathcal{T}_2$ remains silent during the first

time slot, and then $\mathcal{T}_2$ transmits $\sqrt{2P_{\mathcal{T}_2}}w_{\mathcal{T}_2}^{(k)}$ while $\mathcal{T}_1$ remains silent during the second time slot.

4.6.2 Decoding Procedure at the Communicating Terminals with Direct Link

Using the direct link transmission, the estimated value $\hat{\mathbf{s}}_{\mathcal{R},\mathcal{T}_2}$ can be found using

$$\arg\min_{\mathbf{s}_{\mathcal{R}}^{(k)}} \left\| \mathbf{y}_{\mathcal{T}_2}^{(k)} - \frac{\mathbf{U}^{(k)}\mathbf{y}_{\mathcal{T}_2}^{(k-1)}}{\hat{a}_{\mathcal{T}_2}^{(k-1)}} \right\|^2 + \left\| y_{\mathcal{T}_2,dl}^{(k)} - \frac{x_{\mathcal{T}_1}^{(k)}\, y_{\mathcal{T}_2,dl}^{(k-1)}}{\left|\hat{x}_{\mathcal{T}_1}^{(k-1)}\right|} \right\|^2, \tag{4.34}$$

where

$$x_{\mathcal{T}_1}^{(k)} = \mathcal{G}_{\mathcal{T}_2}\left(\mathcal{F}_{\mathcal{T}_2}^{-1}\left(\mathbf{s}_{\mathcal{R}}^{(k)}, \mathbf{s}_{\mathcal{T}_2}^{(k)}\right)\right), \tag{4.35}$$

$$\hat{x}_{\mathcal{T}_1}^{(k-1)} = \mathcal{G}_{\mathcal{T}_2}\left(\mathcal{F}_{\mathcal{T}_2}^{-1}\left(\hat{\mathbf{s}}_{\mathcal{R},\mathcal{T}_2}^{(k-1)}, \mathbf{s}_{\mathcal{T}_2}^{(k-1)}\right)\right) \tag{4.36}$$

and $y_{\mathcal{T}_2,dl}^{(k)}$ is the received signal at $\mathcal{T}_2$ using the direct link in the first phase.

4.7 Simulation Results

In our simulations, we have assumed a wireless relay network with $R = 2$, independent flat Rayleigh fading channels and a power distribution equal to $P_{\mathcal{T}_1} = P_{\mathcal{T}_2} = \sum_{r=1}^{R} P_{\mathcal{R}_r}$ where $P_{\mathcal{R}_1} = P_{\mathcal{R}_2} = \cdots = P_{\mathcal{R}_R}$, as in [113]. The relays use the distributed Alamouti code and the DF strategy for the transmission.

We compare first the proposed coherent schemes with the 2-phase PDF and 3-phase PDF from [113] using the combination functions $\mathcal{F}_{\mathrm{m}}(\cdot,\cdot)$ explained in Sec. 4.3, $\mathcal{F}_{\mathrm{xor}}(\cdot,\cdot)$ and $\mathcal{F}_{\mathrm{s}}(\cdot,\cdot)$ explained in Sec. 4.5. The abbreviation DL stands for the use of the direct link in the scheme. The case when the relays always decode the information without errors is denoted as "ideal". To be able to compare the performance of all schemes, the same total power $P_T = P_{\mathcal{T}_1} + P_{\mathcal{T}_2} + \sum_{r=1}^{R} P_{\mathcal{R}_r}$ and bit rate is used.

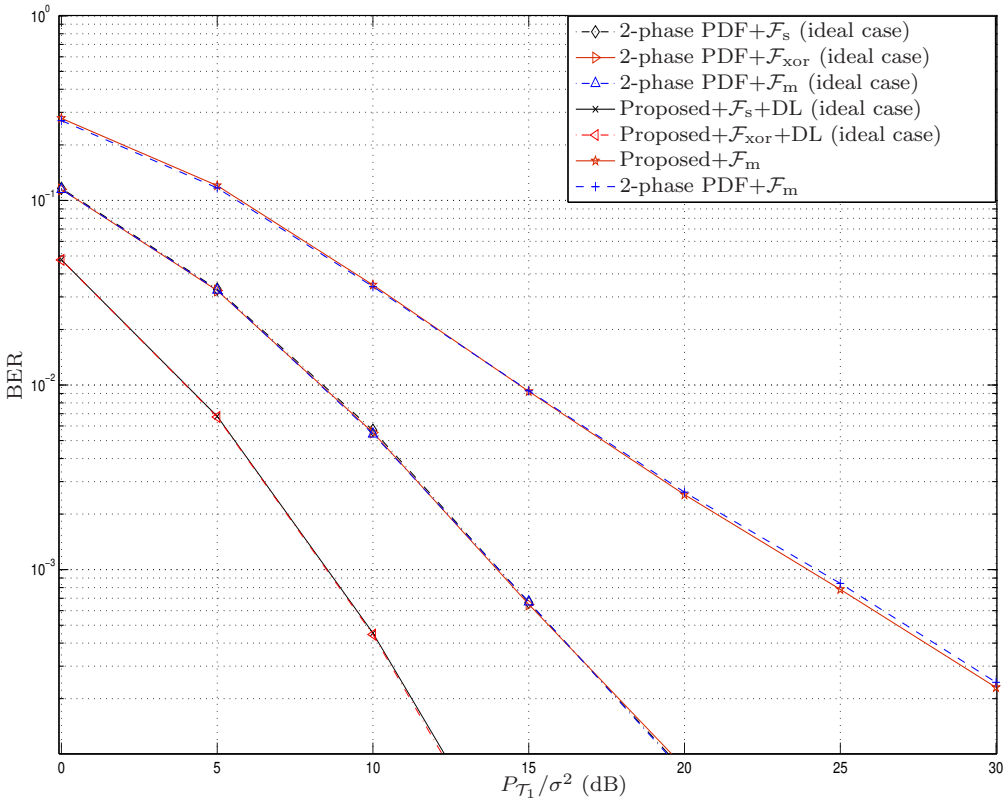

Figure 4.3: Performance of different TWRN protocols with $R = 2$ using BPSK.

Figs. 4.3, 4.4 and 4.5 show the BER at $\mathcal{T}_2$ versus $P_{\mathcal{T}_1}/\sigma^2$ for a total rate of 0.5 bit per channel use (bpcu) using BPSK, 1 bpcu using 4-QAM and 2 bpcu using 16-QAM, respectively.

It can be observed from these figures that, as in the PDF protocols, the full diversity in our proposed schemes can not be obtained unless the decoding at the relays yields a low error probability. This can be achieved using more power in the broadcasting phase, CRC or a forward error correcting code (FEC), for example. The figures show also that the proposed protocol outperforms 2-phase PDF and 3-phase PDF using the same combination function. Note that the transmission

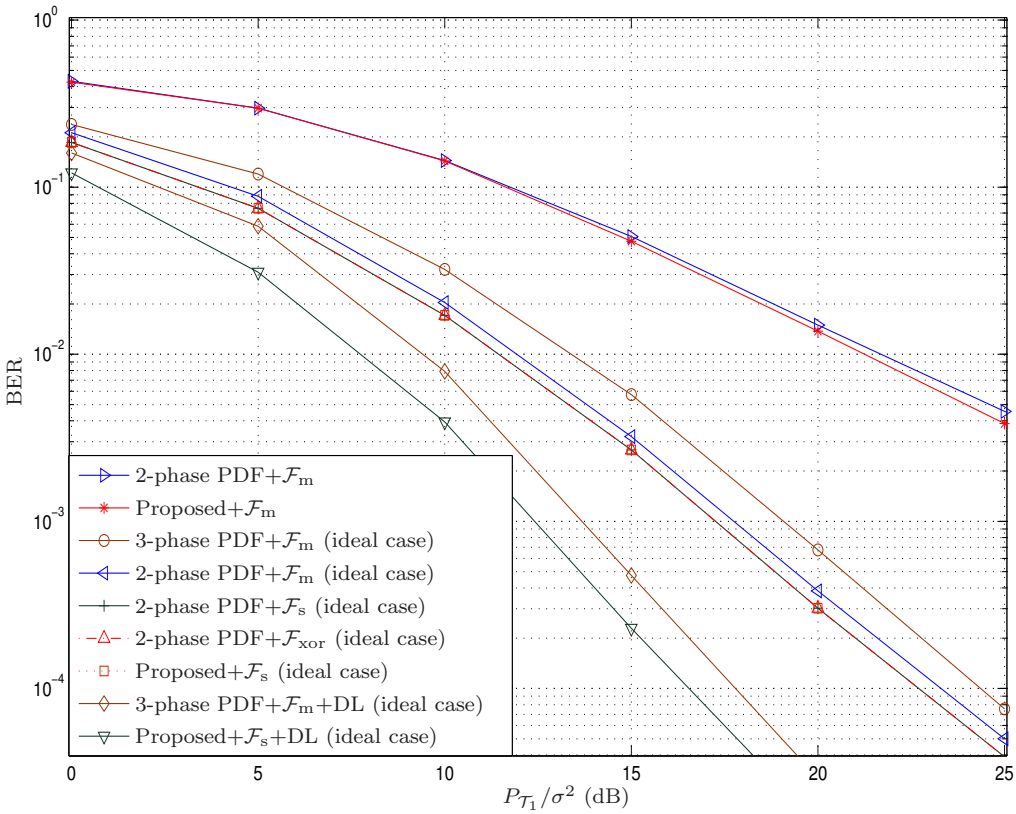

Figure 4.4: Performance of different TWRN protocols with $R = 2$ and a rate of 1 bpcu.

phase from the relays to the terminals in 2-phase PDF and the proposed scheme with the same combination function are equal. Therefore, the performance of both schemes is identical in the ideal case, as the effect of the transmission from the terminals to the relays is not taken into account. If the direct link is used, the proposed scheme obtains a substantial performance advantage with respect to 3-phase PDF. Note that 2-phase PDF can not use the direct link.

From Figs. 4.4 and 4.5, we observe the expected result that the use of $\mathcal{F}_{\mathrm{xor}}(\cdot,\cdot)$ explained in Sec. 4.5 and $\mathcal{F}_{\mathrm{s}}(\cdot,\cdot)$, given by (4.17) in Sec. 4.5, provides improved

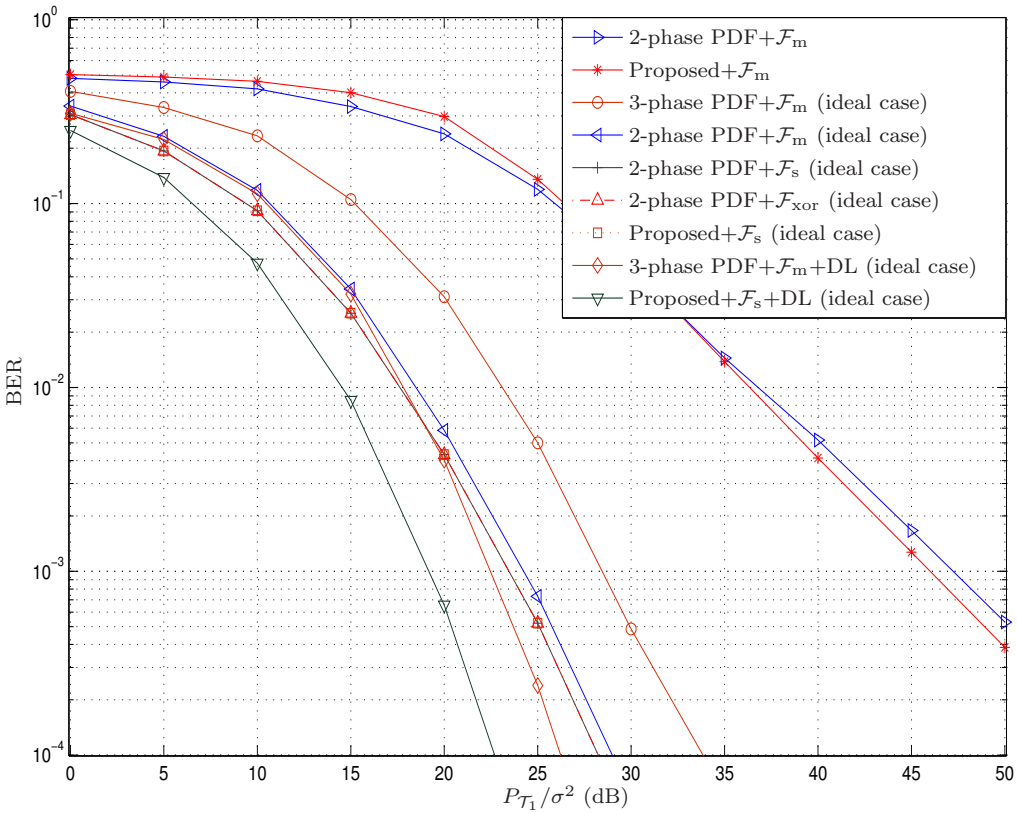

Figure 4.5: Performance of different TWRN protocols with $R = 2$ and a rate of 2 bpcu.

performance as compared to the case where the mapping function $\mathcal{F}_{\mathrm{m}}(\cdot,\cdot)$ explained in Sec. 4.3 is used. Furthermore, the performance of $\mathcal{F}_{\mathrm{xor}}(\cdot,\cdot)$ and $\mathcal{F}_{\mathrm{s}}(\cdot,\cdot)$ is equivalent. However, $\mathcal{F}_{\mathrm{s}}(\cdot,\cdot)$ uses the modulation symbols directly.

Finally, we compare the non-coherent extension of the proposed scheme with the four-phase differential transmission using DF, i.e., the four-phase scheme can be viewed as the conventional one way relaying scheme applied twice. In the first phase, the relays receive the signal from $\mathcal{T}_1$, decode the signal and forward it in the second phase to $\mathcal{T}_2$. Similarly, in the third phase, the relays receive, decode

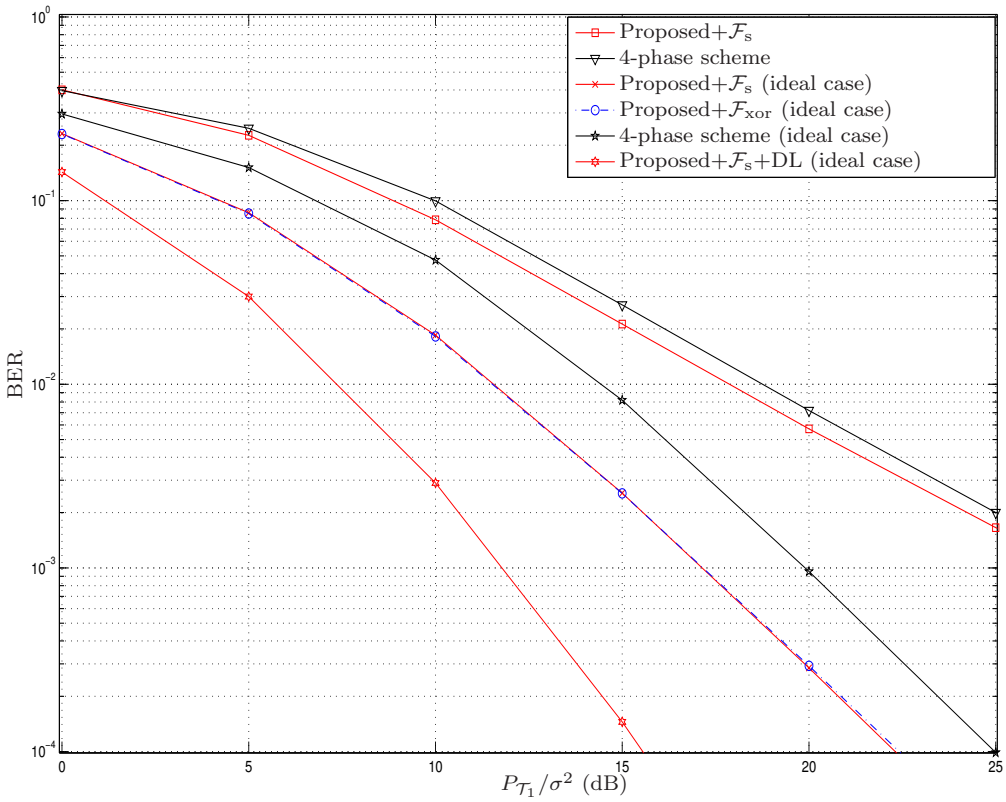

Figure 4.6: Performance of different non-coherent TWRN protocols with $R = 2$ using BPSK.

and forward the signal from $\mathcal{T}_2$ in the fourth phase to $\mathcal{T}_1$.

Figs. 4.6 and 4.7 display the BER at $\mathcal{T}_2$ versus $P_{\mathcal{T}_1}/\sigma^2$ for a total rate of 0.5 bpcu using BPSK and 1 bpcu using 4-QAM. As in the previous figures, it can be observed that $\mathcal{F}_{\text{xor}}(\cdot,\cdot)$ and $\mathcal{F}_{\text{s}}(\cdot,\cdot)$ achieve identical performance. It can also be observed that the proposed scheme achieves significantly better performance than the four-phase protocol.

The error probability at the end terminals is limited by the error probability at the relay nodes. Therefore, the error probability at the relay nodes should be

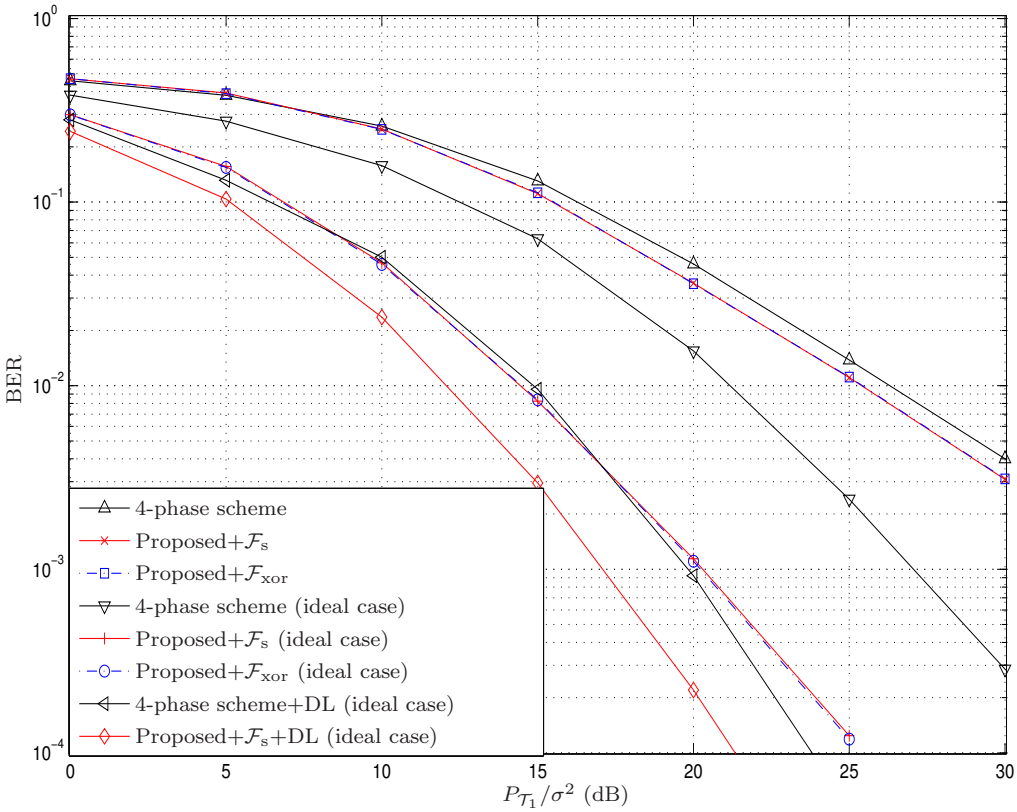

Figure 4.7: Performance of different non-coherent TWRN protocols with $R = 2$ and a rate of 1 bpcu.

lower than the error probability at the end terminal. Fig. 4.8 displays the BER at $\mathcal{T}_2$ of the proposed scheme without direct link versus $P_{\mathcal{T}_1}/\sigma^2$ in a relay network with $R = 2$ using 4-QAM and $\mathcal{F}_{\rm m}(\cdot,\cdot)$. In Fig. 4.8, three cases are shown: i) the relays decode the received signal without errors, denoted as $\text{BER}_{\mathcal{R}} = 0$, ii) the relays decode the received signal with the same BER achieved at the end terminal for the ideal case, denoted as $\text{BER}_{\mathcal{R}} = \text{BER}_{\mathcal{T}_2}^{(\text{ideal})}$ where $\text{BER}_{\mathcal{T}_2}^{(\text{ideal})}$ denotes the BER achieved at $\mathcal{T}_2$ using ideal relays, iii) the relays decode the received signal with a lower BER than the one achieved at the end terminal (1/10 of the BER at $\mathcal{T}_2$), denoted as $\text{BER}_{\mathcal{R}} = \text{BER}_{\mathcal{T}_2}^{(\text{ideal})}/10$.

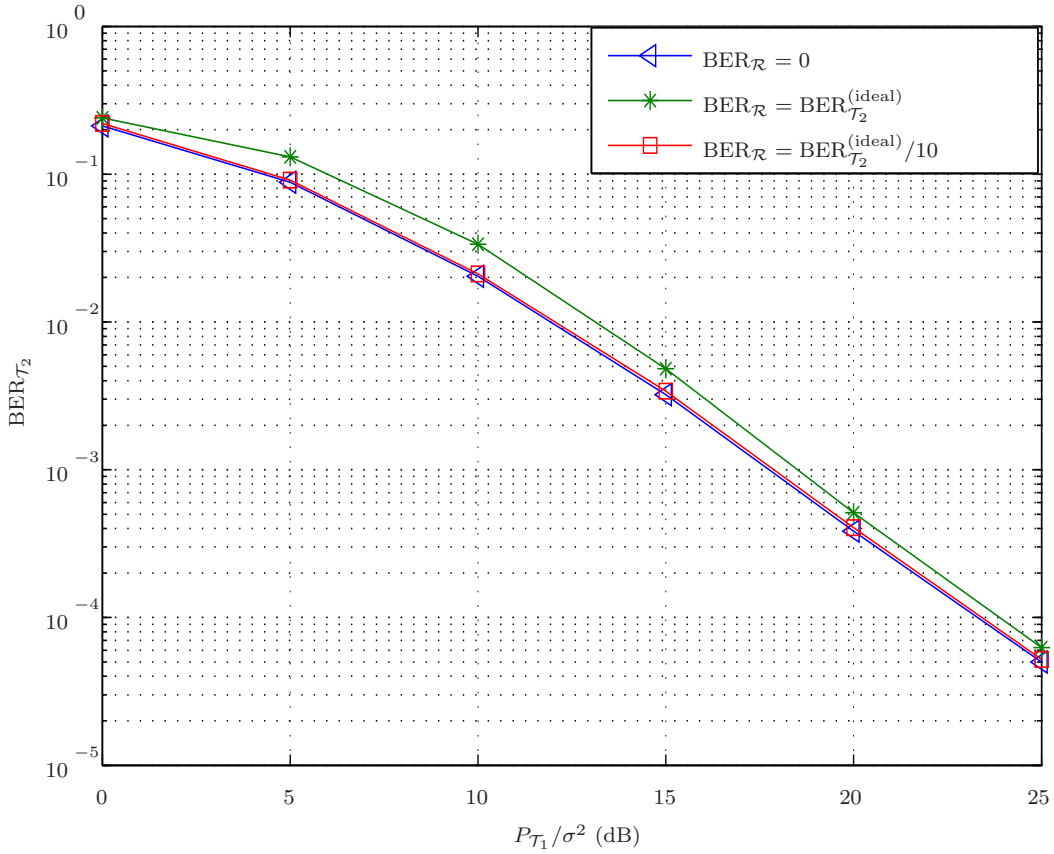

Figure 4.8: Performance of the proposed protocol in a relay network with $R = 2$ using 4-QAM.

From Fig. 4.8, it can be observed that the maximum diversity gain can be achieved when the error probability at the relay nodes is lower than that at the end terminal.

4.8 Conclusion

In this chapter, a simple strategy for distributed space-time coded TWRNs using the decode-and-forward protocol is proposed. Our strategy enjoys a lower

decoding complexity at the relays than the previously proposed methods with simultaneous transmission from both terminals at the same symbol rate. Furthermore, the proposed scheme allows the communicating terminals to use the direct link between them. We also propose an extension of our protocol to networks without CSI using differential DSTC. Our simulations demonstrate a substantially improved performance of the proposed schemes as compared to the earlier strategies.

Chapter 5

Distributed Differential Space-Time Block Coding in Amplify and Forward Relay Networks

Several differential DSTC techniques for TWRNs using the AF protocol have been proposed which do not require CSI either at the relays or at the terminals. In this chapter, we propose novel differential DSTC strategies for TWRNs using the AF protocol. Simulations show a substantially improved BER performance of the proposed strategies as compared to the known strategies.

5.1 Introduction

Efficient cooperative strategies based on DSTC which requires CSI only at the receive terminal have been proposed in [18, 29]. To overcome the overhead involved with the channel estimation, differential DSTC schemes which avoid channel estimation either at the relays or at the terminals have been proposed in [78, 79, 86, 126, 127].

In [128], a simultaneous AF bidirectional differential DSTC scheme for TWRNs using the two-phase protocol has been proposed. The authors in [128] have shown that the two-phase protocol, see Fig. 2.13, outperforms the conventional four-phase protocol, see Fig. 2.11, except for the high SNR region due to the error floor effect where additional research is required to analyze and reduce it. Although the simultaneous bidirectional AF protocol using DSTC has been shown to outperform the conventional four-phase DSTC strategy at low SNR due to its higher symbol rate, it has mainly three disadvantages: i) the relay power wasted to transmit information known at either side, ii) the impracticality to use the direct link between the communicating terminals, and iii) the considerable error floor experienced at high SNR.

In the DF relay networks discussed in chapter four, the relays decode and re-encode their received symbols before amplifying and transmitting them to the terminals. To overcome the overhead involved with the decoding process at each relay, we propose, in this chapter, two novel three-phase differential DSTC strategies for TWRNs using the AF protocol. The proposed strategies combine the received symbols from both terminals at the relays into one symbol, without decoding them, so that each terminal can decode the transmitted symbol of the other terminal using the information of its own transmitted symbol as explained in Sec. 2.4.3. In this way, the BER performance is improved as the relays do not waste any power to transmit known information symbols and the direct link between the communicating terminals can easily be incorporated. In the first proposed strategy, the relays amplify the received signal including the noise, while in the second strategy, they carefully scale the received signal in order to avoid amplifying the relay noise before transmitting it to both terminals.

5.2 The proposed Differential Distributed Space-Time Coding Techniques

Similar to Sec. 2.4.3.1, we consider a half-duplex TWRN with $R+2$ single-antenna nodes where the terminals, $\mathcal{T}_1$ and $\mathcal{T}_2$, communicate with each other through R

relays ($\mathcal{R}_1, \ldots, \mathcal{R}_R$) as shown in Fig. 2.14. In this chapter, similar assumptions as in Sec. 2.4.3.1 are considered. We further assume extended block fading channel model where the channels remain constant during $3T$ time slots and the CSI is neither known at the transmitting nor at the receiving nodes. During the first two phases of this protocol from time slot 1 to T, and time slot $T+1$ to $2T$, the terminals $\mathcal{T}_1$ and $\mathcal{T}_2$ transmit in the kth block the differentially encoded $T \times 1$ symbol vectors $\mathbf{x}_1^{(k)}$ and $\mathbf{x}_2^{(k)}$, respectively, to the relays where

$$\begin{aligned} \mathbf{x}_t^{(k)} &= \mathrm{diag}(\mathbf{s}_\mathrm{t}^{(\mathrm{k})})\ \mathbf{x}_\mathrm{t}^{(\mathrm{k}-1)} \\ &= \mathbf{S}_t^{(k)}\ \mathbf{x}_t^{(k-1)}, \end{aligned} \tag{5.1}$$

$t = 1, 2$, $\mathbf{s}_1^{(k)} = [[s_1^{(k)}]_1, \cdots, [s_1^{(k)}]_T]^T$ and $\mathbf{s}_2^{(k)} = [[s_2^{(k)}]_1, \cdots, [s_2^{(k)}]_T]^T$ denote the kth information symbol vectors of dimension $T \times 1$ transmitted by terminal $\mathcal{T}_1$ and $\mathcal{T}_2$, respectively, $\mathbf{S}_t^{(k)}$ is a unitary matrix containing the information symbols of the kth block, $\mathbf{x}_t^{(0)} = [1,\ 1,\ 1,\ \cdots,\ 1]^T$ defines the initial symbol vector in the first transmission that can be used as a reference at the receiver to start the differential decoding procedure, $\left|[\mathbf{x}_t^{(k)}]_i\right| = \left|[\mathbf{s}_t^{(k)}]_i\right|$, and $\mathrm{diag}(\mathbf{s}_\mathrm{t}^{(\mathrm{k})})$ denotes the diagonal matrix whose diagonal elements are the elements of the vector $\mathbf{s}_t^{(k)}$. We assume that $[\mathbf{x}_t^{(k)}]_i$ and $[\mathbf{s}_t^{(k)}]_i$ are taken from a M-PSK constellation denoted by the set $\mathcal{S}_t$ corresponding to $\mathcal{T}_t$, hence $[\mathbf{x}_t^{(k)}]_i \in \mathcal{S}_t$ and $[\mathbf{s}_t^{(k)}]_i \in \mathcal{S}_t$.

Note that the initial symbol vector $\mathbf{x}_t^{(0)}$ is only transmitted at the beginning of the transmission. In the next block of symbols, the last transmitted vector of the previous block can be used as a reference in the decoding procedure. In the first phase of the kth block, from time slot 1 to T, the $T \times 1$ vector received at the rth relay is given by:

$$\mathbf{y}_{1,r}^{(k)} = \sqrt{P_1}\ f_r^{(k)}\ \mathbf{x}_1^{(k)} + \mathbf{n}_{1,r}^{(k)} \tag{5.2}$$

where $\mathbf{n}_{1,r}^{(k)}$ denotes the noise vector at the rth relay in the first phase of the kth block. We assume that the noise vector can be modeled as a spatially white independently and identically distributed Gaussian random variable with zero mean and covariance $\sigma^2\mathbf{I}_T$.

Similarly, in the second phase of the kth block, from time slot $T+1$ to $2T$, the $T \times 1$ vector received at the rth relay is given by:

$$\mathbf{y}_{2,r}^{(k)} = \sqrt{P_2}\; g_r^{(k)}\; \mathbf{x}_2^{(k)} + \mathbf{n}_{2,r}^{(k)} \tag{5.3}$$

where $\mathbf{n}_{2,r}^{(k)}$ denotes the noise vector at the rth relay in the second phase of the kth block. Making use of the block fading assumption, i.e., the channel remains constant over $3T$ time slots, for simplicity of notation we write f_r and g_r in the following to represent $f_r^{(k)}$ and $g_r^{(k)}$, respectively.

5.2.1 The First Proposed Technique

In the third phase of the kth block, the rth relay transmits the $T \times 1$ signal vector

$$\begin{aligned} \mathbf{x}_{3,r}^{(k)} &= \mathbf{y}_{1,r}^{(k)} \odot \mathbf{y}_{2,r}^{(k)}, \qquad (5.4) \\ &= \sqrt{P_1 P_2}\; f_r^{(k)}\; g_r^{(k)}\; \mathbf{x}_{\mathcal{R}}^{(k)} + \mathbf{v}_{3,r}^{(k)} \end{aligned}$$

where

$$\begin{aligned} \mathbf{v}_{3,r}^{(k)} &\triangleq \sqrt{P_1}\; f_r^{(k)}\; (\mathbf{x}_1^{(k)} \odot \mathbf{n}_{2,r}^{(k)}) \qquad (5.5) \\ &+ \sqrt{P_2}\; g_r^{(k)}\; (\mathbf{x}_2^{(k)} \odot \mathbf{n}_{1,r}^{(k)}) + (\mathbf{n}_{1,r}^{(k)} \odot \mathbf{n}_{2,r}^{(k)}), \end{aligned}$$

$$\mathbf{x}_{\mathcal{R}}^{(k)} \triangleq \mathbf{x}_1^{(k)} \odot \mathbf{x}_2^{(k)} = \mathbf{S}_{\mathcal{R}}^{(k)}\; \mathbf{x}_{\mathcal{R}}^{(k-1)} \tag{5.6}$$

$[\mathbf{x}_{\mathcal{R}}^{(k)}]_i \in \mathcal{S}_t$ and $\odot$ denotes the Hadamard (or Schur) product. In the following, we only consider the received signals at $\mathcal{T}_2$. The signal received at $\mathcal{T}_1$ can be computed correspondingly. Depending on the chosen STC, the rth relay precodes the symbol vector $\mathbf{x}_{3,r}^{(k)}$ or its conjugate with the $T \times T$ unitary matrix $\mathbf{A}_r$ before broadcasting it to both terminals. The received signal vector at $\mathcal{T}_2$ in the kth

block is then given by:

$$\mathbf{y}_2^{(k)} = \sum_{r=1}^{R} \beta_r \; g_r \mathbf{A}_r \breve{\mathbf{x}}_{3,r}^{(k)} + \mathbf{n}_2^{(k)} \tag{5.7}$$

where either $\breve{\mathbf{x}}_{3,r}^{(k)} = \mathbf{x}_{3,r}^{(k)}$ or $\breve{\mathbf{x}}_{3,r}^{(k)} = (\mathbf{x}_{3,r}^{(k)})^*$, $\beta_r = \sqrt{\frac{P_{\mathcal{R}_r}}{P_1 P_2 + P_1 + P_2}}$ and $\mathbf{n}_2^{(k)}$ denotes the noise vector at $\mathcal{T}_2$. The choice of $\breve{\mathbf{x}}_{3,r}^{(k)}$ and $\mathbf{A}_r$ at each relay depends on the used DSTC scheme as explained in Sec. 2.4.1. For example, in the Alamouti scheme with two relays used in the simulation part, $\breve{\mathbf{x}}_{\mathcal{R}3,r}$ and $\mathbf{A}_r$ are chosen as follows:

$$\mathbf{A}_1 \triangleq \begin{bmatrix} 1 & 0 \\ 0 & 1 \end{bmatrix}, \quad \mathbf{A}_2 \triangleq \begin{bmatrix} 0 & 1 \\ -1 & 0 \end{bmatrix},$$

$$\breve{\mathbf{x}}_{3,1}^{(k)} \triangleq \mathbf{x}_{3,1}^{(k)}, \quad \breve{\mathbf{x}}_{3,2}^{(k)} \triangleq (\mathbf{x}_{3,2}^{(k)})^*.$$

For simplicity and without loss of generality, it is assumed that the first L relays transmit the signal vector $\mathbf{x}_{3,r}^{(k)}$ while the remaining $R-L$ relays transmit $(\mathbf{x}_{3,r}^{(k)})^*$, $P_{\mathcal{R}_1} = P_{\mathcal{R}_2} = \cdots = P_{\mathcal{R}_R}$ and $\beta_1 = \beta_2 = \cdots = \beta_R = \beta$. In the third phase of the kth block, the received signal vector at $\mathcal{T}_2$ can be expressed as:

$$\mathbf{y}_2^{(k)} = \beta \; \mathbf{X}^{(k)} \; \mathbf{h}^{(k)} + \mathbf{v}_2^{(k)} \tag{5.8}$$

where

$$\mathbf{v}_2^{(k)} \triangleq \beta \left(\sum_{r=1}^{L} g_r \mathbf{A}_r \mathbf{v}_{3,r}^{(k)} + \sum_{r=L+1}^{R} g_r \mathbf{A}_r (\mathbf{v}_{3,r}^{(k)})^* \right) + \mathbf{n}_2^{(k)}, \tag{5.9}$$

$$\mathbf{h}^{(k)} \triangleq [f_1^{(k)}(g_1^{(k)})^2, \cdots, f_L^{(k)}(g_L^{(k)})^2, (f_{L+1}^{(k)})^* |g_{L+1}^{(k)}|^2, \cdots, (f_R^{(k)})^* |g_R^{(k)}|^2]^T, \tag{5.10}$$

$$\mathbf{X}^{(k)} \triangleq [\mathbf{A}_1 \mathbf{x}_{\mathcal{R}}^{(k)}, \cdots, \mathbf{A}_L \mathbf{x}_{\mathcal{R}}^{(k)}, \mathbf{A}_{L+1} (\mathbf{x}_{\mathcal{R}}^{(k)})^*, \cdots\cdots, \mathbf{A}_R (\mathbf{x}_{\mathcal{R}}^{(k)})^*]. \tag{5.11}$$

Since $\mathbf{S}_{\mathcal{R}}^{(k)}$ and $\mathbf{A}_r$ are unitary matrices, we have $\mathbf{A}_r \mathbf{S}_{\mathcal{R}}^{(k)} = \mathbf{S}_{\mathcal{R}}^{(k)} \mathbf{A}_r$ and

$\mathbf{A}_r(\mathbf{S}_{\mathcal{R}}^{(k)})^* = \mathbf{S}_{\mathcal{R}}^{(k)}\mathbf{A}_r$. Then from equation (5.1) and (5.11) we obtain:

$$\mathbf{X}^{(k)} = \mathbf{S}_{\mathcal{R}}^{(k)}\ \mathbf{X}^{(k-1)}. \tag{5.12}$$

Making use of the extended block fading assumption where $\mathbf{h}^{(k-1)} = \mathbf{h}^{(k)} = \mathbf{h}$ and inserting (5.12) in (5.8) we have:

$$\mathbf{y}_2^{(k)} \;=\; \beta\ \mathbf{S}_{\mathcal{R}}^{(k)}\ \mathbf{X}^{(k-1)}\ \mathbf{h} + \mathbf{v}_2^{(k)}. \tag{5.13}$$

Clearly from the previous equations, the ML decoder at $\mathcal{T}_2$ can be expressed as:

$$\arg\min_{\mathbf{S}_{\mathcal{R}}^{(k)}} \left\| \mathbf{y}_2^{(k)} - \mathbf{S}_{\mathcal{R}}^{(k)}\ \mathbf{y}_2^{(k-1)} \right\|^2. \tag{5.14}$$

In case of using the direct link, the decoder at $\mathcal{T}_2$ can be expressed as:

$$\arg\min_{\mathbf{s}_{\mathcal{T}_1}^{(k)}} \left\| \mathbf{y}_{\mathcal{T}_2}^{(k)} - \mathbf{S}_{\mathcal{T}_1}^{(k)}\ \mathbf{S}_{\mathcal{T}_2}^{(k)}\ \mathbf{y}_{\mathcal{T}_2}^{(k-1)} \right\|^2 + \left\| \mathbf{y}_{\mathcal{T}_2,\mathrm{dl}}^{(k)} - \mathbf{S}_{\mathcal{T}_1}^{(k)} \mathbf{y}_{\mathcal{T}_2,\mathrm{dl}}^{(k-1)} \right\|^2 \tag{5.15}$$

where $\mathbf{y}_{\mathcal{T}_2,\mathrm{dl}}^{(k)}$ is the received signal at $\mathcal{T}_2$ during the first phase. Note that the direct link case can have a significantly more complex decoder, as a full search over $\mathbf{S}_{\mathcal{T}_1}^{(k)}$ is required. In contrast to (5.15), the decoder of (5.14) can be implemented using the sphere decoder, or in case of using orthogonal DSTCs, a symbol-wise decoder can be used to decode the received symbols at $\mathcal{T}_2$. However, the use of the direct link can provide a higher diversity order. A similar decoding procedure can be applied at $\mathcal{T}_1$.

5.2.2 The Second Proposed Technique

During the third phase of the kth block, the rth relay transmits the signal vector

$$\mathbf{x}_{3,r}^{(k)} \;=\; e^{\left(j\measuredangle \mathbf{y}_{1,r}^{(k)}\right)} \odot e^{\left(j\measuredangle \mathbf{y}_{2,r}^{(k)}\right)}. \tag{5.16}$$

where $\measuredangle$ denotes the argument of a complex number and $e^{(\mathbf{y}_{1,r}^{(k)})}$ returns the exponential for each element of the vector $\mathbf{y}_{1,r}^{(k)}$. Consider our extended block fading assumption, hence, $g_r^{(k)} = g_r^{(k-1)}$, $f_r^{(k)} = f_r^{(k-1)}$ and assume for now the ideal noise-free case where $\mathbf{n}_{t,r}^{(k)} = \mathbf{n}_{t,r}^{(k-1)} = 0$, then (5.16) can be expressed as:

$$\mathbf{x}_{3,r}^{(k)} \;=\; e^{j\measuredangle(f_r\ g_r)}\ \mathbf{x}_{\mathcal{R}}^{(k)} \tag{5.17}$$

where $\mathbf{x}_{\mathcal{R}}^{(k)} = \mathbf{x}_1^{(k)} \odot \mathbf{x}_2^{(k)}$ and $\mathbf{x}_{\mathcal{R}}^{(k)} \in \mathcal{S}_t$. Note that, in this scheme, the noise signals change only the phases of the received signals. Clearly for high SNR, the effect of the noise to the phase-shift of the received signals will become negligible, therefore, $\mathbf{x}_{3,r}^{(k)} \approx e^{j\measuredangle(f_r\ g_r)}\ \mathbf{x}_{\mathcal{R}}^{(k)}$. Similar to the previous strategy, the relays also precode the symbol vector $\mathbf{x}_{3,r}^{(k)}$ or its conjugate with the unitary matrix $\mathbf{A}_r$ before broadcasting it to both terminals. The received signal vector at $\mathcal{T}_2$ in the kth block is given by:

$$\mathbf{y}_2^{(k)} = \sum_{r=1}^{R} \sqrt{P_{\mathcal{R}_r}}\ g_r\ \mathbf{A}_r\ \breve{\mathbf{x}}_{3,r}^{(k)} + \mathbf{n}_2^{(k)} \tag{5.18}$$

where $\mathbf{n}_2^{(k)}$ denotes the noise vector at $\mathcal{T}_2$. In the third phase of the kth block, the received signal vector at $\mathcal{T}_2$ can be expressed as:

$$\mathbf{y}_2^{(k)} \;=\; \sqrt{P_{\mathcal{R}}}\ \mathbf{X}^{(k)}\ \mathbf{h} + \mathbf{n}_2^{(k)} \tag{5.19}$$

where

$$\mathbf{h} \;\triangleq [e^{j\measuredangle(f_1 g_1)} g_1, \cdots, e^{j\measuredangle(f_L g_L)} g_L, e^{-j\measuredangle(f_{L+1} g_{L+1})} g_{L+1}, \cdots, e^{-j\measuredangle(f_R g_R)} g_R]^T, \tag{5.20}$$

$$\mathbf{X}^{(k)} \;\triangleq [\ \mathbf{A}_1\ \mathbf{x}_{\mathcal{R}}^{(k)},\ \cdots,\ \mathbf{A}_L\ \mathbf{x}_{\mathcal{R}}^{(k)},\ \mathbf{A}_{L+1}\ (\mathbf{x}_{\mathcal{R}}^{(k)})^*,\ \cdots,\ \mathbf{A}_R\ (\mathbf{x}_{\mathcal{R}}^{(k)})^*\ ]. \tag{5.21}$$

Since $\mathbf{X}^{(k)} = \mathbf{S}_{\mathcal{R}}^{(k)}\ \mathbf{X}^{(k-1)}$, we can rewrite equation (5.19) as:

$$\mathbf{y}_2^{(k)} \quad = \quad \sqrt{P_{\mathcal{R}}}\ \mathbf{S}_{\mathcal{R}}^{(k)}\ \mathbf{X}^{(k-1)}\ \mathbf{h} + \mathbf{n}_2^{(k)}. \tag{5.22}$$

The decoder at $\mathcal{T}_2$ can be expressed as:

$$\arg\min_{\mathbf{S}_{\mathcal{R}}^{(k)}} \left\| \mathbf{y}_2^{(k)} - \mathbf{S}_{\mathcal{R}}^{(k)}\ \mathbf{y}_2^{(k-1)} \right\|^2 \tag{5.23}$$

and similar decoding procedure can be applied at $\mathcal{T}_1$. In case of using the direct link, the decoder at $\mathcal{T}_2$ can be expressed as:

$$\arg\min_{\mathbf{S}_{\mathcal{T}_1}^{(k)}} \left\| \mathbf{y}_{\mathcal{T}_2}^{(k)} - \mathbf{S}_{\mathcal{T}_1}^{(k)}\ \mathbf{S}_{\mathcal{T}_2}^{(k)}\ \mathbf{y}_{\mathcal{T}_2}^{(k-1)} \right\|^2 + \left\| \mathbf{y}_{\mathcal{T}_2,\mathrm{dl}}^{(k)} - \mathbf{S}_{\mathcal{T}_1}^{(k)} \mathbf{y}_{\mathcal{T}_2,\mathrm{dl}}^{(k-1)} \right\|^2. \tag{5.24}$$

In the proposed schemes, the received symbols from both terminals are combined at the relays into one symbol, without decoding them, so that each terminal can decode the transmitted symbol of the other terminal using the information of its own transmitted symbol. In this way, the overall system performance in terms of BER is improved as the relays do not waste power to transmit redundant information to either side as explained in Sec. 2.4.3. However, the two schemes achieve different BER performance.

In the first scheme, the relays amplify the noise combined with the received symbol, while in the second scheme, they carefully scale the received signal in order not to amplify the relay noise before transmitting it to both terminals. This observation clearly described to our simulation results provided in the next section.

5.3 Simulation Results

In our simulations, we have assumed a wireless relay network with $R = 2$, independent flat Rayleigh fading channels, where the power is distributed equally among the three phases, i.e., $P_1 = P_2 = \sum_{r=1}^{R} P_{\mathcal{R}_r}$. In order to obtain a fair comparison of

the performance of all schemes, the same total power ($P_T = P_1 + P_2 + \sum_{r=1}^{R} P_{\mathcal{R}_r}$, $P_{\mathcal{R}_1} = P_{\mathcal{R}_2} = \cdots = P_{\mathcal{R}_R}$) and bit rate are used.

In Fig. 5.1, the BER at $\mathcal{T}_2$ is displayed versus the SNR and the proposed three-

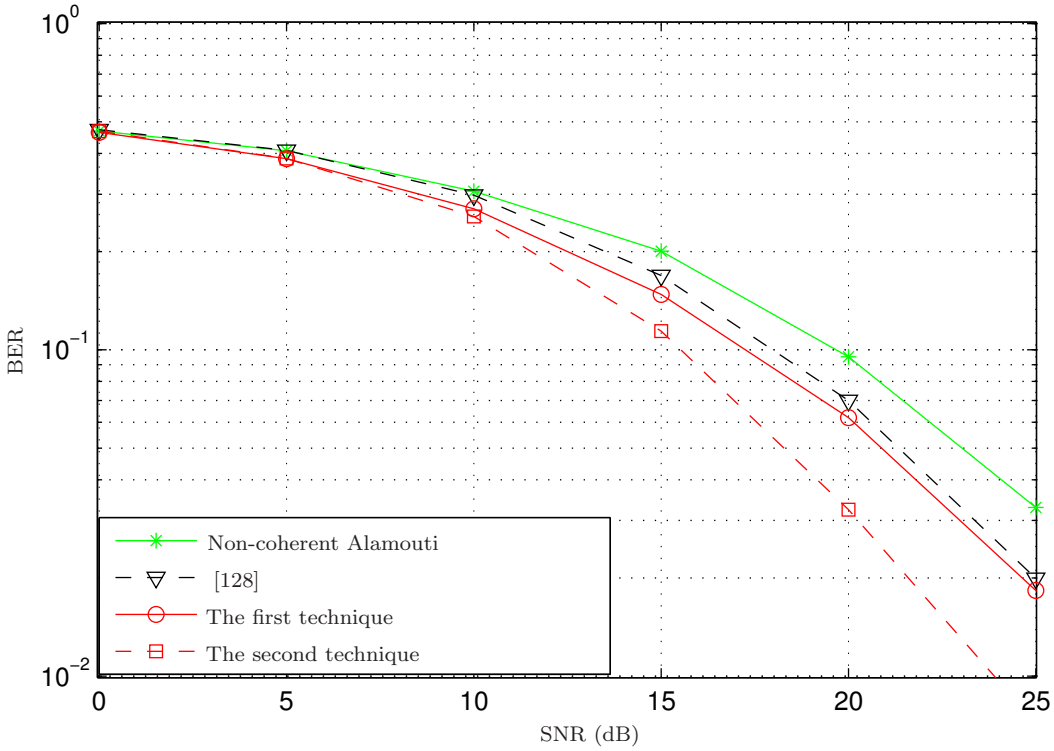

Figure 5.1: BER versus SNR for several differential techniques.

phase non-coherent STC schemes using 8-PSK is compared with the four-phase non-coherent distributed Alamouti STC scheme using 16-PSK and two-phase distributed differential STC scheme for TWRNs proposed in [128] using 4-PSK. It can be seen from Fig. 5.1 that the proposed schemes outperform the two- and four-phase scheme in terms of BER. Note that the second proposed scheme outperforms the first one, since, in the second scheme, the noise signals affect only the phases of the received signals at relays and, for high SNR, the effect of the noise to the phase-shift of the received signals becomes negligible.

5.4 Conclusion

In this chapter, novel strategies for the distributed differential space-time coded TWRNs using the AF protocol are proposed. In the proposed strategies, the relays do not waste power to transmit redundant information at either side and the direct link between the communicating terminals is easily exploited. In the first scheme, the relays combine the received symbols from both terminals into one symbol (without the need to decode them) and amplify it together with the relay noise, while in the second scheme, they carefully scale the combined symbol to not amplify the relay noise before transmitting it to both terminals. Our simulations demonstrate a substantially improved BER performance of the proposed strategies as compared to the known strategies.

Chapter 6

Distributed Differential Beamforming in Amplify and Forward Relay Networks

Various differential DSTC techniques for cooperative relay networks have recently been proposed, which do not require CSI either at the relays or at the terminals. Differential encoding techniques are generally associated with a low BER performance and a comparably high latency and decoding complexity.

Another approach used in relay networks are distributed beamforming techniques which enjoy a high BER performance, a low decoding complexity, and an optimal decoding delay. However, their common requirement is the availability of CSI all nodes. In this chapter, we combine the differential diversity and the distributed beamforming technique while retaining the benefits of both approaches.

6.1 Introduction

Many approaches have recently been proposed to generalize and improve cooperative diversity techniques. Some approaches are based on unrealistic

assumptions such as perfect CSI available at all nodes [123, 124]. Other approaches consider the case of perfect or partial CSI available at the receiver side only [18, 29, 69, 125]. Recent approaches have also been based on the more practical assumption of CSI available neither at the transmitter nor at the receiver [97, 126, 127]. The DSTC techniques require CSI only at the receiver, therefore, differential DSTC techniques which avoid channel estimation at the relays and the terminals have been proposed [78, 79, 86, 97, 126, 127]. These techniques, as explained in Sec. (4.6) and Sec. (5.2), eliminate the overhead involved with channel estimation, however, they have low BER performance, a comparably high latency and a significant decoding complexity for more than two transmit antennas due to unavailability of CSI at the nodes.

Another popular approach used in relay networks relies on coherent processing of the relay signals using distributed beamforming techniques which adjust the phase of the signal at each transmitter and form a beam steering towards the destination. These techniques enjoy a high system performance in terms of BER and low decoding complexity while offering an optimal decoding delay. However, a common requirement in distributed beamforming is the availability of CSI at both transmitter and receiver. Clearly, none of the above pioneer works combines both techniques, the differential diversity and the distributed beamforming technique.
Several efficient techniques have been proposed to synchronize the phase of the received signals at the destination [130, 131, 133]. In [133], the authors proposed a distributed transmit beamforming scheme without CSI at any nodes that periodically uses training symbols to synchronize the phases at the relays. However, in this scheme, the transmission of each information symbol requires three time slots, therefore, its symbol rate is low.

In this chapter, we propose a non-trivial combination of both concepts, i.e., the differential diversity techniques and the distributed beamforming techniques, while retaining the benefits of both approaches. The proposed technique does not require either CSI at any node or feedback bits while achieving high BER performance, optimal end-to-end delay, and low decoding complexity. Simulation

results demonstrate a substantially improved performance in terms of BER of the proposed scheme as compared to the known schemes.

6.2 The Proposed Distributed Differential Transmit Beamforming Technique

Similar as in Sec. 2.4.3.1, we consider a half-duplex TWRN with $R+2$ single-antenna nodes consisting of two terminals, $\mathcal{T}_1$ and $\mathcal{T}_2$, that intend to communicate with each other through R relay nodes $(\mathcal{R}_1, \ldots, \mathcal{R}_R)$, as shown in Fig. 2.14. In this chapter, similar assumptions as in Sec. 2.4.3.1 are considered. We further assume that neither the relays nor the terminals require CSI or feedback bits to decode or process the received signal and the channels remain constant during two consecutive transmission blocks. During the first two time slots of the kth block, the terminals $\mathcal{T}_1$ and $\mathcal{T}_2$ transmit the differential encoded scalars $x_{\mathcal{T}_1}^{(k)}$ and $x_{\mathcal{T}_2}^{(k)}$ where

$$x_{\mathcal{T}_t}^{(k)} = x_{\mathcal{T}_t}^{(k-1)}\ s_{\mathcal{T}_t}^{(k)}, \tag{6.1}$$

$t = 1, 2$; $s_{\mathcal{T}_1}^{(k)}$ and $s_{\mathcal{T}_2}^{(k)}$ denote the information symbols of the kth block transmitted by terminal $\mathcal{T}_1$ and $\mathcal{T}_2$, respectively. Further, $x_{\mathcal{T}_t}^{(0)} = s_{\mathcal{T}_t}^{(0)} = 1$ define the initial symbols in the first transmission that can be used as a reference at the receiver to start the differential decoding procedure and $\left|x_{\mathcal{T}_t}^{(k)}\right| = \left|s_{\mathcal{T}_t}^{(k)}\right|$.

We assume without loss of generality that $s_{\mathcal{T}_t}^{(k)}$ is drawn from a M-PSK constellation denoted by the set $\mathcal{S}_{\mathcal{T}_t}$ corresponding to $\mathcal{T}_t$, hence $s_{\mathcal{T}_t}^{(k)} \in \mathcal{S}_{\mathcal{T}_t}$. Note that the initial symbol $x_{\mathcal{T}_t}^{(0)}$ is only transmitted at the beginning of the transmission. In the next block of symbols, the last symbol from the previous block can be used as a reference to start the decoding procedure. In the first time slot of the kth transmission block, the received signal at the rth relay is given by:

$$y_{\mathcal{R}1,r}^{(k)} = \sqrt{P_{\mathcal{T}_1}} f_r^{(k)}\ x_{\mathcal{T}_1}^{(k)} + n_{\mathcal{R}1,r}^{(k)} \tag{6.2}$$

where $n_{\mathcal{R}1,r}^{(k)}$ denotes the noise at the rth relay in the first time slot of the kth transmission block. We assume that the noise can be modeled as an independent and identically distributed Gaussian random variable with zero mean and variance $\sigma^2 = 1$. Similarly, in the second time slot of the kth block, the received signal at the rth relay is given by:

$$y_{\mathcal{R}2,r}^{(k)} = \sqrt{P_{\mathcal{T}_2}}\ g_r^{(k)}\ x_{\mathcal{T}_2}^{(k)} + n_{\mathcal{R}2,r}^{(k)} \tag{6.3}$$

where $n_{\mathcal{R}2,r}^{(k)}$ denotes the noise at the rth relay in the second time slot of the kth transmission block. In the third and fourth time slot of the kth block, the rth relay transmits the signals

$$x_{\mathcal{R}1,r}^{(k)} = \sqrt{\frac{P_{\mathcal{R}r}}{P_{\mathcal{T}_1}+1}}\ y_{\mathcal{R}1,r}^{(k)}\ e^{j\theta_{\mathcal{R}1,r}^{(k)}}, \tag{6.4}$$

$$x_{\mathcal{R}2,r}^{(k)} = \sqrt{\frac{P_{\mathcal{R}r}}{P_{\mathcal{T}_2}+1}}\ y_{\mathcal{R}2,r}^{(k)}\ e^{j\theta_{\mathcal{R}2,r}^{(k)}}, \tag{6.5}$$

respectively. The optimal value of $\theta_{\mathcal{R}t,r}^{(k)}$, $t = 1, 2$, $r = 1, 2, \cdots, R$, which leads to a coherent superposition of the signals from all relays and maximizes the overall SNR at the both terminals, can be expressed as:

$$\theta_{\mathcal{R}t,r}^{opt} = -\left(\measuredangle f_r^{(k)} + \measuredangle g_r^{(k)}\right) + c \tag{6.6}$$

where c is an arbitrary constant. To proof that the choice of (6.6) is maximizing the SNR, let us first assume, without loss of generality, that $P_{\mathcal{R}_1} = P_{\mathcal{R}_2} = \cdots = P_{\mathcal{R}_R} = P_{\mathcal{R}}$. The overall SNR at $\mathcal{T}_2$ is given by:

$$\mathrm{SNR}_{\mathcal{T}_2} = \frac{\frac{P_{\mathcal{T}_1} P_{\mathcal{R}}}{P_{\mathcal{T}_1}+1}\ \mathrm{E}\left\{\left|\sum_{r=1}^{R} f_r^{(k)}\ g_r^{(k)}\ e^{j\theta_{\mathcal{R}1,r}^{(k)}}\right|^2\right\}}{\mathrm{E}\left\{\left|\sum_{r=1}^{R}\sqrt{\frac{P_{\mathcal{R}}}{P_{\mathcal{T}_1}+1}} g_r^{(k)}\ n_{\mathcal{R}1,r}^{(k)} e^{j\theta_{\mathcal{R}1,r}^{(k)}} + n_{\mathcal{T}_2}^{(k)}\right|^2\right\}}$$

where $n_{\mathcal{T}_2}^{(k)}$ denotes the noise signals at $\mathcal{T}_2$ in the kth block and

$$\left|\sum_{r=1}^{R} f_r^{(k)}\ g_r^{(k)}\ e^{j\theta_{\mathcal{R}1,r}^{(k)}}\right|^2 \leq \left|\sum_{r=1}^{R} \left|f_r^{(k)}\ g_r^{(k)}\right|\right|^2. \tag{6.7}$$

To maximize $\mathrm{SNR}_{\mathcal{T}_2}$, equation (6.7) must hold with equality. This can be achieved if the phase shift $\theta_{\mathcal{R}1,r}^{(k-1)}$ is $-\left(\measuredangle f_r^{(k)} + \measuredangle g_r^{(k)}\right) + c, \quad \forall r$.

In the proposed scheme, it is assumed that there is no CSI available at any node. However, to ensure coherent reception, the phase rotation $\theta_{\mathcal{R}t,r}^{(k)}$ applied at the rth relay in the kth block must be as close as possible to its optimal value $\theta_{\mathcal{R}t,r}^{opt}$ given by (6.6). Using the received signals at each relay from both terminals, then $\theta_{\mathcal{R}1,r}^{(k)}$ and $\theta_{\mathcal{R}2,r}^{(k)}$ can be expressed as:

$$\theta_{\mathcal{R}1,r}^{(k)} = -\left(\measuredangle y_{\mathcal{R}1,r}^{(k-1)} + \measuredangle y_{\mathcal{R}2,r}^{(k)}\right), \tag{6.8}$$

$$\theta_{\mathcal{R}2,r}^{(k)} = -\left(\measuredangle y_{\mathcal{R}1,r}^{(k)} + \measuredangle y_{\mathcal{R}2,r}^{(k-1)}\right), \tag{6.9}$$

respectively. Let us assume that the channels remain constant over two consecutive transmission blocks, hence, $g_r^{(k)} = g_r^{(k-1)}$, $f_r^{(k)} = f_r^{(k-1)}$ and consider for now the ideal noise-free case where $n_{\mathcal{R}t,r}^{(k)} = n_{\mathcal{R}t,r}^{(k-1)} = 0$, $t = 1, 2$, $r = 1, 2, \cdots, R$, then equations (6.8) and (6.9) can be expressed as:

$$\theta_{\mathcal{R}1,r}^{(k)} = -\left(\measuredangle f_r^{(k)} + \measuredangle g_r^{(k)}\right) - \left(\measuredangle x_{\mathcal{T}_1}^{(k-1)} + \measuredangle x_{\mathcal{T}_2}^{(k)}\right), \tag{6.10}$$

$$\theta_{\mathcal{R}2,r}^{(k)} = -\left(\measuredangle f_r^{(k)} + \measuredangle g_r^{(k)}\right) - \left(\measuredangle x_{\mathcal{T}_1}^{(k)} + \measuredangle x_{\mathcal{T}_2}^{(k-1)}\right), \tag{6.11}$$

respectively, where the phase terms $-\left(\measuredangle x_{\mathcal{T}_1}^{(k-1)} + \measuredangle x_{\mathcal{T}_2}^{(k)}\right)$ and $-\left(\measuredangle x_{\mathcal{T}_1}^{(k)} + \measuredangle x_{\mathcal{T}_2}^{(k-1)}\right)$ in (6.10) and (6.11), respectively, are constants, similar as the corresponding phase term c in (6.6), for all relays $r = 1, 2, \cdots, R$. At high SNR, the effect of the noise on the phase-shift becomes insignificant and therefore, $\theta_{\mathcal{R}t,r}^{(k)} \approx \theta_{\mathcal{R}t,r}^{opt}$.

In the third and fourth time slot of the kth transmission block, the received signals at $\mathcal{T}_1$ and $\mathcal{T}_2$ are give by:

$$y_{\mathcal{T}_1}^{(k)} = \sum_{r=1}^{R} f_r^{(k)}\ x_{\mathcal{R}2,r}^{(k)} + n_{\mathcal{T}_1}^{(k)}, \tag{6.12}$$

$$y_{\mathcal{T}_2}^{(k)} = \sum_{r=1}^{R} g_r^{(k)}\ x_{\mathcal{R}1,r}^{(k)} + n_{\mathcal{T}_2}^{(k)}, \tag{6.13}$$

respectively, where $n_{\mathcal{T}_1}^{(k)}$ and $n_{\mathcal{T}_2}^{(k)}$ are the noise signals at $\mathcal{T}_1$ and $\mathcal{T}_2$ in the kth block, respectively. At high SNR, equations (6.12) and (6.13) can be expressed as:

$$y_{\mathcal{T}_1}^{(k)} \approx \sum_{r=1}^{R} \sqrt{\frac{P_{\mathcal{R}r}}{P_{\mathcal{T}_2}+1}} |f_r^{(k)}||g_r^{(k)}| e^{\left(-j\measuredangle x_{\mathcal{T}_1}^{(k)}\right)} s_{\mathcal{T}_2}^{(k)} + w_{\mathcal{T}_1}^{(k)}, \tag{6.14}$$

$$y_{\mathcal{T}_2}^{(k)} \approx \sum_{r=1}^{R} \sqrt{\frac{P_{\mathcal{R}r}}{P_{\mathcal{T}_1}+1}}\ |f_r^{(k)}||g_r^{(k)}| e^{\left(-j\measuredangle x_{\mathcal{T}_2}^{(k)}\right)} s_{\mathcal{T}_1}^{(k)} + w_{\mathcal{T}_2}^{(k)}, \tag{6.15}$$

respectively, where

$$w_{\mathcal{T}_1}^{(k)} = \sum_{r=1}^{R} \sqrt{\frac{P_{\mathcal{R}r}}{P_{\mathcal{T}_2}+1}}\ (f_r^{(k)}\ e^{(j\theta_{\mathcal{R}2,r}^{(k)})}\ n_{\mathcal{R}2,r}^{(k)}) + n_{\mathcal{T}_1}^{(k)}, \tag{6.16}$$

$$w_{\mathcal{T}_2}^{(k)} = \sum_{r=1}^{R} \sqrt{\frac{P_{\mathcal{R}r}}{P_{\mathcal{T}_1}+1}} \left(g_r^{(k)}\ e^{(j\theta_{\mathcal{R}1,r}^{(k)})} n_{\mathcal{R}1,r}^{(k)}\right) + n_{\mathcal{T}_2}^{(k)}. \tag{6.17}$$

The decoder at $\mathcal{T}_1$ can be expressed as:

$$\arg\min_{s^{(k)}} \left\| \frac{y_{\mathcal{T}_1}^{(k)}}{e^{(-j\measuredangle x_{\mathcal{T}_1}^{(k)})}} - \left| \frac{y_{\mathcal{T}_1}^{(k-1)}}{e^{(-j\measuredangle x_{\mathcal{T}_1}^{(k-1)})}} \right| s^{(k)} \right\|^2. \tag{6.18}$$

A similar decoding procedure can be used at $\mathcal{T}_2$ where $s_{\mathcal{T}_1}^{(k)}$ is decoded as:

$$\arg\min_{s^{(k)}} \left\| \frac{y_{\mathcal{T}_2}^{(k)}}{e^{(-j\measuredangle x_{\mathcal{T}_2}^{(k)})}} - \left| \frac{y_{\mathcal{T}_2}^{(k-1)}}{e^{(-j\measuredangle x_{\mathcal{T}_2}^{(k-1)})}} \right| s^{(k)} \right\|^2 . \tag{6.19}$$

6.3 Simulation Results

In our simulations, we have assumed a wireless relay network with $R = 2$, independent flat Rayleigh fading channels and the power is distributed equally among the communicating terminals and relays, i.e., $P_{\mathcal{T}_1} = P_{\mathcal{T}_2} = \sum_{r=1}^{R} P_{\mathcal{R}_r}$.

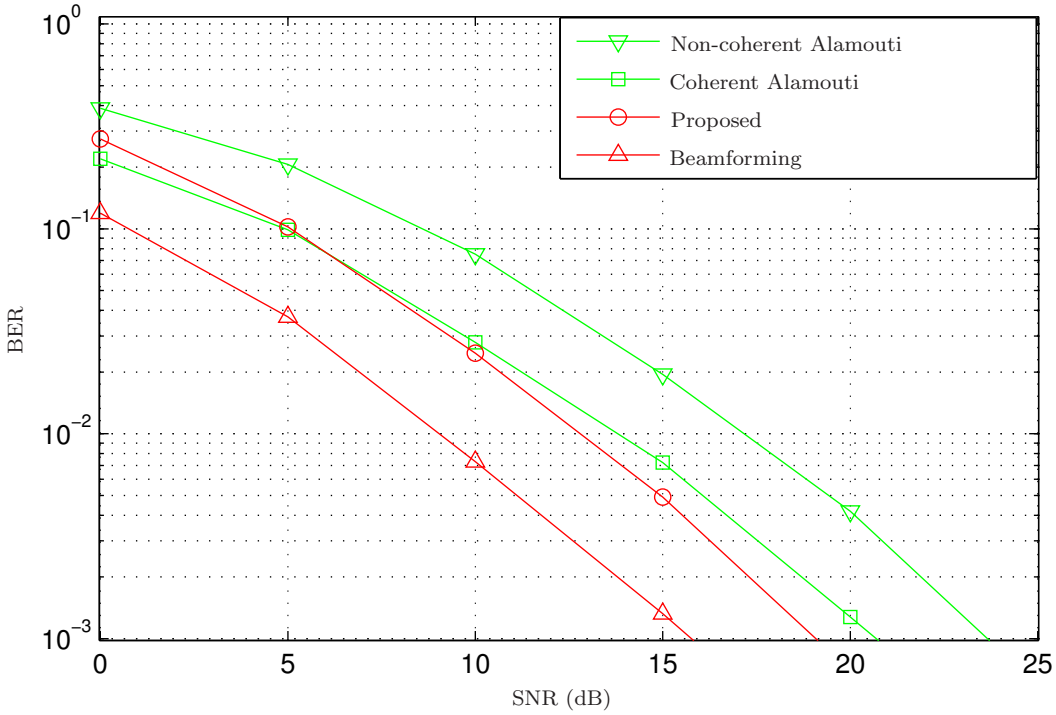

Figure 6.1: BER versus SNR for different coherent and differential schemes using BPSK modulation.

We compare the proposed non-coherent scheme with the four-phase coherent

and non-coherent DSTC scheme using the Alamouti [12] and the random unitary code, four-phase distributed transmit beamforming and the two-phase differential DSTC scheme for TWRNs proposed in [128]. In order to obtain a fair comparison of the performance for all schemes, the same total power ($P_T = P_{\mathcal{T}_1} + P_{\mathcal{T}_2} + \sum_{r=1}^{R} P_{\mathcal{R}_r}$, $P_{\mathcal{R}_1} = P_{\mathcal{R}_2} = \cdots = P_{\mathcal{R}_R}$) and bit rate are used.

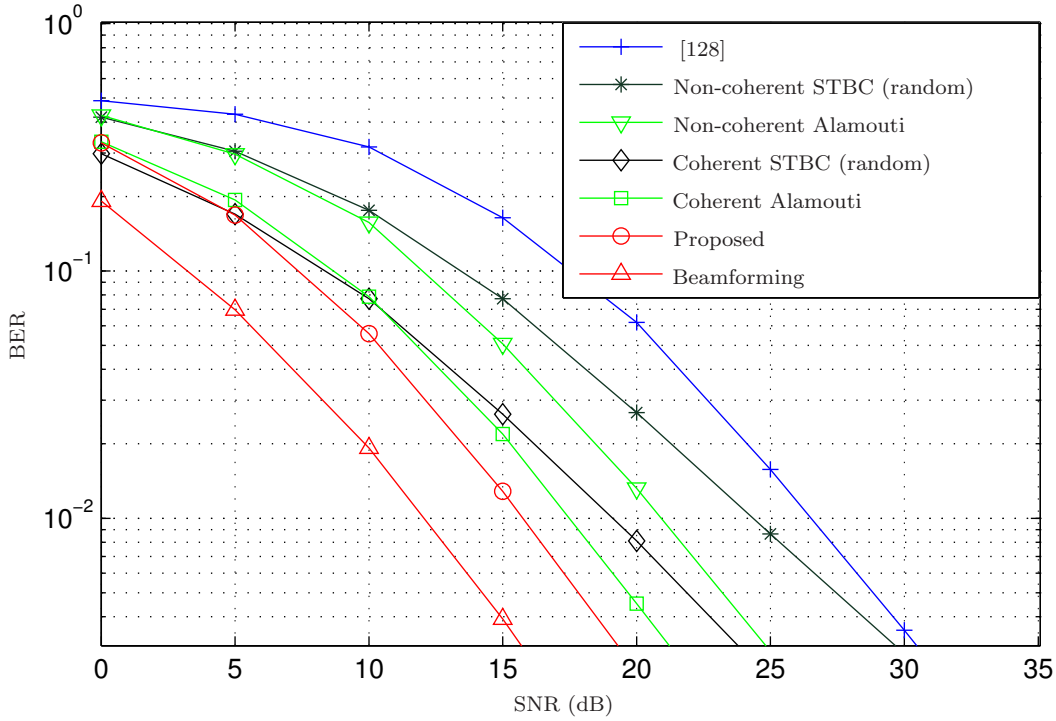

Figure 6.2: BER versus SNR for different coherent and differential schemes.

In Fig. 6.1, the BER at $\mathcal{T}_2$ is displayed versus the SNR using BPSK modulation. In Fig. 6.2, the four-phase schemes using QPSK are compared with two-phase scheme proposed in [128] using BPSK. It can be observed that the proposed scheme outperforms the two- and four-phase schemes in terms of BER.

Note that the difference between the coherent and non-coherent distributed scheme for the random unitary and Alamouti scheme is around 3 dB. Similarly, there exists a 3 dB margin between the proposed non-coherent scheme and the

distributed beamforming scheme. This means that the proposed scheme achieves full diversity gain with coding gain only 3 dB less than that of a system which requires full CSI at all relay transceivers. The 3 dB loss in performance can be explained by the absence of CSI at all transmitting and receiving nodes [19].

6.4 Conclusion

In this chapter, we propose a novel differential distributed relay beamforming scheme, which does not require CSI at any node. The proposed strategy enjoys a low decoding complexity, a high system performance in terms of BER, and an optimal transmission delay without requiring any feedback bits. The proposed scheme can be viewed as a non-trivial combination of two multiple-antenna techniques, the differential diversity and the distributed beamforming technique, while retaining the benefits of both approaches.

List of Abbreviations

AF	Amplify-and-forward
AM	Amplitude modulation
BER	Bit error rate
bpcu	Bits per channel use
bps	Bits per second
CRC	Cyclic redundancy check
CSI	Channel state information
DF	Decode-and-forward
DSTC	Distributed space-time coding/code
FEC	Forward error correction
FM	Frequency modulation
FEC	Forward error correction
IEEE	Institute of electrical and electronics engineers
i.i.d	Independent and identically distributed
ISI	Inter-symbol interference
LOS	Line-of-side
MIMO	Multiple-input multiple-output
MISO	Multiple-input single-output
ML	Maximum likelihood
MMSE	Minimum mean squared error
OSTBC	Orthogonal space-time block coding/code
pdf	Probability density function
PAM	Pulse amplitude modulation
PDF	Partial decode-and-forward

PEP	Pairwise error probability
QAM	Quadrature amplitude modulation
QO-STBC	Quasi-orthogonal space-time block coding/code
QoS	Quality of service
QPSK	Quadrature phase shift keying
SER	Symbol error rate
SIMO	Single-input multiple-output
SISO	Single-input single-output
SNR	Signal-to-noise ratio
STBC	Space-time block coding/code
STC	Space-time coding/code
STTC	Space-time trellis coding/code
TWRN	Two-way wireless relay network
USTC	Unitary space-time coding/code
XOR	Exclusive OR

List of Symbols

M_t	Number of transmit antennas
M_r	Number of receive antennas
T	Block length
j	$\sqrt{-1}$
$h_{m,n}$	Channel state information between the nth transmit and mth receive antenna
$\mathbf{H}$	Channel matrix
$y(t)$	Receive signal
$x_j(t)$	Signal transmit from the jth antenna and t time-slot
$n(t)$	Additive white Gaussian noise signal
$\mathbf{Y}$	$M_r \times T$ complex matrix of the received signals
$\mathbf{X}$	$M_t \times T$ complex matrix of the transmitted signals
$\mathbf{N}$	$M_r \times T$ complex white Gaussian noise matrix
$\mathbf{I}_A$	$A \times A$ identity matrix
$f_X(x)$	Probability density function of X
$\mathbf{n}(t)$	Noise vector
c, K, γ	Constants
R	Number of relay nodes
f_r	Channel gain between the source terminal and the rth relay
g_r	Channel gain between the rth relay and the destination terminal
f_0	Channel gain from the source terminal to the destination terminal
$\mathcal{T}_t$	Terminal t
$\mathbf{s}_{\mathcal{T}_t}$	Information symbol vector transmitted from the tth terminal
μ	Mean
σ^2	Variance

L	The number of transmitted symbols
ϕ	Rotation angle.

List of Notations

$\mathcal{CN}(\cdot,\cdot)$	Gaussian random variable
$(\cdot)^T$	Transpose of a matrix
$(\cdot)^H$	Hermitian transpose
$\|\cdot\|$	Frobenious norm
$f_X(x)$	Probability density function of X
$\|\cdot\|$	Absolute value
$\log_2$	Binary logarithm
$\max(a,b)$	Maximum value between a and b
$\min(a,b)$	Minimum value between a and b
$\mathrm{Re}\{\cdot\}$	Real part
$\Im\{\cdot\}$	Imaginary part
$\det(\cdot)$	Determinant
$(\cdot)^*$	Complex conjugate
$(\cdot)^{(k)}$	Block index
$\oplus$	Exclusive OR (XOR) operation
$\mathrm{E}\{\cdot\}$	Statistical expectation
$[\mathbf{a}]_i$	ith entry of a vector $\mathbf{a}$
$\mathrm{mod}(a,b)$	Remainder of the division of a by b
$\mathrm{sgn}(\cdot)$	Signum function
$\mathcal{G}_{\mathcal{T}_1}(\cdot)$	Mapping function
$\mathcal{P}(\cdot\|\cdot)$	Conditional probability
$\mathcal{F}(\cdot,\cdot)$	Combination function
$\mathcal{F}_{\mathrm{m}}(\cdot,\cdot)$	Modular arithmetic function
$\mathcal{F}_{\mathrm{xor}}(\cdot,\cdot)$	XOR combination function

$\mathcal{F}(\cdot,\cdot)^{-1}$	Inverse of the combination function
$\mathcal{G}_{\mathcal{T}_1}(\cdot)$	Inverse of the mapping function
$\measuredangle$	Argument
$\odot$	Hadamard (or Schur) product
diag($\mathbf{a}$)	Diagonal matrix whose diagonal elements are the elements of the vector $\mathbf{a}$
$I_o(\cdot)$	Modified zero-order Bessel function of the first kind.

Bibliography

[1] G. Foschini and M. Gans, "On limits of wireless communications in a fading environment when using multiple antennas," *Wireless Personal Commun.*, vol. 6, pp. 311–355, 1998.

[2] E. Telatar, "Capacity of multi-antenna Gaussian channels," *European Trans. Telecommun.*, vol. 10, pp. 585–595, June 1999.

[3] J. G. Proakis, "Digital communications," Fourth Edition, McGraw Hill, New York, 2001.

[4] J. H. Winters, "Switched diversity with feedback for DPSK mobile radio systems," *IEEE Trans. on Vechnology*, vol. 32, pp. 134–150, 1983.

[5] A. Wittneben, "A new bandwidth efficient transmit antenna modulation diversity scheme for linear digital modulation," *In Proc. of 1993 International Conference on Communications (ICC'93)*, pp. 1630–1634, May 1993.

[6] G. L. Stuber, "Principles of mobile communications," Kluwer Academic Publishers (KAP), second edition, 2000.

[7] T. S. Rappaport, "Wireless communications: principles and practice," Prentice Hall PTR, second edition, 2002.

[8] Alex B. Gershman and N. D. Sidiropoulos, "Space-time processing for MIMO communications," John Wiley and Sons, Ltd, 2005.

[9] V. Tarokh, N. Seshadri, and A. R. Calderbank, "Space-time codes for high data rate wireless communication: Performance analysis and code

construction," *IEEE Trans. Inform. Theory*, vol. 44, no. 2, pp. 744–765, Mar. 1998.

[10] V. Tarokh, H. Jafarkhani, and A. Calderbank, "Space-time block coding for wireless communications: Performance results," *IEEE J. Select. Areas Commun.*, vol. 17, pp. 451–460, Mar. 1999.

[11] V. Tarokh, H. Jafarkhani, and A. Calderbank, "Space-time block codes from orthogonal designs," *IEEE Trans. Inform. Theory*, vol. 45, pp. 1456–1467, July 1999.

[12] S. Alamouti, "A simple transmitter diversity scheme for wireless communications," *IEEE J. Select. Areas Commun.*, vol. 16, pp. 1451–1458, Oct. 1998.

[13] S. Sandhu, R. Heath, and A. Paulraj, "Space-time block code versus space-time trellis code," *IEEE Proc. Conf. Commun.*, Helsinki, Finland, vol. 4, pp. 1132–1136, Jun. 2001.

[14] A. Sendonaris, E. Erkip, and B. Aazhang, "User cooperation diversity Part-I: system description," *IEEE Trans. Commun.*, vol. 51, no. 11, pp. 1927–1938, Nov. 2003.

[15] A. Sendonaris, E. Erkip, and B. Aazhang, "User cooperation diversity Part-II: Implementation aspects and performance analysis," *IEEE Trans. Commun.*, vol. 51, no. 11, pp. 1939–1948, Nov. 2003.

[16] R. Nabar, H. Boelcskei, and F. Kneubuhler, "Fading relay channels: performance limits and space-time signal design," *IEEE Journal Selected Areas Commun.*, vol. 22, no. 6, pp. 1099–1109, Aug. 2004.

[17] J. Laneman, D. Tse, and G. Wornell, "Cooperative diversity in wireless networks: efficient protocols and outage behavior," *IEEE Trans. Inform. Theory*, vol. 50, pp. 3062–3080, Dec. 2004.

[18] Y. Jing and B. Hassibi, "Distributed space-time coding in wireless relay networks," *IEEE Trans. on Wireless Communications*, vol. 5, no. 12, pp. 3524–3536, Dec. 2006.

[19] H. Jafarkhani, "Space-Time Coding: Theory and Practice," *Cambridge, U.K. Cambridge Univ. Press,* 2005.

[20] G. M. Calhoun, "The third generation wireless systems, Volume I: post Shannon signal architectures," *artech house,* 2003.

[21] J. W. Mark and W. Zhuang, "Wireless communications and networking," Prantice Hall, New Jersey, 2003.

[22] J. N. Laneman and G. W. Wornell, "Energy-efficient antenna sharing and relaying for wireless networks," *Proc. of WCNC 2000*, vol. 1, pp. 7–12, Sep. 2000.

[23] M. C. Valenti and B. Zhao, "Distributed turbo codes: towards the capacity of the relay channel," *Proc. Of IEEE Vehicular Technology Conference (VTC)*, Orlando (USA), vol. 1, pp. 322–326, Oct. 2003.

[24] A. Nosratinia, T. E. Hunter, and A. Hedayat, "Cooperative communication in wireless networks," *IEEE Communications magazine*, vol. 42, pp. 74–80, Oct. 2004.

[25] T. E. Hunter and A. Nosratinia, "Performance analysis of coded cooperation diversity," *Proc. of ICC*, vol. 4, pp. 2688–2698, 2003.

[26] V. Emamian and M. Kaveh, "Combating shadowing effects for systems with transmitter diversity by using collaboration among mobile users," *Proc. of Intern. Symp. On Commun., Taiwan*, vol. 9, pp. 1051–1054, Nov. 2001.

[27] A. Sendonaris, E. Erkip, and B. Aazhang, "Increasing uplink capacity via user cooperation diversity," *In Proceeding IEEE International Symposium on Information Theory (ISIT)*, pp. 156–156, Aug. 1998.

[28] J. N. Laneman and G. W. Wornell, "Distributed space-time coded protocols for exploiting cooperative diversity in wireless networks," *Proc. of GLOBECOM*, pp. 77–81, Nov. 2002.

[29] J. Laneman and G. Wornell, "Distributed space-time-coded protocols for exploiting cooperative diversity in wireless networks," *IEEE Trans. Inform. Theory,* vol. 49, no. 10, pp. 2415–2425, Oct. 2003.

[30] J. C. Guey, M. P. Fitz, M. R. Bell, and W. Y. Kuo, "Signal design for transmitter diversity wireless communication systems over Rayleigh fading channels," *IEEE Trans. on Communications*, vol. 47, no. 4, pp. 527–37, Apr. 1999.

[31] A. Narula, M. Trott, and G. Wornell, "Performance limits of coded diversity methods for transmitter antenna arrays," *IEEE Trans. on Information Theory*, vol. 45, pp. 2418–2433, Nov. 1999.

[32] G. Raleigh and J. M. Ciof., "Spatio-temporal coding for wireless communications," *IEEE Globecom.*, vol. 3, pp. 1809–1814, 1996.

[33] N. Seshadri and J. H. Winters, "Two signaling schemes for improving the error performance of frequency-division-duplex (FDD) transmission systems using transmitter antenna diversity," *IEEE Vehicular Technology Conference,* vol. 1, pp. 508–511, May 1993.

[34] A. Wittneben, "Base station modulation diversity for digital SIMULCAST," *IEEE Vehicular Technology Conference*, vol. 1, pp. 848–853, May 1991.

[35] L. Zheng and D. Tse, "Communication on the Grassman manifold: a geometric approach to the noncoherent multiple-antenna channel," *IEEE Trans. on Information Theory*, vol. 48, pp. 359–383, Feb. 2002.

[36] D. Chizhik, G. J. Foschini, and M. J. Gans, "Keyholes, correlations, and capacities of multielement transmit and receive antennas," *IEEE Trans. on Wireless Communications*, vol. 1, pp. 361–368, Apr. 2002.

[37] C. N. Chuah, D. Tse, and J. M. Kahn, "Capacity scaling in MIMO wireless systems under correlated fading," *IEEE Trans. on Information Theory*, vol. 48, pp. 637–650, Mar. 2002.

[38] D. S. Shiu, G. Foschini, M. Gans, and J. Kahn, "Fading correlations and effect on the capacity of multielement antenna systems," *IEEE Trans. on Communications*, vol. 48, pp. 502–512, Mar. 2000.

[39] G. J. Foschini "Layered space-time architecture for wireless communication in fading environment when using multi-element antennas," *Bell Labs. Tech. J.*, vol. 1, no. 2, pp. 41–59, 1996.

[40] B. M. Hochwald and T. J. Marzetta "Unitary space-time modulation for multiple-antenna communication in Rayleigh flat fading," *IEEE Trans. Inform. Theory*, vol. 46, pp. 543–564, Mar. 2000.

[41] A. Stefanov and T. M. Duman, "Turbo-coded modulation for systems with transmit and receive antenna diversity over block fading channels: system model, decoding approaches, and practical considerations," *IEEE Jour. on Selected Areas in Communications*, vol. 19, pp. 958–968, May 2001.

[42] H. J. Su and E. Geraniotis, "Space-time turbo codes with full antenna diversity," *IEEE Trans. on Communications*, vol. 49, pp. 47–57, Jan. 2001.

[43] Y. J. Liu, M. P. Fitz, and O. Y. Takechita, "Full rate space-time turbo codes," *IEEE Jour. on Selected Areas in Communications*, vol. 19, pp. 969–980, May 2001.

[44] S. L. Ariyavisitakul, "Turbo space-time processing to improve wireless channel capacity," *IEEE Trans. on Communications*, vol. 48, pp. 1347–1359, Aug. 2000.

[45] S. Baro, G. Bauch, and A. Hansmann, "Improved codes for space-time trellis-coded modulation," *IEEE Trans. on Communications Letters*, vol. 4, pp. 20–22, Jan. 2000.

[46] W. Firmanto, B. S. Vucetic, and J. H. Yuan, "Space-time TCM with improved performance on fast fading channels," *IEEE Trans. on Communications Letters*, vol. 5, pp. 154–156, Apr. 2001.

[47] Y. Gong and K. B. Letaief, "Concatenated space-time block coding with trellis coded modulation in fading channels," *IEEE Trans. on Wireless Communications*, vol. 1, pp. 580–590, Oct. 2002.

[48] Bahceci and T. M. Duman, " Trellis coded unitary space-time modulation," *In Proc. of IEEE Global Telecommunications Conference (GLOBECOM'01)*, vol. 2, pp. 25–29, Nov. 2001.

[49] X. T. Lin and R. S. Blum, "Systematic design of space-time codes employing multiple trellis-coded modulation," *IEEE Trans. on Communications*, vol. 50, pp. 608–615, Apr. 2002.

[50] H. Jafarkhani and N. Seshadri, "Super-orthogonal space-time trellis codes," *IEEE Trans. on Information Theory*, vol. 49, pp. 937–950, Apr. 2003.

[51] C. Cheng and C. Lu, "Space-Time Code Design for CPFSK Modulation Over Frequency-Nonselective Fading Channels," *IEEE Trans. Commun*, vol. 53, no. 9, pp. 1477–1489, Sep. 2005.

[52] J. K. Cavers, "Space-Time Coding Using MSK," *IEEE Trans. Wireless Commun.*, vol. 4, no. 1, pp. 185–191, Jan. 2005.

[53] H. Jafarkhani, "A quasi-orthogonal space-time block code," *IEEE Trans. Commun.*, vol. 49, pp. 1–4, Jan. 2001.

[54] O. Tirkkonen, "Optimizing STBCs by constellation rotations," *in Proc. Finnish Wireless Commun. Workshop*, pp. 59–60, Tampere, Finland, Oct. 2001.

[55] W. Su and X. Xia, "Signal constellations for quasi-orthogonal space-time block codes with full diversity," *IEEE Trans. Inform. Theory*, vol. 50, pp. 2331–2347, Oct. 2004.

[56] N. Sharma and C. Papadias, "Improved quasi-orthogonal codes through constellation rotation," *IEEE Trans. Commun.*, vol. 51, pp. 332–335, Mar. 2003.

[57] S. Tsai, X. Yu, and C. Kuo, "Channel diagonalization using a full-rate space-time block code," *IEEE Globecom*, vol. 5, pp. 2951–2955, Dallas, TX, Nov. 2004.

[58] X. B. Liang, "Orthogonal designs with maximal rates," *IEEE Trans. Inform. Theory*, vol. 49, pp. 2468–2503, Oct. 2003.

[59] X. B. Liang, "A high-rate orthogonal space-time block code," *IEEE Commun. Lett.*, vol. 7, pp. 222–223, May 2003.

[60] W. Su, X. Xia, and K. Liu, "A systematic design of high-rate complex orthogonal space-time block codes," *IEEE Commun. Lett.*, vol. 8, no. 6, pp. 380–382, Jun. 2004.

[61] X. B. Liang, "A complex orthogonal space-time block code for 8 transmit antennas," *IEEE Commun. Lett.*, vol. 9, no. 2, pp. 115–117, Feb. 2005.

[62] A. F. Naguib, N. Seshadri, and A. R. Calderbank, "Space-time coding and signal processing for high data rate wireless communications," *IEEE Signal Processing Mag.*, vol. 17, no. 3, pp. 76–92, 2000.

[63] D. Gesbert, M. Shafi, D. Shiu, P. Smith, and Naguib, " From theory to practice: an overview of MIMO space-time coded wireless systems," *IEEE Jour. Selected Areas in Commun.*, vol. 21, no. 3, Apr. 2003.

[64] B. Hassibi and B. M. Hochwald, "Cayley differential unitary space-time codes," *IEEE Trans. Inform. Theory*, vol. 48, pp. 1485–1503, Jun. 2002.

[65] B. Hochwald and W. Sweldens, "Differential unitary space-time modulation," *IEEE Trans. Commun.*, vol. 48, pp. 2041–2052, Dec. 2000.

[66] G. Ganesan and P. Stoica, "Differential modulation using space-time block codes," *IEEE Signal Processing Lett.*, vol. 9, pp. 57–60, Feb. 2002.

[67] Y. Zhu and H. Jafarkhani, "Differential modulation based on quasi-orthogonal codes," *IEEE Trans. Wireless Commun.*, vol. 4, pp. 3018–3030, Nov. 2005.

[68] T. M. Cover and A. A. El Gamal, "Capacity theorems for the relay channel," *IEEE Trans. on Information Theory*, vol. 25, no. 5, pp. 474–584, Sep. 1979.

[69] M. Janani, A. Hedayat, T. E. Hunter, and A. Nosratinia, "Coded cooperation in wireless communications: space-time transmission and iterative decoding," *IEEE Trans. Signal Processing*, vol. 52, pp. 362–371, Feb. 2004.

[70] J. Boyer, D. D. Falconer, and H. Yanikomeroglu, " Multihop diversity in wireless relaying channels," *IEEE Trans. Commun.*, vol. 52, pp. 1820–1830, Oct. 2004.

[71] K. Azarian, H. El Gamal, and P. Schniter, "On the achievable diversity-multiplexing tradeoff in half-duplex cooperative channels," *IEEE Trans. on Inform. Theory*, vol. 51, no. 12, pp. 4152–4172, Dec. 2005.

[72] P. Mitran, H. Ochiai, and V. Tarokh, "Space-time diversity enhancements using collaborative communications," *IEEE Trans. Inform. Theory*, vol. 51, pp. 2041–2057, Jun. 2005.

[73] P. Maurer and V. Tarokh, "Transmit diversity when the receiver does not know the number of transmit antennas," *In Proceedings of the International Symposium on Wireless Multimedia Communications (WPMC), Aalborg, Denmark*, pp. 2688–2692, Sep. 2001.

[74] S. Yang and J. Bel, "Optimal space-time codes for the amplify-and-forward cooperative channel," *IEEE Trans. Inform. Theory*, vol. 53, no. 2, pp. 647–663, Feb. 2007.

[75] B. A. Sethuraman, B. S. Rajan, and V. Shashidhar, "Full-diversity, high-rate space-time block codes from division algebras," *IEEE Trans. Inform. Theory*, vol. 49, pp. 2596–2616, Oct. 2003.

[76] P. Tarasak, H. Minn, and V. K. Bhargava, "Differential modulation for two-user cooperative diversity systems," *IEEE J. Select. Areas Commun.*, vol. 23, pp. 1891–1900, Sep. 2005.

[77] T. Wang, Y. Yao, and G. B. Giannakis, "Non-coherent distributed space-time processing for multiuser cooperative transmissions," *IEEE Trans. on Wireless Comm.*, vol. 5, no. 12, pp. 3339–3343, Dec. 2006.

[78] S. Yiu, R. Schober, and L. Lampe, "Distributed space-time block coding," *IEEE Trans. Commun.*, vol. 54, no. 7, pp. 1195–1206, Jul. 2006.

[79] S. Yiu, R. Schober, and L. Lampe, "Non-coherent distributed space-time block coding," *In Proceedings of the IEEE Vehicular Technology Conference (VTC), Dallas, USA*, Sep. 2005.

[80] P. A. Anghel and M. Kaveh, "On the performance of distributed space-time coding systems with one and two non-regenerative relays," *IEEE Trans. Wireless Commun.*, vol. 5, no. 3, pp. 682–692, Mar. 2006.

[81] S. Barbarossa and G. Scutari, "Distributed space-time coding for multihop networks," *In Proc. of IEEE Proc. of IEEE International Conference on Communications*, vol. 2, pp. 916–920, Jun. 2004.

[82] S. Barbarossa and G. Scutari, "Distributed space-time coding strategies for wideband multihop networks: regenerative vs. non-regenerative relays," *In Proc. of IEEE Inter. Conf. on Acoustics, Speech, and Signal Process. (ICASSP)*, vol. 4, pp. 501–504, May 2004.

[83] J. Mietzner, R. Thobaben, and P. A. Hoeher, "Analysis of the expected error performance of cooperative wireless networks employing distributed space-time codes," *In Proc. IEEE Global Telecomm. Conf. (Globecom 2004)*, vol. 5, pp. 2854–2858, Dec. 2004.

[84] Y. Hua, Y. Mei, and Y. Chang, "Parallel wireless mobile relays with space-time modulations," *In Statistical Signal Processing, IEEE Workshop,* pp. 375–378, Oct. 2003.

[85] Y. Chang and Y. Hua, "Application of space-time linear block codes to parallel wireless relays in mobile ad hoc networks," *In Signals, Systems and Computers, 2003, The Thrity-Seventh Asilomar Conference*, vol. 1, pp. 1002–1006, Nov. 2003.

[86] T. Wang, Y. Yao, and G. B. Giannakis, "Non-coherent distributed space time processing for multiuser cooperative transmissions," *IEEE Transactions on Wireless Communications*, vol. 5, no. 12, pp. 3339–3343, Dec. 2006.

[87] H. E. Gamal and D. Aktas, "Distributed space-time filtering for cooperative wireless networks," *In Proc. IEEE Global Telecomm. Conf. (Globecom 2003)*, vol. 4, pp. 1826–1830, Dec. 2003.

[88] S. Wei, D. Goeckel, and M. Valenti, "Asynchronous cooperative diversity," *IEEE Transactions on Wireless Communications*, vol. 5, pp. 1547–1557, 2006.

[89] B. Sirkeci Mergen and A. Scaglione, "Randomized distributed space time coding for cooperative communication in self-organized networks," *IEEE Workshop on Signal Processing Advances in Wireless Communications (SPAWC)*, pp. 500–504, Jun. 2005.

[90] M. Yuksel and E. Erkip, "Diversity-multiplexing tradeoff in cooperative wireless systems," *In Proceedings of 40th CISS*, pp. 1062–1067, Mar. 2006.

[91] S. J. Alabed, J. M. Paredes, and A. B. Gershman, "A Low Complexity Decoder for Quasi-Orthogonal Space-Time Block Codes," *IEEE Transactions on Wireless Communications*, vol. 10, no. 3, March 2011.

[92] S. J. Alabed, J. M. Paredes, and A. B. Gershman, "A Simple Distributed Space-Time Coded Strategy for Two-Way Relay Channels," *accepted for publication in IEEE Transactions on Wireless Communications*, 2011.

[93] S. J. Alabed, M. Pesavento, and A. B. Gershman, "Distributed Differential Space-Time Coding Techniques for Two-Way Wireless Relay Networks,"

accepted for publication in Proceedings of the Fourth IEEE International Workshop on Computational Advances in Multi-Sensor Adaptive Processing (CAMSAP'11), San Juan, Puerto Rico, December 2011.

[94] S. J. Alabed and M. Pesavento, "A Simple Distributed Differential Transmit Beamforming Technique for Two-Way Wireless Relay Networks," *accepted for publication in Proceedings of the 16th International IEEE/ITG Workshop on Smart Antennas (WSA 2012)*, Mar. 2012.

[95] D. Tse and P. Viswanath, "Fundamentals of wireless communication," *Cambridge: Cambridge University Press*, 2005.

[96] S. Boyd and L. Vandenberghe, "Convex optimization," *Cambridge University Press*, 2004.

[97] Z. A. Khan and S. B. Rajan, "Single-symbol maximum likelihood decodable linear STBCs," *IEEE Trans. Inform. Theory*, vol. 52, pp. 2062–2091, May 2006.

[98] C. Yuen, Y. L. Guan, and T. T. Tjhung, "Quasi-orthogonal STBC with minimum decoding complexity," *IEEE Trans. Wireless Commun.*, vol. 4, pp. 2089–2095, Sep. 2005.

[99] J. Paredes and A. B. Gershman, "High-rate space-time block codes with fast maximum-likelihood decoding," *in Proc. ICASSP'08*, pp. 2385–2388, Las Vegas, USA, Apr. 2008.

[100] H. Wang, D. Wang, and X. G. Xia, "On optimal quasi-orthogonal space-time block codes with minimum decoding complexity," *IEEE Trans. Inform. Theory*, vol. 55, pp. 1104–1130, Mar. 2009.

[101] L. He and H. Ge, "Fast maximum likelihood decoding of quasi-orthogonal space-time codes," in *Proc. Asilomar Conf. on Signals, Systems and Computers*, vol. 1, pp. 1022–1026, Monterey, CA, Nov. 2003.

[102] C. Jiang, H. Zhang, D. Yuan, and H. Chen, "A low complexity decoding scheme for quasi-orthogonal space-time block coding," in *Proc. IEEE SAM Workshop*, pp. 9–12, Jul. 2008.

[103] C. F. Mecklenbräuker and M. Rupp, "Generalized Alamouti codes for trading quality of service against data rate in MIMO UMTS," *EURASIP J. Applied Signal Processing*, vol. 5, pp. 662–675, 2004.

[104] A. Wong, J. Zhang, and K. M. Wong, "Full diversity group decodable orthogonal linear dispersion codes for MISO flat fading channels," in *Proc. ICASSP'08*, pp. 2929–2932, Las Vegas, USA, Apr. 2008 .

[105] O. Tirkkonen, A. Boariu, and A. Hottinen, "Minimal non-orthogonality rate 1 space-time block code for 3+ tx antennas," in *IEEE ISSSTA*, vol. 2, pp. 429–432, 2000.

[106] C. B. Papadias and G. J. Foschini, "Capacity-approaching space-time codes for systems employing four transmitter antennas," in *IEEE Trans. on Information Theory*, vol. 49, pp. 726– 733, Mar. 2003.

[107] C. Yuen, Y. L. Guan, and T. T. Tjhung, "Decoding of quasi-orthogonal space-time block code with noise whitening," in *IEEE PIMRC*, pp. 2166–2170, 2003.

[108] L. Zheng and D. Tse, "Diversity and multiplexing: a fundamental tradeoff in multiple-antenna channels," *IEEE Transactions on Information Theory*, vol. 49, pp. 1073–1096, 2003.

[109] E. Agrell, T. Eriksson, A. Vardy, and K. Zeger, "Closest point search in lattices," *IEEE Trans. Inform. Theory*, vol. 48, pp. 2201-2214, Aug. 2002.

[110] B. Rankov and A. Wittneben, "Spectral efficient protocols for half-duplex relay channels," *IEEE J. Select. Areas Commun.*, vol. 25, pp. 379–389, Feb. 2007.

[111] C. Esli and A. Wittneben, "One- and Two-Way Decode-and-Forward Relaying for Wireless Multiuser MIMO Networks," in *Proc. IEEE Globecom*, New Orleans, USA, vol. 6, pp. 1–6, Dec. 2008.

[112] C. E. Shannon, "Two-way communication channels," in *Proc. 4th Berkeley Symp. Math. Stat. Prob.*, pp. 611–644, 1961.

[113] T. Cui, F. Gao, T. Ho, and A. Nallanathan, "Distributed Space-Time Coding for Two-Way Wireless Relay Networks," *IEEE Trans. Signal Processing*, vol. 57, pp. 658–671, May 2009.

[114] P. Larsson, N. Johansson, and K. E. Sunell, "Coded bi-directional relaying," in *Proc. IEEE Vehicular Technology Conf.*, Melbourne, Australia, vol. 2, pp. 851–855, May 2006.

[115] I. Hammerstrom, M. Kuhn, C. Esli, J. Zhao, A. Wittneben, and G. Bauch, "MIMO two-way relaying with transmit CSI at the relay," in *Proc. SPAWC '07*, pp. 1–5, Helsinki, Finland, Jun. 2007 .

[116] P. Popovski and H. Yomo, "Physical network coding in two-way wireless relay channels," in *IEEE Int. Conf. Communications (ICC)*, pp. 707–712, Glasgow, Scotland, Jun. 2007.

[117] I. Baik and S. Chun, "Network coding for two-way relay channels using lattices," in *IEEE Int. Conf. Communications (ICC)*, pp. 3898-3902, May 19–23, 2008.

[118] C. Hausl and J. Hagenauer, "Iterative network and channel decoding for the two-way relay channel," *in Proc. IEEE Int. Conf. Communications (ICC)*, pp. 1568–1573, Istanbul, Turkey, Jun. 2006.

[119] T. Unger and A. Klein, "Applying Relay Stations with Multiple Antennas in the One- and Two-Way Relay Channel," *in Proc. International Symposium on Personal, Indoor and Mobile Radio Communications*, Athens, Greece, Sep 2007.

[120] T. Unger and A. Klein, "On the performance of two-way relaying with multiple-antenna relay stations," *in Proc. IST Mobile and Wireless Communications Summit*, Budapest, Hungary, Jul 2007.

[121] T. Unger and A. Klein, "On the performance of distributed space-time block codes," *IEEE Communications Letters*, vol. 11, No. 5, pp. 411-413, May 2007.

[122] M. Tao and R. Cheng, "Differential Space-time Block Codes," in *Proc. IEEE Globecom*, vol. 2, pp. 1098–1102, Nov. 2001.

[123] H. Boelcskei, R. U. Nabar, O. Oyman, and A. J. Paulraj, "Capacity scaling laws in MIMO relay networks," *IEEE Trans. Wireless Commun.*, vol. 5, no. 6, pp. 1433-1444, Jun. 2006.

[124] A. F. Dana and B. Hassibi, "On the power-efficiency of sensory and ad-hoc wireless networks," *IEEE Trans. Inf. Theory*, vol. 52, no. 7, pp. 2890-2914, Jul. 2006.

[125] R. U. Nabar, H. Boelcskei, and F. W. Kneubuhler, "Fading relay channels: Performance limits and space-time signal design," *IEEE J. Sel. Areas Commun.*, vol. 23, no. 7, pp. 1099-1109, Aug. 2004.

[126] Y. Jing and H. Jafarkhani, "Distributed differential space-time coding in wireless relay networks," *IEEE Trans. Commun.*, vol. 56, no. 7, pp. 1092-1100, Jul. 2008.

[127] F. Oggier and B. Hassibi, "A coding strategy for wireless networks with no channel information," *in Proc. Allerton Conf. Communications, Control, and Computing*, Monticello, IL, pp. 113-117, Sep. 2006.

[128] Z. Utkovski, G. Yammine, and J. Lindner, "A Distributed differential space-time coding scheme for two-way wireless relay networks," *ISIT 2009*, Seoul, Korea, pp. 779-783, Jun. 2009.

[129] A. Hottinen, O. Trikkonen, and R. Wichman, "Multi-Antenna Transciever Techniques for 3G and Beyond," New York, Willey, 2003.

[130] R. Mudumbai, B. Wild, U. Madhow, and K. Ramchandran, "Distributed beamforming using 1 bit feedback: from concept to realization," *in Proceedings of the 44th Allerton Conference on Communication Control and Computing* , Monticello, Ill, USA, September 2006.

[131] P. Jeevan, S. Pollin, A. Bahai, and P. P. Varaiya, "Pairwise algorithm for distributed transmit beamforming," *in Proceedings of the IEEE International Conference on Communications (ICC '08)*, pp. 4245-4249, Beijing, China, May 2008.

[132] M. F. Ahmed and S. A. Vorobyov, "Collaborative beamforming for wireless sensor networks with Gaussian distributed sensor nodes," *IEEE Transactions on Wireless Communications*, vol. 8, no. 2, pp. 638-643, 2009.

[133] C. Wang, Q. Yin, J. Zhang, B. Hao, and W. Li, "Distributed Transmit Beamforming without Phase Feedback," *EURASIP Journal on Wireless Communications and Networking*, vol. 2010, 2010.

Samer Alabed

Curriculum Vitae

Personal Details

Address	Darmstadt, Germany
Telephone	+49615116-6271
	+4917645156888
E-Mail	salabed@nt.tu-darmstadt.de
	dr.samer_alabed@yahoo.com
Nationality	Jordanian
Birthday	18-08-1981

Academic Degrees

Ph.D. Candidate in Communication Systems Oct. 2008-2012

Name of University	Darmstadt University of Technology, Darmstadt, Germany.
Research Interests	MIMO communication systems, cooperative communications, space-time coding, wireless relay networks, and speech processing, such as speech source coding and speech enhancement.

M.Sc in Electrical Engineering / Communications 2003 - 2005

Name of University	University of Jordan, Amman, Jordan.
Thesis Title	Enhancement of the design of high quality, low-bite rate speech coder based on analysis/synthesis sinusoidal model
Evaluation	3.88 out of 4 (excellent with highest honors)

B.Sc in Electrical and Computer Engineering 1999 - 2003

Name of University	Hashemite University, Jordan.
Evaluation	3.5 out of 4

Work Experience

Research and Teaching Assistant 2003-2005

Name of employer	Electrical engineering department, University of Jordan, Amman, Jordan.
Main activities	Teaching and supervising electrical, electronic, computer, and communication engineering Labs and participating in the preparation and grading of exams and reports.

Lecturer 2005-2006

Name of employer	Electrical engineering department, University of Jordan, Amman, Jordan.
Main activities	Teaching several electrical, electronic, and communication engineering courses and Labs.

Lecturer 2006-2008

Name of employer	Wadi Al-Sir international college (U.N.R.W.A), Amman, Jordan.
Main activities	Teaching several electrical, electronic, and computer engineering courses.

Research Scientist 2008-present

Name and address of employer	Communication Systems Group, Darmstadt University of Technology, Germany.

Skills and Awards

Awards	1. The second place in IEEE (Jordan branch) competition in 2003 and granted a reward due to the graduation project titled as "sinusoidal speech coding". 2. The third place in IEEE/IEE (Jordan branch) competition in 2004 and granted a reward due to the project titled as "techniques in speech coding". 3. The best student award. 4. DAAD (German Academic Exchange Service) scholarship from 2008-2010.
Teaching Experience	Tutorial for MIMO Communications and Space-Time Coding, Quick and Turbo Basic, Circuit Analysis 1 and 2 (Theory and Lab), Electronics 1 and 2 (Theory and Lab), Digital Design (Theory and Lab), Electrical Measurements (Theory and Lab), Microprocessors (Theory and Lab), Computer Networks (Theory and Lab), Assembly Language (Theory and Lab), C-Language (Theory and Lab), Communication Lab, Supervising Graduation Projects, CCNA, WLAN, IT Essential, Matlab, and Computer Maintenance.

Studied Courses	Interconnecting Cisco Networking Devices (CCNA) - 40 hours, Global System for Mobile (GSM) - 30 hours, ASP.Net - 36 hours, Orientation Course for Cisco Academy - 16 hours, CCNA Academy Course for Instructors -280 hours, Fundamentals of Wireless LANs - 48 hours, IT Security -30 hours, Advanced ICDL certificates in (Microsoft Word, Microsoft Excel, and Microsoft PowerPoint), C-Language, Assembly Language, ORACLE - 60 hours, Web Page Design - 30 hours, Linux -30 hours, Autotronic Systems -30 hours, AutoCAD, Workbench, Maple, Mathematica, and MathCAD.
Software	Windows Operating Systems (DOS, Windows 9X, 2000, Millennium, XP, Vista, 7), Linux, MS-Office, LaTex, Web Page Design (HTML, Front Page and ASP.net), Matlab, Simulink, C-language, Qbasic, C++, Assembly Language, AutoCAD, Workbench, Maple, Mathematica and MathCAD.

Journal Papers

- S. J. Alabed, J. M. Paredes, and A. B. Gershman, *A Low Complexity Decoder for Quasi-Orthogonal Space-Time Block Codes*, IEEE Transactions on Wireless Communications, vol. 10, no. 3, March 2011.
- S. J. Alabed, J. M. Paredes, and A. B. Gershman, *A simple distributed space-time coded strategy for two-way relay channels*, IEEE Transactions on Wireless Communications, pp. 1260-1265, vol. 11, no. 4, April, 2012.
- I. Mansour and S. Alabed, *A New Architecture Model for Multi Pulse Linear Predictive Coder for Low Bit Rate Speech Coder*, Engineering Sciences, Dirasat Journal, vol. 33, no. 2, October 2006.

Conference Papers

- S. J. Alabed, M. Pesavento, and A. B. Gershman, *Distributed Differential Space-Time Coding Techniques for Two-Way Wireless Relay Networks*, Proceedings of the Fourth International Workshop on Computational Advances in Multi-Sensor Adaptive Processing (CAMSAP'2011), pp. 221-224, San Juan, Puerto Rico, December 2011.

- S. J. Alabed and M. Pesavento, *A Simple Distributed Differential Transmit Beamforming Technique for Two-Way Wireless Relay Networks*, Proceedings of the 16th International IEEE/ITG Workshop on Smart Antennas (WSA 2012), pp. 243-247, Dresden, March 2012.

- X. Wen, K. Law, S. J. Alabed, and M. Pesavento, "*Rank-two beamforming for single-group multicasting networks using OSTBC*", accepted for publication in the 7th IEEE Sensor Array and Multichannel Signal Processing Workshop (SAM), January 2012.

- I. Mansour and S. J. Alabed, *Using Sinusoidal Model to Implement Sinusoidal Speech Coder with Speech Enhancer*, The 6th Jordanian International Electrical and Electronics Engineering Conference (JIEEEC), vol. 1, pp. 1-8, March 2006.

- I. Mansour and S. J. Alabed, *A New Technique for Regular Pulse Predictive Coding of Speech at Low Bit Rates*, 6th ICEENG, 27-29 May, 2008.